1966

Electrical resistivity of carbon granules in a fluidized bed

Arthur Lowell Jones
Iowa State University

JONES, Arthur Lowell, 1928-
ELECTRICAL RESISTIVITY OF CARBON GRANULES IN A FLUIDIZED BED.

Iowa State University of Science and Technology, Ph.D., 1966
Engineering, chemical

ELECTRICAL RESISTIVITY OF CARBON GRANULES IN A FLUIDIZED BED

by

Arthur Lowell Jones

A Dissertation Submitted to the

Graduate Faculty in Partial Fulfillment of

The Requirements for the Degree of

DOCTOR OF PHILOSOPHY

Major Subjects: Mechanical Engineering
Chemical Engineering

Approved:

Signature was redacted for privacy.

In Charge of Major Work

Signature was redacted for privacy.

Heads of Major Departments

Signature was redacted for privacy.

Dean of Graduate College

Iowa State University
Of Science and Technology
Ames, Iowa

1966

TABLE OF CONTENTS

LIST OF FIGURES

LIST OF TABLES

ABSTRACT

The purpose of this investigation was to study the parameters affecting the apparent resistivity of a fluidized bed of carbon granules, to determine which parameters were important, and to correlate these parameters by means of a mathematical expression which could be used to predict the apparent resistivity. All determinations were made at room temperature. The method used in determining resistivity values was the four terminal method of resistance measurement which employed two current terminals and two potential terminals. The use of this method eliminated any contact resistance between the potential terminals and the bed. Measurements of current and voltage drop together with bed dimensions gave values for the apparent resistivity according to the relationship $R = \rho L/A$, where R is resistance, ρ is apparent resistivity, L is the distance between probes and A is the cross-sectional area of the fluidized bed.

It was observed that the resistivity of a given bed of material increased with the time length of use. The resistivity increased rapidly at first and then it subsequently increased more gradually. The increase in resistivity was probably due to the elutriation of fines from the bed and perhaps polishing of individual particles by attrition. Materials used were petroleum coke, calcined coke and graphite having Tyler mesh sizes from -65 to +250 and in some cases, from -65 to +400.

As the gas flow rate through a bed was increased from zero, the resistivity remained constant at the relatively low value of the settled bed resistivity. When the flow rate approached the minimum fluidization rate,

the resistivity began a rapid increase. With further increases in flow rate, the resistivity reached a peak, decreased to a minimum and began to increase again. For individual size fractions, the resistivity reached a peak at lower flow rates as the particle size was decreased. For mixtures containing smaller size fractions, the peaks were higher and steeper than for mixtures of larger size fractions. The resistivity of graphite increased rapidly as the minimum fluidization flow rate was reached. As flow rate was increased further, the resistivity reached a plateau and remained constant.

A statistically designed study of the resistivity of calcined coke used nine levels of particle size and two levels each of gas density, bed height and bed diameter. Analysis of the data was made by using the techniques of analysis of variance, stepwise regression analysis and multiple regression analysis. Since it did not appear feasible to correlate the apparent resistivity over the entire range of flow rates, correlations were made for the resistivity of the settled bed, for the peak resistivity and for the minimum fluidized resistivity. Settled bed resistivity was found to be a function of bed diameter, bed height and average particle size; peak resistivity was a function of particle size, bed diameter and gas density; minimum fluidized resistivity was a function of bed diameter, tangent of the angle of repose of the bed material and the average particle size. Mathematical expressions were determined for each of these three resistivities correlating them with the above mentioned independent variables.

INTRODUCTION

The term "fluidized bed" is used to describe a method of contacting granular solids with a fluid. As an example, consider a vertical column having a porous plug near the bottom which would support the granular solids, yet allow a gas to pass through. As upward gas flow is established and flow is increased, a certain flow rate will be reached where the solids will become suspended in the gas stream and will have a well defined upper surface and the bed will appear much like a boiling liquid. As flow is progressively increased, bubbles will form and become larger until ultimately the bed materials are swept out of the column.

The numerous small particles of the bed provide an extremely large ratio of surface area to bed volume. This large surface area in a small volume suggests that the fluidized bed be used as a chemical reactor and since most chemical reactions involve the addition or removal of heat, some means of temperature control must be provided. One method which has been employed for the heating of fluidized beds is the passing of electric current through electrically conducting fluidized solids. This investigation was primarily concerned with the measurement of the electrical resistivity of fluidized beds of carbon particles.

Probably the earliest recorded application of fluidization was for the purification of ores in 1556 (1) and scattered references to early observations of fluidization can be found in the published literature as far back as 1878 according to Zenz and Othmer (2). Apparently the first

patent using a form of fluidization was issued in 1910 for the contacting of a gas and a finely divided catalyst. Probably the first attempt to operate a fluidized unit on a commercial scale was the Winkler gas generator developed in 1921 in Germany for the manufacture of water gas and producer gas (1). The fluidization technique as it is now known was initiated in the early 1940's by the pioneering work of the petroleum industry in an effort to find a better catalytic-cracking process for oil vapors (2).

Uses have been found for fluidized beds varying from the freezing or cooking of foods such as peas and kernel corn, to chemical reactors having temperatures up to 7000°F., to the quenching of 12,500°F. products from plasma jet reactors (3).

One of the outstanding characteristics of fluidized beds is the extremely rapid heat transfer between gases and solids and from solids to solids. This characteristic can be used to advantage in processes requiring controlled temperatures or large quantities of heat.

Heat can be supplied to or removed from a fluidized bed by several methods such as:

1. Heating or cooling the walls of the bed.
2. Supplying a heated or cooled fluidizing medium.
3. Heating or cooling an internal surface element such as a helical coil.
4. Placing electrodes in the bed and heating the bed solids directly by self-resistive heating.

The latter scheme has come to be known as the "electro-thermal fluidized bed."

Within the last six or seven years, several patents have been issued for apparatus in which electrodes are inserted in a fluidized bed of conductive carbon particles. A voltage potential is applied and the electrical energy is converted to heat by the flow of current through the carbon particles. The heat thus generated is used in various chemical reactions (4, 5, 6, 7).

To date, the design of electro-thermal fluidized bed reactors has been based more on experience and trial and error procedures than on quantitative information. Some of the basic questions that arise in designing such a reactor are:

1. What is the range of values for the apparent electrical resistivity of a fluidized bed of carbon granules?
2. Of the many variables which one might suspect would affect this apparent resistivity, which are significant and which of little or no importance?
3. Can the significant variables be correlated into a mathematical relationship by which apparent resistivity may be predicted?
4. Does apparent resistivity change with the time length of use of the fluidized bed?
5. How does apparent resistivity vary with gas flow rate and with granule size?

The development of reliable answers to these questions was the objective

of this investigation. This required developing experimental methods and techniques for measuring the resistivity of both the fluidized and settled beds.

Although several investigators have measured the resistivity of fluidized beds in order to study solids mixing, bubble formation and the conduction mechanism, there have been few concerned with determining the factors upon which the resistivity depends. Some have reported on a few of the factors affecting the overall resistance of fluidized beds but due to the experimental techniques used, the resistance is not readily convertible into resistivity.

In this work the effects of particle size, particle size distribution, bed dimensions, angle of repose, gas velocity, gas viscosity and gas density on the resistivity of both settled and fluidized beds were investigated. Although most measurements were made on calcined coke particles, some were made on graphite particles. All of the determinations were made at room temperature and pressure.

The electrical resistivity referred to throughout this work was actually the apparent or effective electrical resistivity of the bed of granulated carbon material as determined by measuring the resistance of a volume element in the center section of the bed.

REVIEW OF THE LITERATURE

General Characteristics of Fluidized Beds

Stages of fluidization

The stages of fluidization as well as the following general characteristics of fluidized beds are discussed by several authors (1, 2, 8, 9). In the process of fluidizing a bed of granular material, there are three stages which can be recognized:

1. At very low velocity the gas percolates through the bed without agitating individual particles. Gas flow is generally streamlined. The pressure drop increases linearly with velocity and is less than the static weight of the bed per unit cross-sectional area.
2. When the velocity is increased sufficiently, the pressure drop becomes equivalent to or slightly in excess of the weight per unit area of solids present. At this point, the solids are suspended in the gas and the bed is fluidized. The fluid flows uniformly through the bed, and the loose packing adopted by the solids give the particles some freedom to move about. This state of fluidization is known as the "particulate" or emulsion phase.
3. Further increase in gas flow can be accommodated by "bubble" flow where the excess of gas required for the emulsion phase rises in the form of "bubbles."

Bed expansion

A large bed expansion is characteristic of systems which fluidize

easily and smoothly. The amount of expansion depends on the properties of both solids and gas. For example, particle size has a marked effect. With cracking catalyst, the expansion is large if the solid particles have an average size in the range of 30 to 80 microns. If the particles are larger than about 100 microns, there is much less expansion. If the particles are less than 20 microns, they adhere to each other so firmly that they agglomerate in spheres several millimeters in diameter, and the gas flows through well defined channels in the bed. Generally, a bed of fine solids expands more than one of coarse solids. As an example of gas properties affecting bed expansion, a bed of cracking catalyst expanded 25 per cent when fluidized with air at atmospheric pressure but expanded 40 per cent when fluidized with nitrogen at 200 lb./sq.in.gage. Increased gas density results in larger bed expansion.

Entrainment

At low gas velocity the fluidized bed has a high density, and only a small amount of very fine material is carried out by the gas. However, as gas velocity is raised, entrainment rate increases rapidly. The rate may increase in proportion to the velocity raised to the second power or even higher. Entrainment is also influenced by the gas and solids properties and the amount of freeboard (distance between the upper surface of the bed and the outlet of the fluidization column).

Thermal characteristics

One of the outstanding characteristics of the fluidized bed is its uniformity of temperature, even when reactions involving rather large heat

effects are carried out. The reasons for this are, first, circulation of solids from top to bottom of the bed, second, the rapid heat transfer in a fluidized bed, and, third, the large heat capacity of the solids which prevents any rapid change in temperature. Heat transfer coefficients are large and in addition, the total surface area of the fine particles making up the bed is large. This combination makes for rapid equalization of temperature between the solid particles and the adjacent gas. The early observation that temperature gradients within the bed are low is due principly to the astounding solids circulation from top to bottom of the bed. This mixing action is in turn caused by the action of gas bubbles rising through the bed. Effective thermal conductivities in the vertical direction as large as 20,000 to 30,000 Btu./hr.sq.ft.^{o}F./ft. have been measured in the laboratory. These conductivities are 100 times that of silver.

Bubble formation

Romero and Smith (10) used a flash x-ray technique in studying bubble flow within fluidized beds. Their results supported the two phase theory according to which the flow of gas through a fluidized bed is composed of both a streamline or laminar interstitial flow within the emulsion phase and a flow in the form of bubbles. The streamline interstitial flow is equal to that required for incipient fluidization. This flow within the emulsion phase provides the initial expansion of the bed. Further expansion is due to the formation of gas bubbles. Wace and Burnett (11) injected bubbles of nitrogen dioxide, a dark brown gas, into a fluidized bed having a thin section in depth as compared to width and height so that it was essentially a two dimensional fluidized bed. From their studies they

concluded that gas bubbles have a spherical shape with an indented bottom and that gas flows through the bubbles at a greater velocity than through the emulsion phase. Bubbles coalesce by the lower bubble elongating and the roof of the lower bubble penetrating the bottom of the upper bubble. Bubbles aid in the mixing of solids since particles follow in the wake of the bubble. The general tendency is for particles to move upward in the center of the bed and downward around the outside.

Applications of Fluidized Beds

The fluidized solids technique may have application to any gas-solids process in which:

1. Large quantities of heat are to be transferred.
2. Large quantities of solids must be circulated.
3. Intimate contact between gases and solids is desired.

Fluidized beds may be used not only for chemical reactors but also for drying, humidifying, gas adsorption, encapsulating, agglomerating and coating processes and as heat exchangers. Some examples of processes where it should be advantageous to use fluidized bed reactors include the preparation of carbon monoxide by reaction of carbon dioxide with carbon (4), the preparation of titanium tetrachloride by chlorination of a titanium bearing material mixed with carbon at an elevated temperature (5), the preparation of carbon disulphide by reaction of hydrogen sulfide with carbon particles (12), the preparation of carbon disulphide by reaction of sulphur vapor with carbon (13) and the preparation of hydrocyanic acid

from a mixture of ammonia and hydrocarbon gases passed through an electrically heated bed of fluidized carbon particles (14, 15, 16).

Examples of fluidized bed encapsulating, agglomerating and coating processes which have been suggested are the coating of seeds with a water soluble gum and dye for the prupose of protection and identification; the coating of phthalic anhydride with carboxylmethylcellulose for protection from attack by a second component; the simultaneous removel of dust and fumes from industrial exhaust gases by a fluidized bed agglomerator which not only agglomerates the dust but by means of chemical reaction removes the fumes; the coating of heated metal parts by immersion in a fluidized bed of thermoplastic resin.

Examples of proposed heat exchangers are the cooking of foods such as breaded shrimp, cashew nuts, peanuts, potatoes and onion rings in fluidized beds of monosodium glutamate, limestone, sugar, salt, limestone-salt mixtures or rice; the freezing of peas, kernel corn and diced carrots in a stream of cold air; the quenching of products from a plasma jet reactor in a fluidized bed. Cooling rates in excess of 2×10^{7}°F./sec. have been achieved by injecting a plasma directly into a low temperature fluidized bed (3).

Waterhouse (17) suggested the use of fluidized bed dryers for the drying of foundry sand as an economically attractive alternative to rotary drum dryers. He also suggested that fluidized bed techniques might find applications in the thermal reclamation of resin bonded sand and as an alternative to conventional furnaces for the heat treatment of small castings.

Methods of Heating Fluidized Beds

Various means have been devised for either the removal of heat from or the supply of heat to a fluidized bed. As previously mentioned, some of the methods used are the heating or cooling of the column wall, supplying a heated or cooled gas as the fluidizing medium, and heating or cooling an internal surface such as a tube, plate or a helical coil. Within the last five years, patents (6, 18) have been issued for apparatus in which electrodes are inserted in a fluidized bed of conductive carbon particles thus converting the electrical energy to heat and using this heat for various chemical reactions. Johnson (19) indicated that the advantages of this type of reactor are:

1. Large quantities of heat energy can be generated.
2. High temperatures in excess of 2000^{o}F. can be obtained.
3. Rapid heating of the bed is possible.

Electrothermal Fluidized Reactors

Apparatus for obtaining high temperatures in a bed of fluidized electrically conductive particles heated by the passage of electric current was described as early as 1932 by Winkler (20). Winkler's apparatus consisted of a fluid bed reaction chamber with flat alloy plates as electrodes located in opposite walls of the reactor so that electric current flowing between the electrodes passed through the fluidized bed of carbon particles. This particular apparatus was designed for production of water gas from steam and granular coke.

Although apparatus of the type described by Winkler was known for over 25 years, and suggestions for the use of this type of apparatus had been made as recently as 1949 by Garbo (21) for the reduction of zinc compounds to metallic zinc vapor and by Schenck et al. (6) for the melting of ores and by Pevere et al. (22) in 1957 for spark discharge activated reactions, no commercial use of the apparatus was made until about 1960 when Shawinigan Chemicals Limited of Canada (23) built a commercial unit for the production of hydrogen cyanide.

High temperature operation

Difficulties were encountered at Shawinigan by Johnson (18) especially when attempts were made to operate at temperatures above 1800°F. The principal difficulty was the apparent breakdown of the electrical insulating properties of structural elements separating electrodes thus causing short circuits. A method of shielding was devised to prevent breakdown of the insulating properties. A system of baffles protected the area around the electrode entrance from radiant energy. The electrodes were inserted through the top of the fluidization column. Johnson (7) also found that electrodes which penetrate the walls of the fluidized bed structure below the surface of the fluidized bed are very unsatisfactory at temperatures above 1800°F. Conductive paths develop on the walls and form short circuits between the electrodes.

Goldberger et al. (24) apparently overcame these difficulties and has built an electrothermal fluidized bed and operated it at a temperature of 6500°F. for extended periods of time. They indicate that operation at

Temperatures up to 8000°F. appears possible.

Conductivity of the bed

Johnson and Anderson (12) found that at least some of the solids in a bed of fluidized solids must have good conductivity in order to carry sufficient current through the bed to supply the required heat at convenient voltages. Carbon in some of its numerous forms is suitable for providing electrical conductivity in a fluidized bed. It is well known that coke is electrically conductive and the petroleum coke by-product of fluidized bed petroleum coking processes is in a particulate form which is readily suitable for use in other fluidization processes. As produced in the coking operation, petroleum coke has a very high resistance (of the order of 500 megohms between two parallel $\frac{1}{4}$ in. graphite electrodes immersed to a depth of one inch and spaced $\frac{1}{2}$ in. apart in a stationary bed of coke), but upon calcination at elevated temperature, the resistance decreases greatly (to about 10 ohms) and the calcined coke has ample conductivity to carry electric current through a fluidized bed at convenient voltages. Metallurgical coke, in suitable particle size, is also an effective electrical conductor in a fluidized bed. Stoker coke and silicon carbide of appropriate particle size can also be used as electrical conductors in fluidized beds.

For numerous reasons, including its ready availability, low cost, and very low ash content, calcined fluid coke seems to be preferred in an electrothermal fluid bed operation. However, it is sometimes very high in sulfur content. Johnson and Anderson (12) found that without calcination

the electrical conductivity of fluid petroleum coke is too low to permit significant resistive heating of the coke by conduction of an electric current even with the application of voltage gradients as high as 1000 volts per inch.

The range of conductivity which the solids in a fluidized bed can have in order to be suitable for an electrothermal fluidized bed is not critical but it is important. Obviously if the conductivity is too high there might not be enough resistance in a fluidized bed to control the current and a short circuit could result. If the conductivity is too low, the voltage required to supply sufficient power to obtain the bed temperature may be sufficient to cause continuous arcs between the electrodes. Arcs involve a breakdown in the gas and the formation of ions creating a conductive path through the gas. Arcs are objectionable in electrofluid beds in that they make it difficult to regulate the heating current and they disturb and upset the smooth operation of a fluidized bed by causing momentary local overheating.

Electrical Resistivity and Calcining of Carbon

Pinnick (25) describes the effect that calcining has on the electrical resistivity of petroleum coke. The term "carbon" includes a class of solids which are formed by heating organic compounds in the absence of air or in a reducing atmosphere to about $400^{\circ}C$. As the temperature is increased, polymerization occurs and regardless of whether the starting material was composed of long chain molecules or aromatic molecules, the

result of the polymerization is a system of cross-linked planar condensed benzene-ring molecules. Between 400°C. and 700°C. these condensed ring systems grow slowly, but all the peripheral carbon atoms are attached by chemical bonds to hydrogen atoms or hydrocarbon groups and therefore these substances are called condensed molecular solids. These substances have very high resistivities. During heat treatment in the temperature range of 700°C. to 800°C., large evolution of gases occurs which is due to the hydrogen and hydrocarbon groups being driven off from the periphery of the condensed ring system leaving small crystallites with a structure similar to graphite. Over the range of heat treatment from 500°C. to 800°C., coinciding with the range where the large evolution of gases occurs, the resistivity decreases from 10^{7} ohm-cm. to 10^{-2} ohm-cm. As heat treatment is increased from 800°C. to 2000°C., the crystallites grow gradually. The resistivity begins to level off and reaches a plateau between 1200°C. to 2000°C. at which time the resistivity is essentially constant. For heat treatment above 2000°C., the crystallites continue to grow and the planes begin to align into the regular graphitic structure until it all becomes polycrystalline graphite for heat treatment greater than 2500°C. At this point the electrical resistivity begins to decrease again, however, the decrease is much more gradual than during the early stage of heat treatment.

Mrozowski (26) and Pinnick (25) offer explanations based on principles of solid state physics for the behavior of resistivity and molecular structure.

Electrical Resistivity of Fixed Beds of Carbon

A considerable amount of work has been done on the electrical resistivity of carbon granules in fixed beds under pressures up to several thousand pounds per square inch and also in the freely heaped condition. This interest has been prompted by the great use of carbon granules in carbon microphones and in particular, the telephone transmitter. Walker and Rusinko (27) studied the resistivity of particulate carbons under pressures up to about 51,000 lb./sq.in. Moisture in the air was found to have a small but detectable effect on resistivity. An experimental procedure was recommended for determining the resistivity of carbon under pressure. Takahashi (28, 29) has investigated the resistivity of freely heaped carbon powders. However, he was unable to get good reproducibility of results and felt that his electrodes measuring the voltage drop were too close together and were affected unduly by the random arrangement of carbon granules.

Thus far there has been no really satisfactory measurement standard devised for determining the resistivity of carbon granules.

Contact resistance

Goucher (30) studied the effect of compressive forces on the contact resistance between two carbon granules. This investigation led to the view that carbon surfaces are submicroscopically rough and that both the number of surface projections in intimate contact between the two surfaces and the area of contact vary due to elastic deformations of the crystallites. Grisdale (31) determined that the force between two carbon

granules in the telephone transmitter averages only a few dynes, yet experiment and theory show the contact areas to be so small that only the hardest materials will support the stress without plastic deformation. The contact resistance between two carbon granules is confined largely to a minute volume of material directly beneath the contact interface since the two surfaces are in intimate contact over but a small fraction of the apparent contact area and, therefore, is critically dependent on the resistivity of the material in this region.

The orientation of carbon crystals has a bearing on the contact resistance because of the anisotropic properties of carbon. It has been found by several investigators (31, 32, 33) that the resistance to electric current flowing perpendicular to the basal plane of a crystal of natural graphite is 100 to 10,000 times as great as the resistance parallel to the basal plane. For example, Gopalaswamy et al. (34) stated the resistivity of graphite crystals in the direction parallel to the graphite plane is about 5×10^{-5} ohm-cm. while the resistivity in the transverse direction is of the order of 3 ohm-cm. or more.

The resistance of a bed of carbon granules is the sum of two parts--first, the resistance of the intergranular contacts themselves, and, second, the resistance of the carbon body acting in series with the contact resistance. Grisdale (31) found that for pyrolitic carbon having a resistivity of 1.0 to 1.8×10^{-3} ohm-cm. that the body resistance is small relative to the contact resistance for carbon thicknesses exceeding 0.00003 cm. Thus the contact resistance is dependent upon the resistivity

of the carbon and on the degree of orientation of the graphitic crystals in the surfaces.

Resistance of a single contact

Grisdale (31) discussed the properties of single carbon contacts and stated that when the force on a single carbon contact is held constant while the voltage across it is increased, the contact resistance is decreased; and, if the contact potential drop is not more than about two volts, the change is reversible. This decrease in resistance is the result of Joule heating of the contact.

The change in resistance of a carbon contact with change in applied voltage is reversible only if a certain critical voltage is not exceeded. The value of the critical voltage, in general, lies between 2 and 3 volts. If the voltage exceeds this value, large and random fluctuations in contact resistance arise; and, upon subsequent decrease of voltage, it is found that the contact resistance has permanently increased as much as fivefold from its initial value. This phenomenon has been termed "burning" and, since it is not observed when the contact is thoroughly degassed and sealed in a vacuum, it has been presumed that it is due to oxidation of the contact material. It has been determined that the theoretical voltage to cause "burning" for graphite crystals in a contact which are oriented with their basal planes perpendicular to the flow of current at the contact interface will reach a temperature sufficient to produce oxidation at 0.42 volt and those parallel at 2.94 volts. Experiments have shown that a "burning noise" associated with oxidation and the

resulting small fluctuations of resistance is first detectable in a range from 0.4 to 0.5 volts. The noise and resistance fluctuations increase greatly as the potential drop is increased to about 3 volts.

Effect of particle size, ash content, surface films

Benson et al. (35) found that for a given volume of particles, as the particle size increases, the resistance decreases. This is reasonable since the total number of individual contact resistances would be fewer between electrodes for the large particles. Joglekar et al. (36) and Gopalaswamy et al. (34) have studied the resistance of petroleum coke, retort carbon and graphite powders and made the same observation. They also found that the resistivity increases with ash content and that surface films such as oil will increase the resistivity.

Resistivity of Fluidized Beds of Carbon

Mechanism of current flow

Goldschmidt and Le Goff (37) studied the possible mechanisms by which electric current could pass through a fluidized bed. They concluded that three possible mechanisms were:

1. A diffusion of charge between colliding particles to give a current flow.
2. A conducting system of chains of particles which would allow current flow.
3. Arcing between particles.

The third mechanism was avoided by operating at voltages below that at

which arcing would occur. The first mechanism was ruled out when the calculated resistivity by diffusion of charge was 10^7 times greater than the actual measured value. Therefore, the conclusion was that the current flows by conducting paths through chains of particles if arcing is not present. In a study of the electrical resistance of fluidized bed of coke and graphite, Graham and Harvey (38) also concluded that the most probable mechanism for conduction of electric current in a fluidized bed of conducting particles was along chains of touching particles.

Some studies of fluidized bed resistivity

Recently some investigators have made studies of fluidized beds of carbon materials which have involved some of the electrical properties of the fluidized bed. Johnson (19) determined that Ohm's law applied to the fluidized bed until applied voltages became great enough to cause arcing at which time the current-voltages relationship becomes non-linear. Hayakawa et al. (39) used a resistance probe for determining the rate of mixing of conducting and non-conducting solids in a fluidized bed, but local resistances were determined rather than the resistance of the entire bed. Graham and Harvey (40) determined that there is a trend to higher resistivity as the size of the particles in a bed is decreased. They determined that the net effect of bubbles in a fluidized bed was to decrease the resistivity. It was also found that as the gas velocity reached the incipient or minimum fluidizing velocity that the resistance of the bed increased rapidly until it reached a peak and then decreased slowly with further increase of gas velocity. This decrease in resistivity was thought to be due to the effect of the bubbles causing an

increased particle aggregate density.

Goldschmidt (41) used a resistance probe to study the mechanism of bubbles in a fluidized bed and determined the fraction of volume of the bed occupied by the bubbles, the distribution of bubble sizes and the velocity of the bubbles as a function of their diameter.

Reed and Goldberger (42) made a study to determine if the basic resistivity relationship

$$R = \frac{\rho L}{A} \tag{1}$$

where R = resistance, ohms

ρ = resistivity, ohm-cm.

L = length of current path, cm.

A = cross-sectional area of current path, sq.in.

would hold true for a fluidized bed. This relationship appeared to be valid since the resistance of a conductive fluidized bed was found to increase linearly with current path and decrease linearly with the reciprocal of cross-sectional area for current travel. A generalized graphical correlation of resistivity was also determined which was a plot of resistivity against the ratio of the gas flow rate to the incipient or minimum fluidizing gas flow rate. However, this correlation would only hold for their particular column size, bed height and bed material.

Graham and Harvey (43) have investigated the resistivity of fluidized beds of coke and graphite at temperatures up to 1200^{o}C. and found that for

A given gas flow rate, the resistivity of a coke bed decreased with temperature, reached a minimum at about 600°C. and then increased. Whereas the resistivity of the graphite bed decreased until the temperature was about 600°C. and then remained constant. The explanation offered for this was that the higher resistivity of the coke was accompanied by higher supply voltages with arcing occurring at about 600°C. Further voltage increases only increased the amount of energy dissipated in arcs but had little influence on the current to the bed. The over-all result was an increase in apparent bed resistivity when voltages were increased above the value for producing the 600°C. temperature.

EQUIPMENT AND PROCEDURE

Description of Equipment and Apparatus

In general, the apparatus used in this investigation consisted of a fluidized bed column; a means for supplying, drying and filtering the gas in a closed loop system; a gas storage tank; and the necessary instrumentation for measuring gas flow rates, voltages and currents in the test section.

Flow diagram

By referring to Figure 1, which is a schematic diagram of the apparatus, the gas flow through the system can be followed beginning at the compressor. Gas from the storage tank was compressed to about 10 lb./sq.-in.gage by a model 2065-P9 Gast rotary vane-type compressor. The gas then passed through a felt element oil trap and then through a finned tube heat exchanger which had sufficient cooling capacity to remove the heat of compression so that the gas entered the drier at essentially room temperature. The drier used was a refrigeration type drier containing two silica gel cartridges as the desiccant.

The finned tube heat exchanger was not in the original design but was found necessary when the dew point temperature of the circulated gas was not constant. It was determined that after a period of operation the silica gel was reaching a temperature at which it would no longer adsorb water but was releasing part of the adsorbed water vapor to the gas stream. Nitrogen was received from a supply cylinder at a dew point of

Figure 1. Schematic diagram of the fluidized bed apparatus

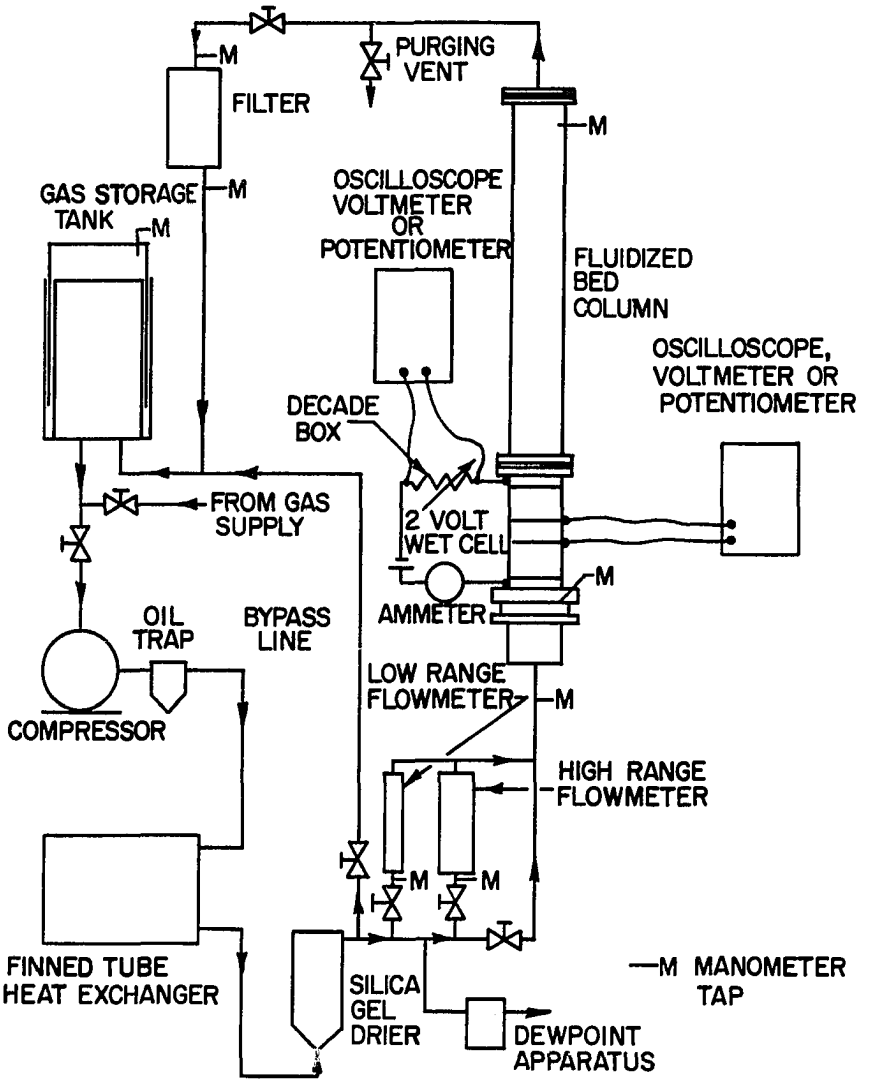
M
PURGING VENT
FILTER
M
GAS STORAGE TANK
M
M
OSCILLOSCOPE VOLTMETER OR POTENTIOMETER
FLUIDIZED BED COLUMN
OSCILLOSCOPE, VOLTMETER OR POTENTIOMETER
DECADE BOX
FROM GAS SUPPLY
2 VOLT WET CELL
M
AMMETER
OIL TRAP
BYPASS LINE
LOW RANGE FLOWMETER
M
COMPRESSOR
HIGH RANGE FLOWMETER
M
M
FINNED TUBE HEAT EXCHANGER
SILICA GEL DRIER
DEWPOINT APPARATUS
—M MANOMETER TAP

about -54°C. but after the circulation system had been operating for 15 to 30 min. the dew point of the gas in the system would be up to about -10°C. With the finned tube heat exchanger in the line so that the drier remained at about room temperature, it was possible to maintain operating dew point temperatures between -45°C. and -50°C. Occasionally it was necessary to remove the cartridges and replace them with cartridges that had been regenerated. The regeneration procedure was to place the cartridges in an oven at about 300°F. for a total period of 4 hr. At about 1 hr. intervals the cartridges were removed from the oven and dry gas blown through them to remove the water vapor. The source of moisture was from the atmosphere or the bed materials. Moisture would get into the system when the bed materials were changed, were added to, or when the columns were changed. Any water vapor not removed by a purging operation would be adsorbed by the drier.

Following the drier was a by-pass line. Since the compressor was of the positive displacement type, the by-pass line was used to return to the gas storage tank excess gas not used in fluidizing the bed. Gas flowing to the column passed through either one of two flow meters. The high range flow meter was a Brooks Rotameter, Type 1110, with a R-8M-25-2 tube having a range of 0.2 to 2.4 std.cu.ft./min. of air at 70°F. and 14.7 lb./sq.in.abs. The low range flow meter was a Brooks Rotameter, Type 1110, with a 4-15-2 tube having a range of 0.03 to 0.28 std.cu.ft./min. of air. Manometer taps at the entrance to each of the rotameters allowed pressure readings to be taken so as to determine the density of the gas flowing through the rotameters.

Dew point temperatures of the gas being circulated could be taken with a dew point apparatus manufactured by the Pittsburgh Lectrodryer Division of McGraw Edison Company. Acetone and dry ice were used to lower the temperature of a polished cup on which a sample of gas impinged. The acetone mixture was stirred with a thermometer and the dew point was read when the frost first appeared on the outside of the cup.

From the flow meters the gas entered the base of the fluidized bed column and passed through a porous plate diffuser. The diffuser was a Norton Alundum P-2120 (standard fine) disc, 1 in. thick by $4\frac{1}{2}$ in. in diameter. A P-260 (standard medium) and a P-236 (standard course) porous disc were also tried, but the best fluidization was obtained with the fine disc. In order to prevent gas leakage around the periphery of the porous plate, it was placed within a 5 in. inside diameter steel ring, and Devcon Flexane, a flexible urethane casting material, was poured in the space between the plate and the steel ring. A mold release agent was applied to the steel ring so that the plate could be removed and different porous plates could be used in the same steel ring. Since the urethane adhered to the porous plate, it gave an excellent seal around the periphery of the plate. Rubber gaskets were placed on both sides of the porous plate between the flanges to give a good seal there.

Manometer taps were placed at the base of the bed (near the top side of the porous plate) and near the top of the column for the purpose of measuring the pressure drop across the bed.

A front view of the apparatus is shown in Figure 2. In this picture

Figure 2. Photograph showing the front view of the fluidized bed apparatus

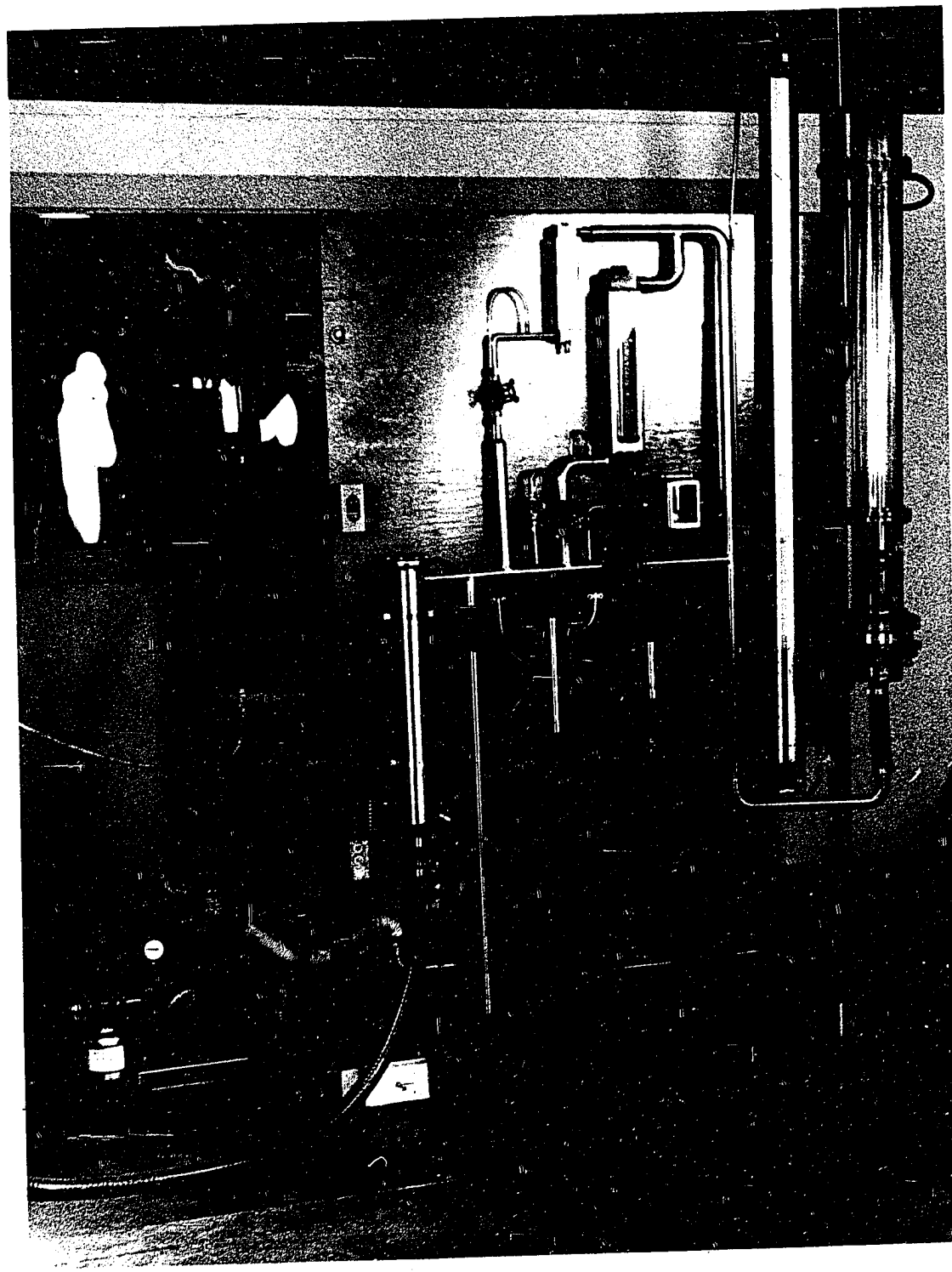

can be seen the relative locations of the compressor, drier, flow meters, dew point apparatus and column. The gas supply cylinder and finned tube heat exchanger were out of view to the left. The bottom portion of the gas storage tank is visible behind the panel.

After leaving the column, the gas passed through a Pall Trinity Micro Corporation filter, model MCC 1001 EC 16, having a pleated paper filter element. The purpose of this filter was to remove from the gas stream any dust or bed materials which might be elutriated from the bed. Manometer taps were placed at the entrance and exit of the filter to determine if and when the filter was becoming plugged. The gas then proceeded to the storage tank which supplied the compressor. In Figure 3 can be seen the gas storage tank and just above it is the filter.

Nitrogen or helium was added to the gas storage tank from cylinders. The storage tank was built locally according to design specifications. The pressure of gas in the tank was maintained at a pressure of 1 to 2 in. of water above atmospheric pressure by counter-weighting the floating head. A manometer manifold was connected to a tap in the floating head to measure the pressure within the tank.

Instrumentation

The method used in measuring resistance in this investigation was the four terminal method described by Silsbee (44, 45). The reason for using this method is that it allows the resistance of a material to be measured independently of any contact resistance. Referring to Figure 4, the principle of this method is to have two current terminals of comparatively

Figure 3. Photograph showing the rear view of the fluidized bed apparatus

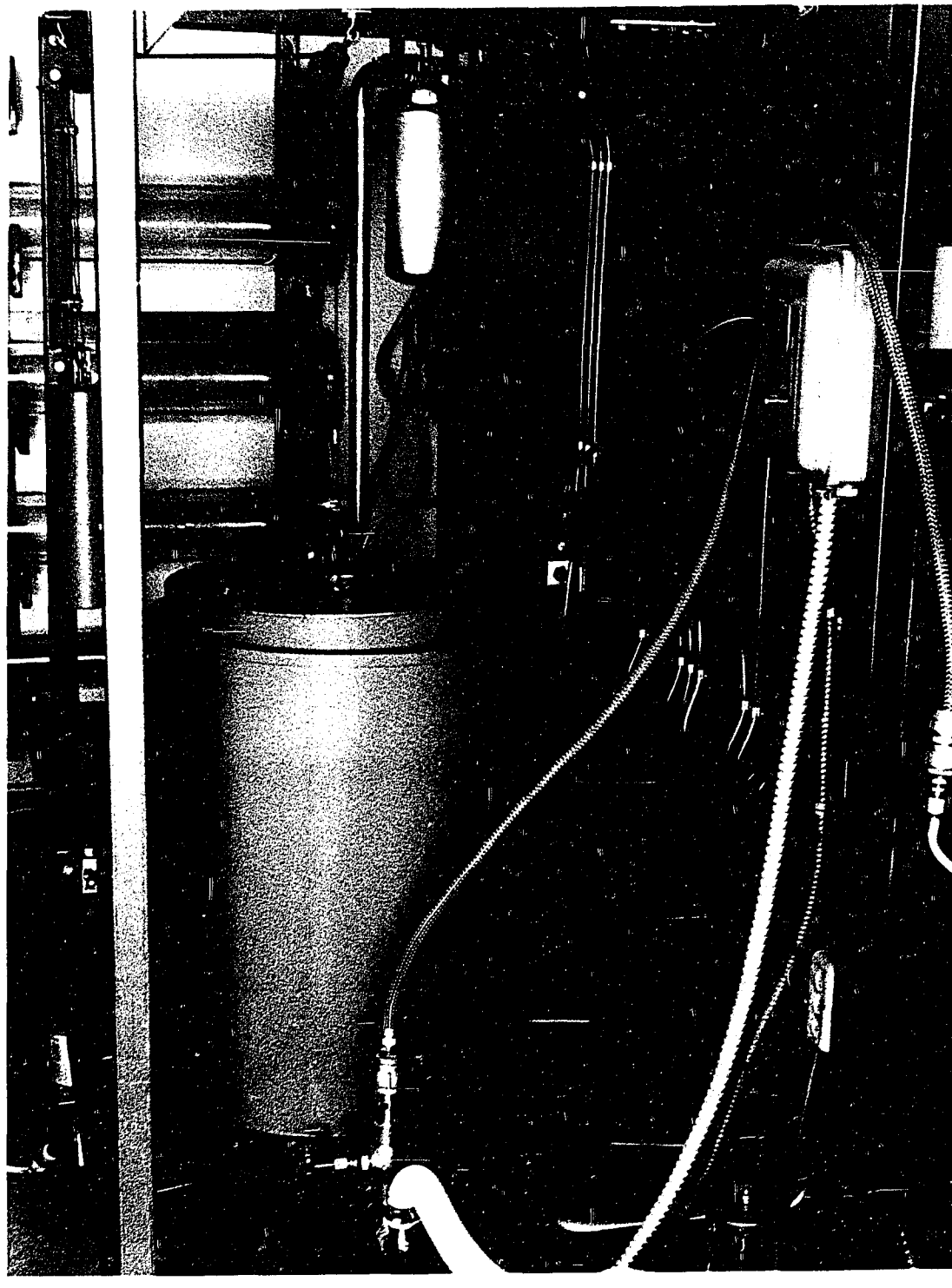

Figure 4. Schematic diagram of the four terminal method of resistance measurement

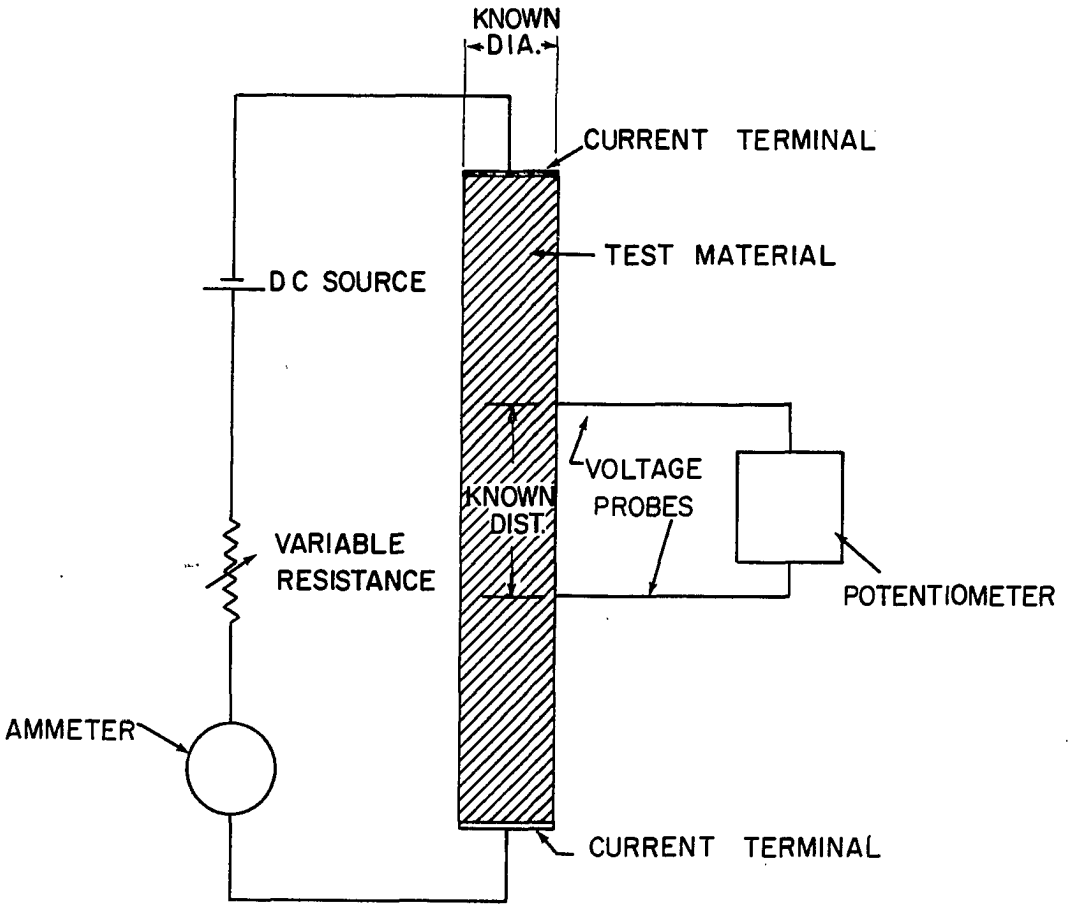
KNOWN
DIA.
CURRENT TERMINAL
TEST MATERIAL
DC SOURCE
VOLTAGE
PROBES
KNOWN
DIST.
VARIABLE
RESISTANCE
POTENTIOMETER
AMMETER
CURRENT TERMINAL

massive construction which are intended to carry the current to be measured, while the other pair of terminals, the potential terminals, are smaller and are intended to be connected to some apparatus for measuring a difference in potential. In this investigation, the potential terminals were two size 12 "bead" needles measuring 2 1/8 in. in length and 0.019 in. in diameter. Two of these needles were used as probes by inserting them through holes in the wall of the column. These holes were drilled perpendicular to the axis of the bed.

Settled bed resistivity Two different instrument arrangements were used depending upon whether the resistance of a settled bed or a fluidized bed was being measured. In the case of a settled bed, the potential drop across the probes was determined by using either a Leeds and Northrup model 8686 millivolt potentiometer having a range of 100.00 millivolts or a Hewlett-Packard model 425-A Microvolt-Ammeter having a range from 10 microvolts to 1 volt with an input imedance of 1 megohm. The variable resistance (decade resistance box) was used to keep the voltage drop across the probes within the limits of range of the potentiometer. The value of current was determined with the ammeter which was a Hewlett-Packard model 410-C electronic Voltmeter having a range of 1.5 microamps to 150 milliamps. Figure 5 shows the electrical circuit used in determining the resistivity of the settled bed.

Fluidized bed resistivity In the case of the fluidized bed, the potential drop across the probes was measured with a Tektronix model 502 dual beam oscilloscope with a Du Mont type 450 oscilloscope record camera.

Figure 5. Schematic diagram of electrical circuitry used for measuring the settled bed resistivity

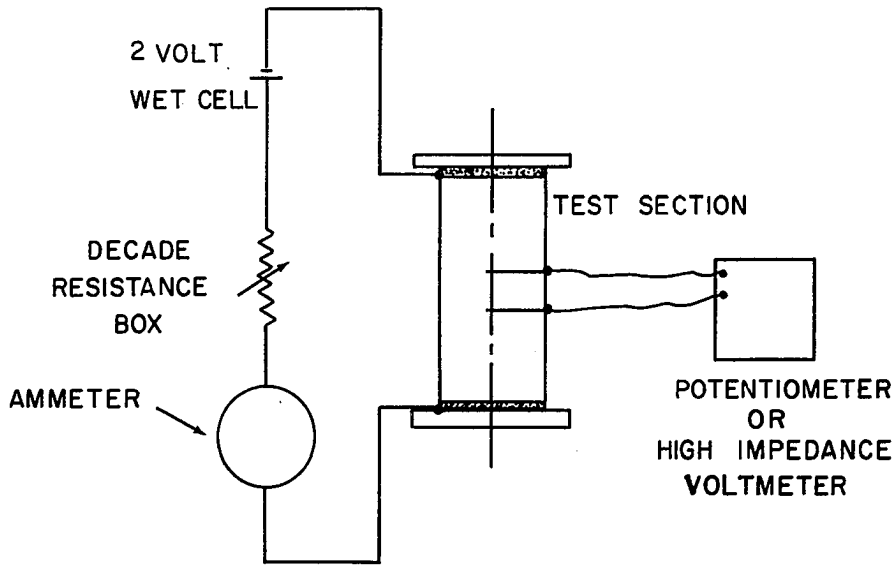
2 VOLT
WET CELL
DECADE
RESISTANCE
BOX
AMMETER
TEST SECTION
POTENTIOMETER
OR
HIGH IMPEDANCE
VOLTMETER

The decade resistance box was a Leeds and Northrup model 4776 decade box having a range of 0.1 to 999.99 ohms. By measuring the voltage drop across the known resistance of the decade box it was possible to calculate the current flowing in the bed circuit. The voltage drop across the decade box and the voltage drop across the potential probes were both measured simultaneously by the dual beam oscilloscope. The upper beam was used to measure the probe voltage drop and the lower beam the decade box voltage drop. Pictures of the simultaneous voltages were then taken with the scope camera, and the average values of the voltage readings taken from the pictures. Figure 6 shows a schematic of the electrical circuitry for measuring the fluidized bed resistivity. A typical oscilloscope picture is shown in Figure 7. The uppermost trace represents the variation in direct current voltage drop across the probes during a 5 sec. period. The center trace is the zero position for both the upper and lower beams. The lowest trace is the variation of direct current voltage drop across the decade resistance box. The average of each trace was estimated and a straight line drawn in at that position. The magnitude of the average voltage was determined from the distance between the line and the zero trace. In Figure 7, the ordinate for the upper trace had a scale of 200 millivolts per division, while that of the lower trace had a scale of 50 millivolts per division. The scale of the abscissa was 0.5 sec. per division.

Peak fluidized bed resistivity Shown in Figure 8 is the arrangement of instrumentation for the measurement of resistivity. The two channel Brush oscillograph shown in the picture was used to locate the

Figure 6. Schematic diagram of electrical circuitry used for measuring the fluidized bed resistivity

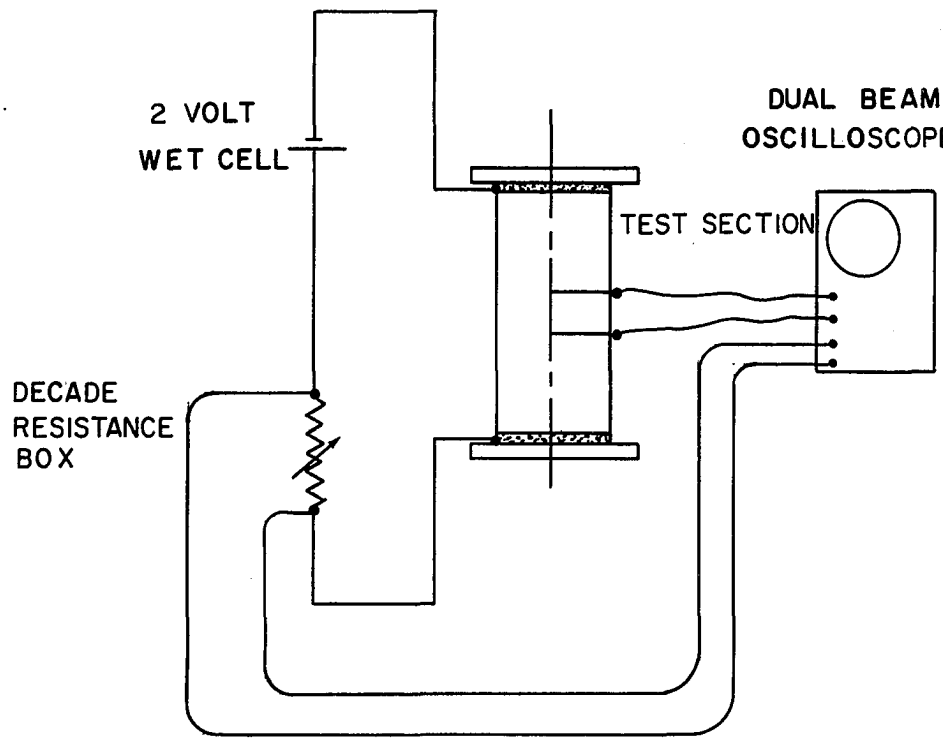
2 VOLT
WET CELL
DUAL BEAM
OSCILLOSCOPE
TEST SECTION
DECADE
RESISTANCE
BOX

Figure 7. A typical oscilloscope trace of voltages during fluidization of the bed

Upper trace -- voltage drop across the potential probes

Center trace -- zero position of both beams

Lower trace -- voltage drop across decade resistance box from which the bed current was calculated

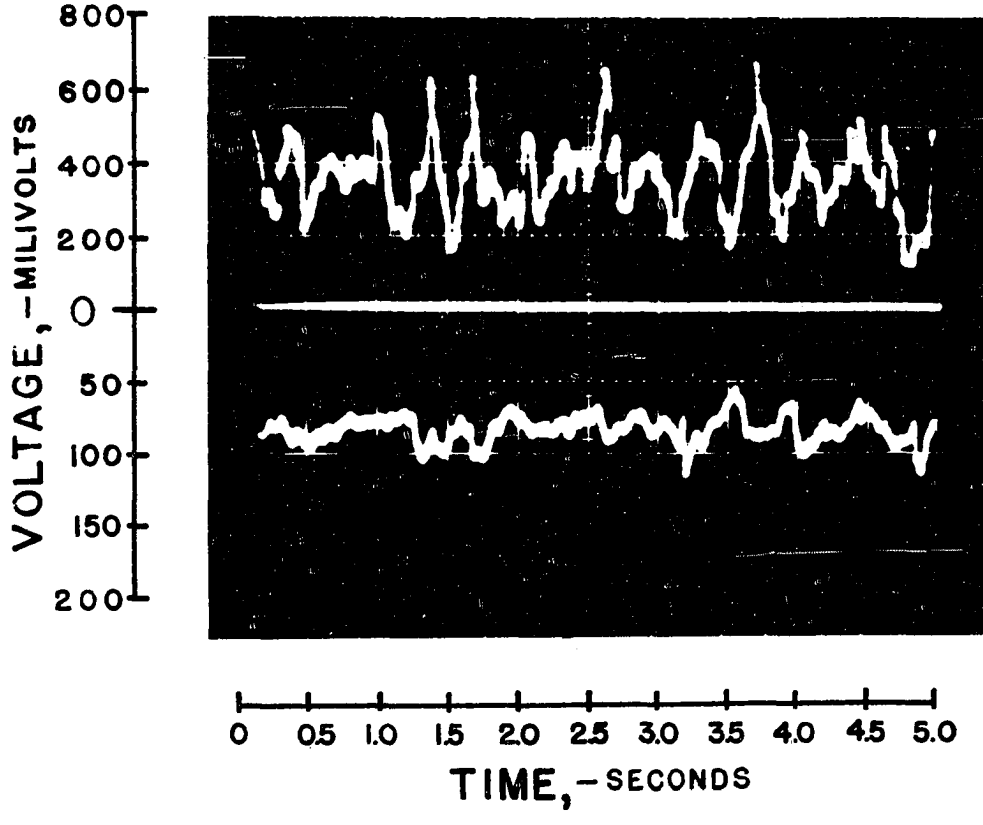
800
600
400
200
0
50
100
150
200
VOLTAGE, - MILIVOLTS
0
0.5
1.0
1.5
2.0
2.5
3.0
3.5
4.0
4.5
5.0
TIME, - SECONDS

Figure 8. Photograph showing the arrangement of instrumentation

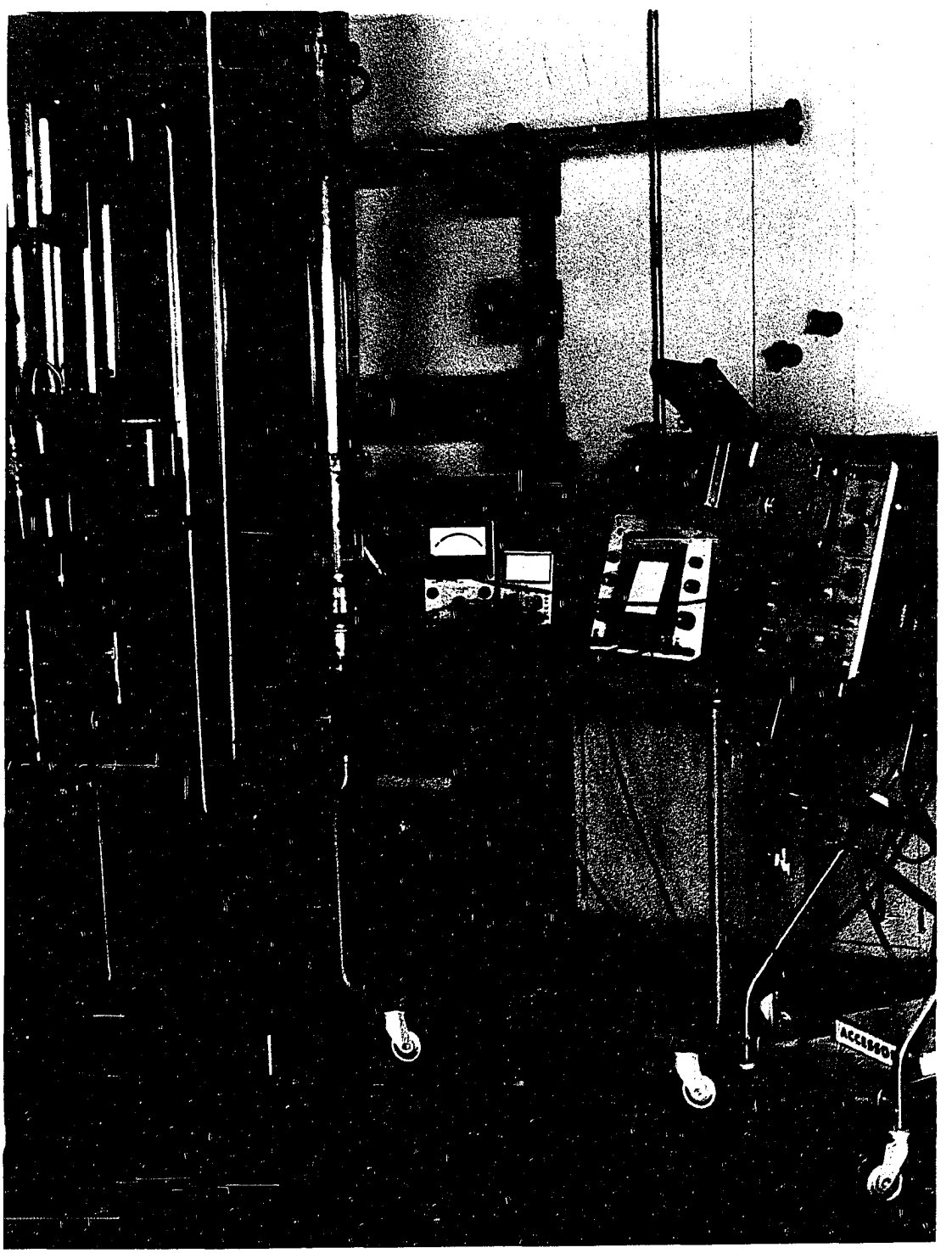

flow rate at which the peak resistivity occurred. By slowly increasing the flow rate in small increments and watching the bed current and probe potential drop history, it was possible to locate very closely the point of peak resistivity.

Voltage source

The voltage source for the resistance measuring circuit was one cell of a six volt storage battery. All resistance readings were taken using direct current. However, as a matter of interest the direct current power source was replaced by a Variac transformer and the wave form observed on the oscilloscope while the bed was fluidized. Figure 9 shows the amplitude modulating effect of the bed resistance on the probe voltage. The upper trace is the voltage applied across the current terminals with the ordinate scale of 10 volts per division. The lower trace is the voltage drop across the probes. The ordinate scale is 1 volt per division. The abscissa is sweep time and is 0.1 sec. per division or a total sweep time of 1 sec.

Test sections

Details of the two and four inch fluidized bed test sections are shown in Figures 10 and 11 respectively. The voltage probes were located $1\frac{1}{2}$ in. apart in the midsection between the current terminals. Since carbon granules are extremely sensitive to pressure, the amount of material above the probes would influence the measured resistance. In order to have meaningful and consistent results, the upper surface of the settled bed was maintained at constant heights above the upper potential

Figure 9. An oscilloscope trace when 60 cycle/sec. alternating current is applied to a fluidized bed

Upper trace -- voltage applied across the current terminals

Lower trace -- voltage drop across the potential probes

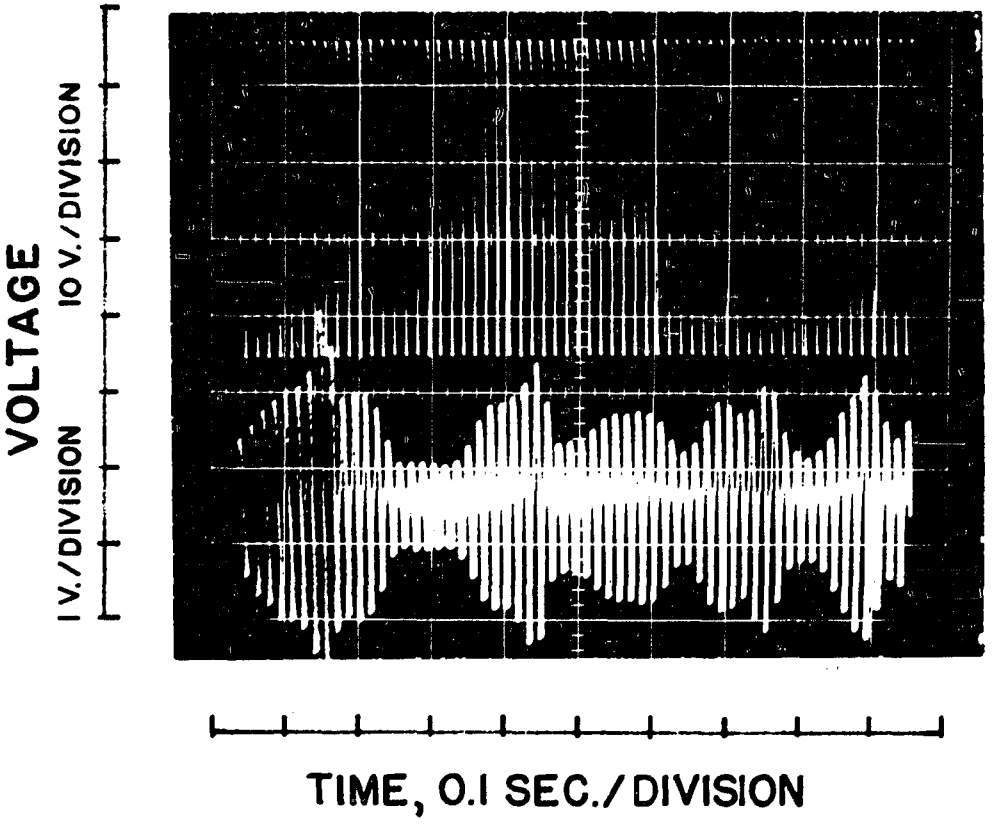
VOLTAGE
10 V./DIVISION
1 V./DIVISION
TIME, 0.1 SEC./DIVISION

Figure 10. Detailed drawing of the two inch fluidized bed test section

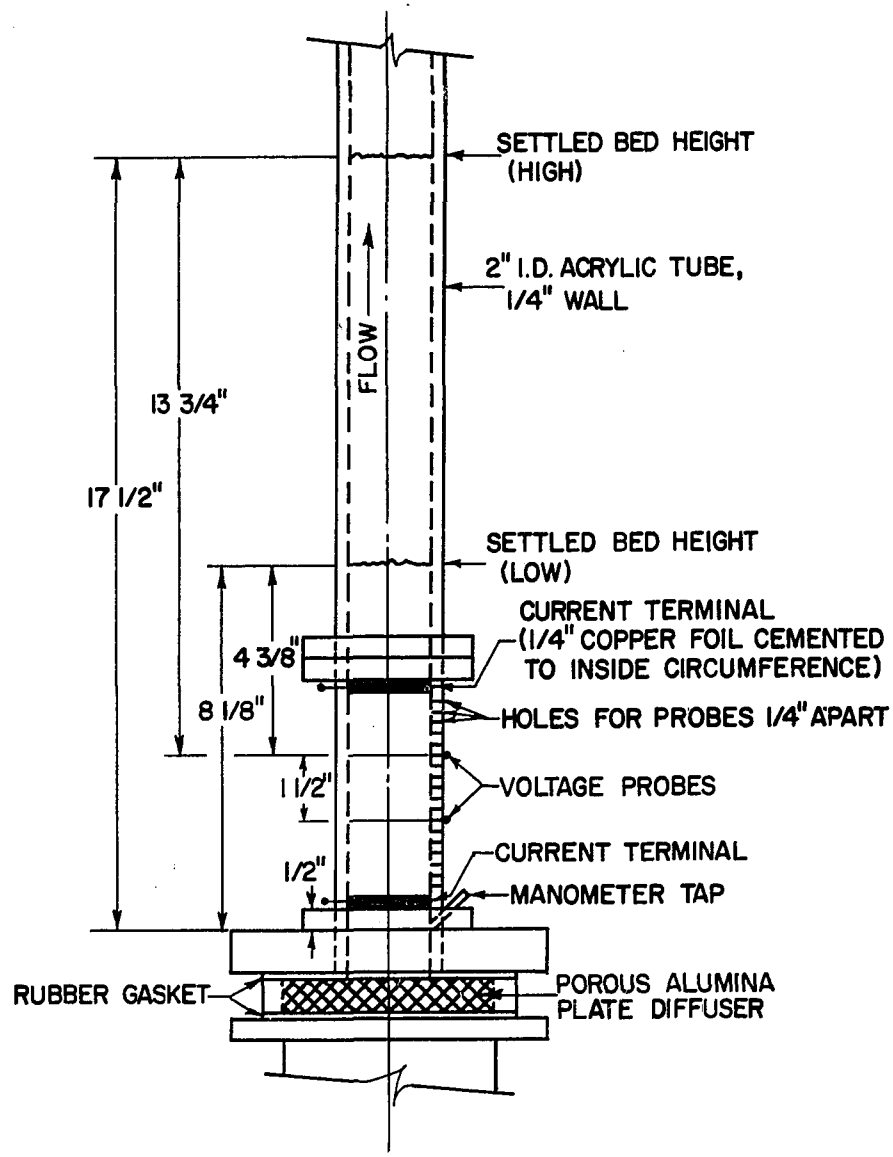
SETTLED BED HEIGHT
(HIGH)
2" I.D. ACRYLIC TUBE,
1/4" WALL
FLOW
13 3/4"
17 1/2"
SETTLED BED HEIGHT
(LOW)
CURRENT TERMINAL
(1/4" COPPER FOIL CEMENTED
TO INSIDE CIRCUMFERENCE)
4 3/8"
8 1/8"
HOLES FOR PROBES 1/4" APART
1 1/2"
VOLTAGE PROBES
1/2"
CURRENT TERMINAL
MANOMETER TAP
RUBBER GASKET
POROUS ALUMINA
PLATE DIFFUSER

Figure 11. Detailed drawing of the four inch fluidized bed test section

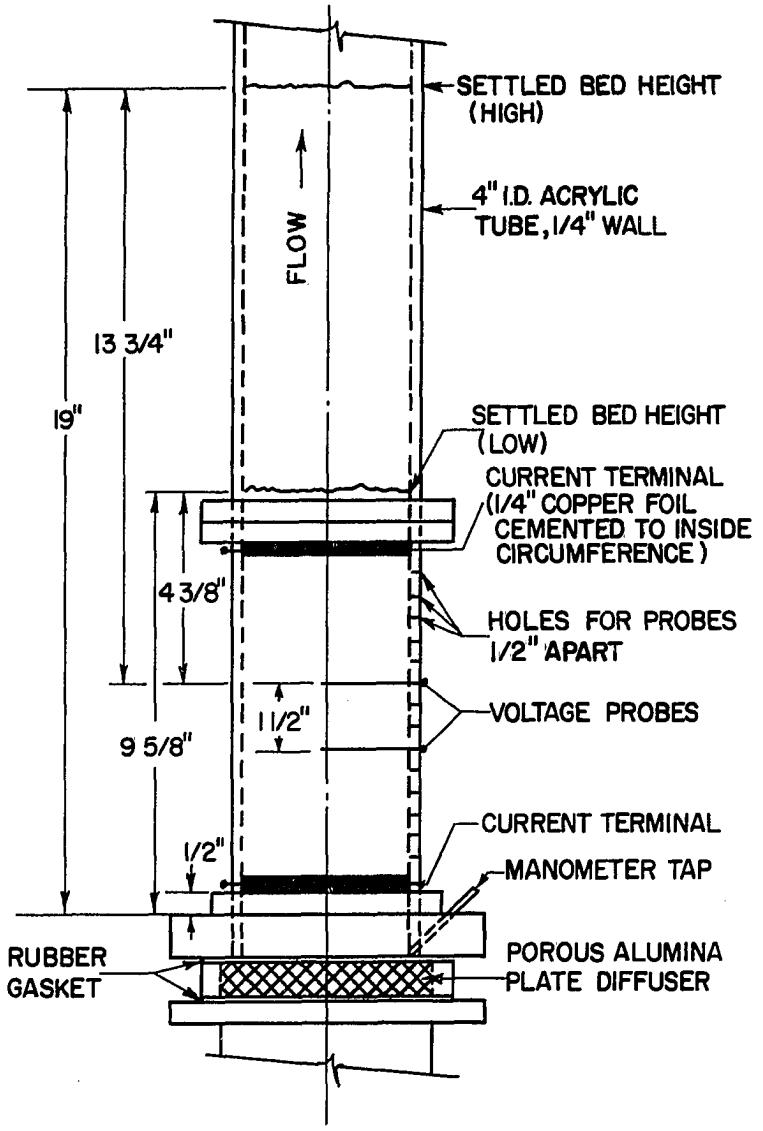
SETTLED BED HEIGHT
(HIGH)
4" I.D. ACRYLIC
TUBE, 1/4" WALL
FLOW
13 3/4"
19"
SETTLED BED HEIGHT
(LOW)
CURRENT TERMINAL
(1/4" COPPER FOIL
CEMENTED TO INSIDE
CIRCUMFERENCE)
4 3/8"
HOLES FOR PROBES
1/2" APART
1 1/2"
VOLTAGE PROBES
9 5/8"
CURRENT TERMINAL
1/2"
MANOMETER TAP
RUBBER
GASKET
POROUS ALUMINA
PLATE DIFFUSER

probe. Two different bed heights were used during this investigation. The low bed height was 4 3/8 in. above the upper probe and the high bed height was 13 3/4 in. above the probe. Figure 12 shows a close-up view of the four inch test section with its electrical connections.

In the original construction of the test sections, the current terminals were $\frac{1}{4}$ inch wide strips of aluminum foil which were cemented to the inside surface of the acrylic tube using rubber cement. Copper wires were then connected to the aluminum foil from outside of the tube through holes in the tube wall. The end of the copper wire was flattened with a hammer and the connection with the foil made secure using a thick, silver-filled paint which is commonly used in electronic circuitry. After experiencing considerable difficulty with erratic readings, it was determined that the oxide surface coating of the aluminum foil had an extremely high resistance and was causing the difficulty. The aluminum foil was then replaced by copper foil and this eliminated the problem.

Before deciding on the type of current terminal to use, a study was made of the current field that one could expect in a cylinder with current entering and leaving through rings at the ends of the cylinder. Figure 13 shows the instrumentation for a two dimensional analog study using conductive paper with a Sunshine Scientific Instrument Company Analog Field Plotter. Figure 14 shows lines of constant potential between points in the bed and the current terminal. Lines of constant current flux would be perpendicular to the lines of constant potential. From this analog, it appeared that in the center portion of the bed the lines of constant

Figure 12. Close-up photograph of the four inch fluidized bed test section

Figure 13. Photograph of the Sunshine Scientific Instrument Company Analog Field Plotter used in the two dimensional analog study of a conducting bed

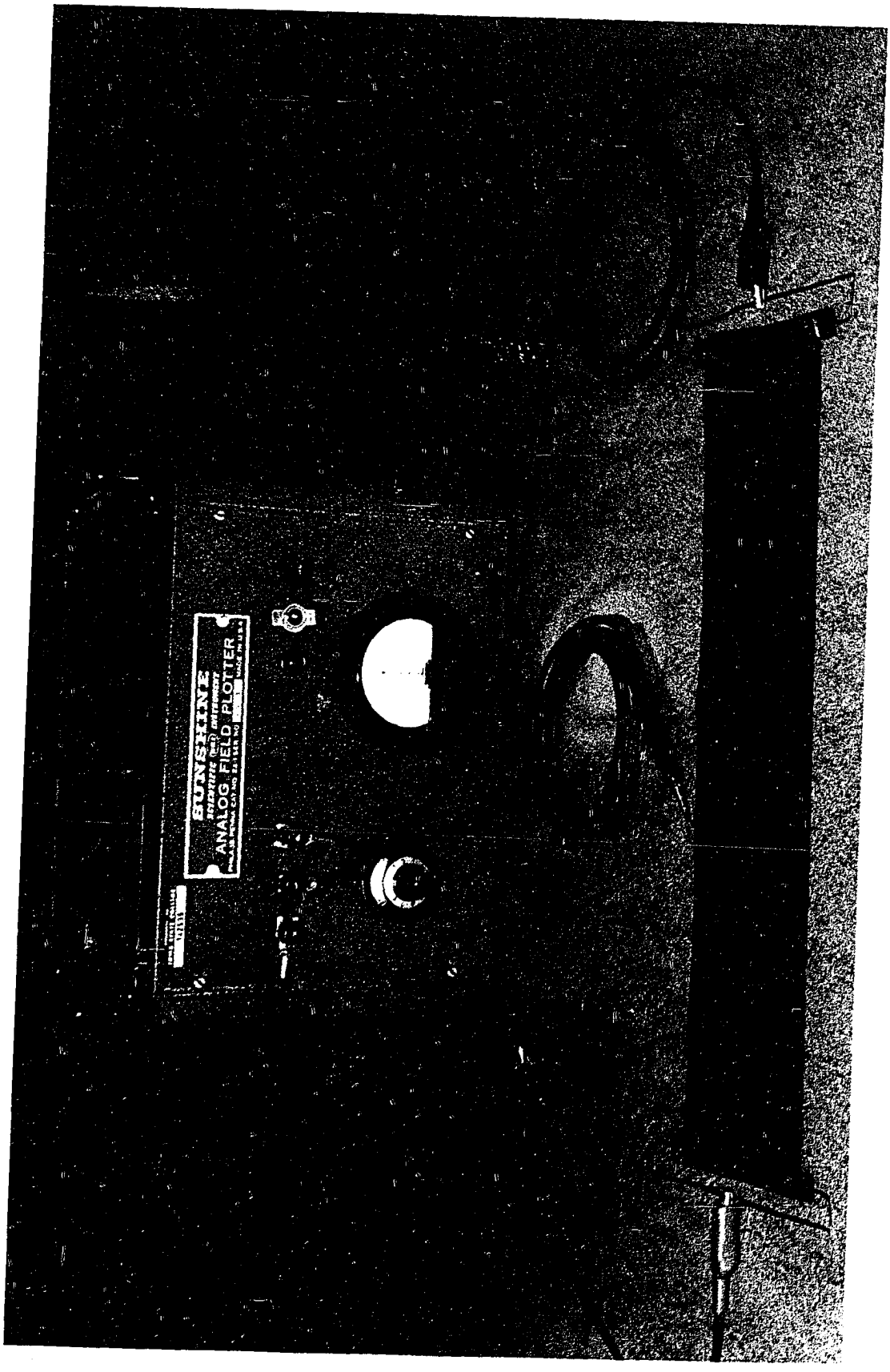
SUNSHINE
ANALOG FIELD PLOTTER

Figure 14. Close-up photograph of conducting paper used in the two dimensional analog study showing lines of constant voltage potential

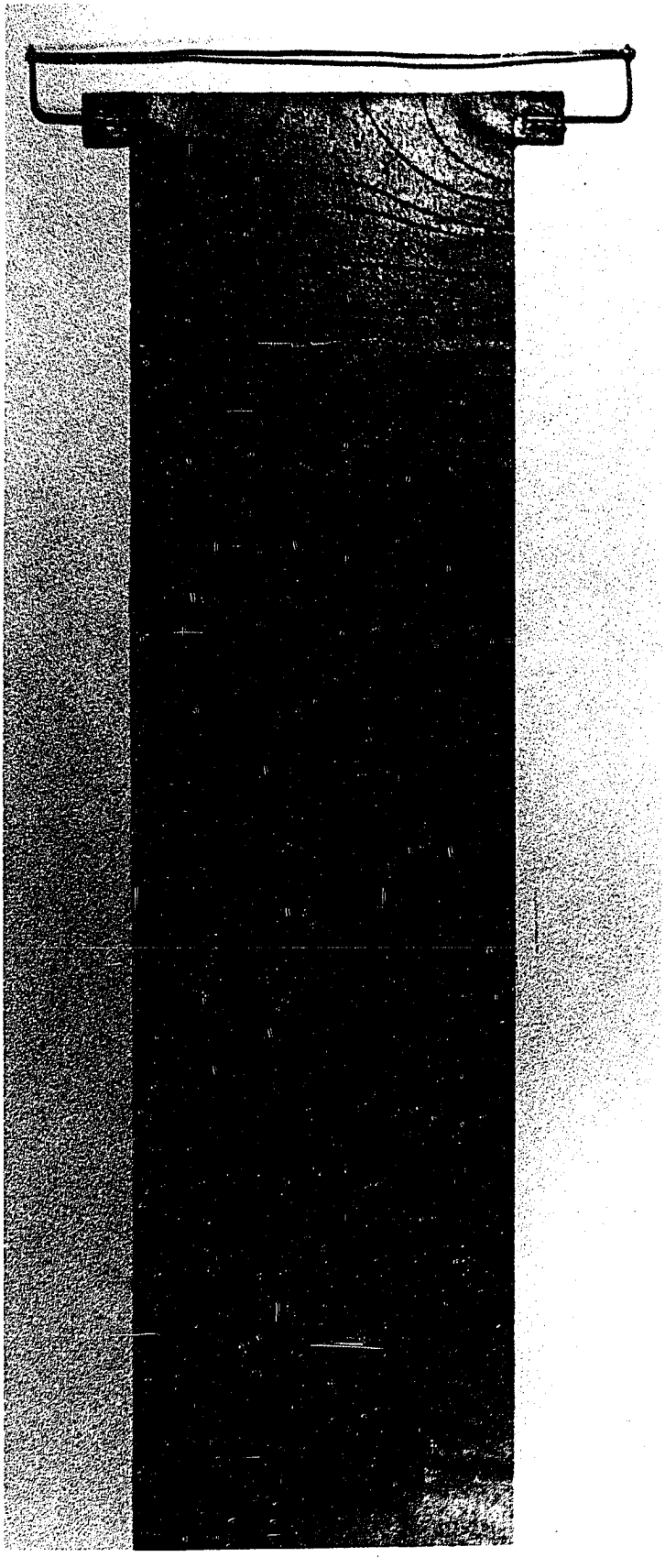

potential would be perpendicular to the axis of the bed, and the current flux would be evenly distributed across the bed.

In order to compare the analog and the actual bed, a point probe was made by plastic coating a steel needle except for a 1/16 in. tip. However, the high contact resistance between the small area of the needle tip and the carbon granules gave erratic readings. This difficulty was overcome by increasing the uninsulated length of the tip to 1/8 in. and copper plating the tip. The point probe was inserted into the bed at different heights and different radial positions and the potential drop measured between the probe and the upper current terminal. This technique was similar to that used by the Analog Field Plotter. The potential drops were found to be constant in a radial direction across the bed in the center portion of the column but near the ends there was considerable variation as was to be expected. It was determined that the center 4 in. of the two inch diameter column would be well within the limits of that portion of the bed having lines of constant potential which were perpendicular to the axis of the bed.

Fluidized bed materials

Three different materials were used during the course of this investigation. A graphite material was purchased from National Carbon Company, Division of Union Carbide Corporation, as catalog number GP BB-6 P4 Electric Furnace Graphite Powder. Specifications were as follows:

> Guaranteed specifications: A minimum of 75 per cent will pass through an 8 mesh screen and be retained on a 20 mesh.

Typical sieve analysis:

Per cent retained on	8 mesh	1 per cent
	10	14
	20	65
	35	18
	65	1
	pan	1

A calcined coke was also purchased from National Carbon Company as catalog number W 8306 Calcined Coke Particles. Specifications were:

Ash: approximately 1.25 per cent or less

Volatile at 1000°C.: negligible

Typical sieve analysis:

Per cent retained on	10 mesh	6 per cent
	20	84
	35	8
	65	2

Humble Oil and Refining Company of Billings, Montana, furnished fluid petroleum coke. Typical specifications were:

Sieve analysis:

Per cent retained on	10 mesh	2 per cent
	48	23
	65	25
	100	25
	200	23
	pan	2

Particle density, gr./cu.cm.	1.3
Bulk density, lb./cu.ft.	61
Calorific value, BTU/lb. (ASTM D-271)	14,100

Proximate Analysis, Weight per cent (ASTM D-271)

Moisture	0.3
Volatile matter	6
Fixed carbon	93.4
Ash	0.3

Ultimate analysis, weight per cent (ASTM D-271)

Carbon	91
Hydrogen	2
Sulfur	5.5

Metals:	Weight per cent on coke
Nickel	0.013
Vanadium	0.034
Iron	less than 0.01
Calcium	less than 0.01
Silicon	less than 0.005
Titanium	less than 0.001
Sodium	less than 0.02

It was found that the resistivity of the petroleum coke was so high that it was not suitable for resistivity tests without a calcining treatment and was not used. All bed materials were crushed and ground using a roll mill and a burr mill and then screened using a set of 8 in. diameter, half height, brass Tyler testing screen sieves in either a Tyler Ro-tap shaker or a Tyler RX-8 portable shaker.

Eight major tests were made during this investigation. A description of materials used in these tests is as follows:

Run A petroleum coke, -65/+250 mesh, fluidized 33 hr.

Run B graphite, -65/+250 mesh, fluidized 72 hr.

Run C calcined coke, -65/250 mesh, fluidized 304 hr.

Run D calcined coke, individual size fractions, -65/+80, -80/+100, -100/+115, -115/+150, -150/+170, -170/+200, -200/+250, fluidized 89 hr.

Run E calcined coke, mixed fractions, -65/+100, -65/+115, -65/+150, -65/+170, -65/+200, -65/+250, -65/+270, -65/+325, -65/+400, (same material as used in Run D), fluidized 89 hr.

Run F graphite, -65/+80, -80/+100, -65/+100, only fluidized for sufficient time to remove fines.

Procedure

Purging the system

Purging the system was accomplished by closing the valve ahead of the filter and opening the purging vent valve in the line just upstream from the filter valve. Whenever the column was opened or material added to the bed, the column could be purged to remove air and moisture. In order to change the gas in the entire system, the procedure followed was to vent as much gas as could be pumped out; fill the storage tank with the new gas; and again vent the system until the storage tank was empty. A gas analysis was made to determine the number of purgings necessary in changing from one gas to another. The gas analysis was begun with the system initially full of helium. Samples of the system gas were taken after repeated venting and filling with nitrogen. The volume per cent helium remaining in the system gas was determined using a gas chromatograph. It was found after six purgings that 0.1 per cent helium remained and after seven purgings only 0.06 per cent helium remained. It was decided to use six purgings in changing gases. Figure 15 shows the volume per cent of helium remaining after each purging in a series of purgings.

Calibration of rotameters

The low range flow meter was calibrated with both nitrogen and helium using a Sargent Wet Test Meter having a capacity of 20 cu.ft./hr. The high range flow meter was also calibrated with both nitrogen and helium but it was calibrated using the gas storage tank. In calibrating by means of the gas storage tank it was first necessary to accurately determine the

Figure 15. Graph showing the volume per cent helium remaining in the fluidized bed system after each of a series of purgings with nitrogen

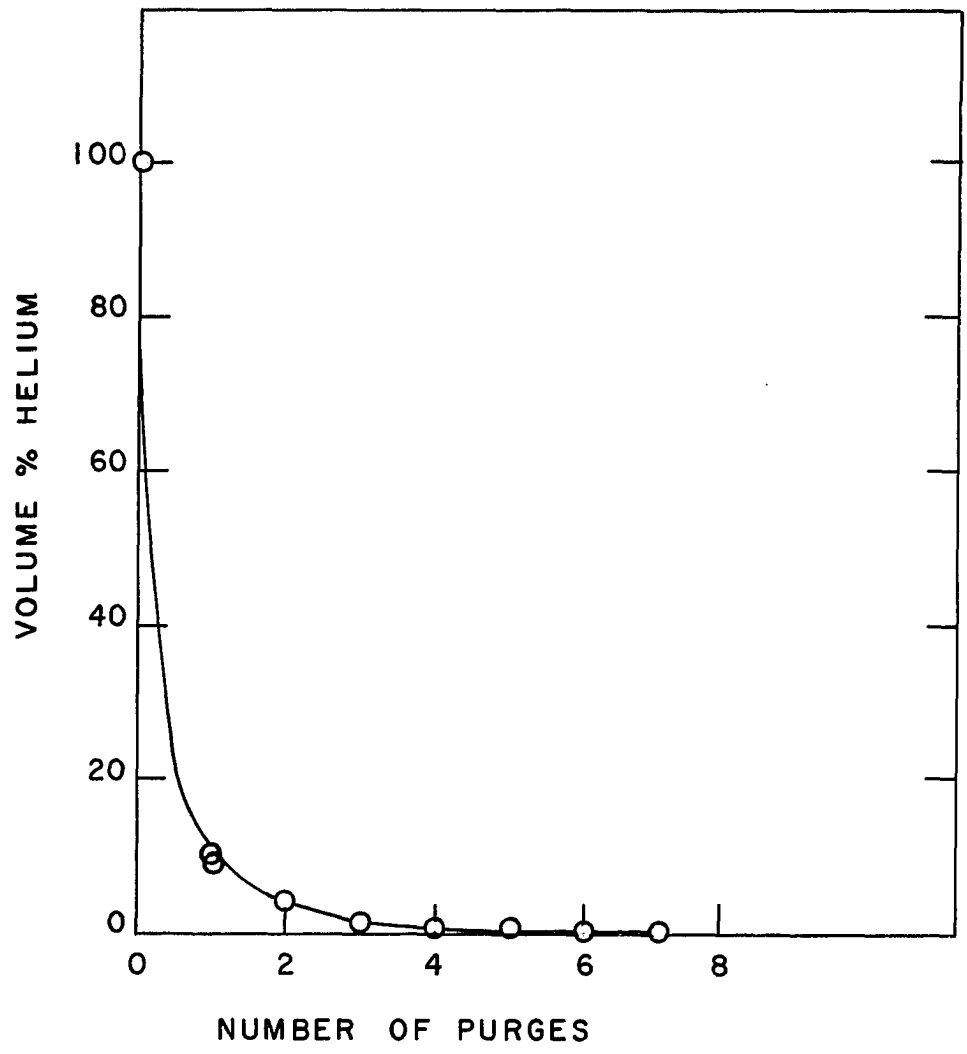
VOLUME % HELIUM
100
80
60
40
20
0
0
2
4
6
8
NUMBER OF PURGES

volume of the storage tank. This was done by inverting the floating head, filling it with water to various heights and weighing the water. Using a hook gage, the height of the water was determined accurately and knowing the density of the water, the volume of the tank for each inch of height was determined. Then with the system in operation, the displacement of the floating head and the time required to displace a given distance gave the flow rate of gas through the rotameter.

Preparation of materials

All bed materials were ground and screened before they were used in the tests. Grinding was done by a burr mill. Screens were 8 in. diameter, half height, Tyler brass screen sieves. A complete set of screen sizes from 65 to 400 mesh were available. This included 65, 80, 100, 115, 150, 170, 200, 250, 270, 325 and 400 mesh sizes. The range of sizes ordinarily used included 80 through 250 mesh. The notation -65/+250 means that the material passed through the 65 mesh screen and was retained on the 250 mesh screen. After grinding the material, a sample of approximately 100 grams was placed on top of eight or more nested screens. The screens were placed in a Tyler Ro-tap shaker for 15 min. The over-size material was ground once again and the under-size material was discarded. This was a slow and tedious process but if larger samples were used, the screens would become overloaded and some fine mesh particles would never get a chance to get to their proper sieve. Blinding of the meshes occurs from overloading the sieves and results in unreliable data.

Settled bed tests

After the bed material had been prepared by grinding and screening, the desired column was connected to the system and the column charged with the material. Charging was accomplished by pouring the material in at the top of the column. The proper bed height was obtained by fluidizing the bed; allowing it to settle; and if the settled bed height was too great, some material was removed by using a tap located low on the side wall of the column. Pressure within the column when the compressor was running would force the material through the tap. The material was collected in a beaker. The bed was then fluidized and allowed to settle again to see if the proper height had been obtained. If not, the procedure was repeated. If too much was removed, it was necessary to add more material through the top of the bed. When the proper bed height was obtained, the column was purged of air and water vapor by opening the vent valve. No gas was allowed to recirculate to the storage tank. If there was no change of gas in the system, the storage tank was emptied once for the two inch column and twice for the four inch column. If there was a change of gas, the system was purged as described under "Purging the system."

Instruments were then connected to the test section as described under "Instrumentation." In taking resistance readings of the settled bed, it was found that the rate at which a fluidized bed was allowed to settle made a difference in the density of the settled bed and hence a difference in the resistivity of the settled bed. After trying several settling techniques, it was decided to settle the fluidized bed after

fluidizing it at approximately three times the incipient fluidization velocity by shutting off the compressor and allowing the bed to settle. This procedure gave about the same result as closing the valve at the rotameter, thereby shutting off the supply of gas to the bed. The reason for shutting off the compressor was to eliminate all vibration from the system. After compressor shutoff the bed would settle at an exponential rate for about 3 min. Thereafter, the current and voltage readings would remain essentially constant. Therefore, all settled bed readings were taken after the 3 min. settling period.

The settled bed was extremely sensitive to vibration. Any disturbance such as the slamming of a door or someone walking down the hallway would cause the bed to settle an additional amount and give a different resistance reading. When this occurred it would be necessary to refluidize the bed and allow it to settle again before taking readings.

The compressor was originally mounted with rubber vibration mountings on the same frame as the fluidized bed column but because of the vibration transmitted to the bed, it was necessary to remove the compressor from the frame and place it on the floor on the vibration mountings. Furthermore, the connections to and from the compressor had to be flexible hose connections. A steel spring reinforced vacuum cleaner hose was tried at first. It worked well for the suction side but could not hold the pressure of the supply side. A length of steel wire reinforced polyvinyl hose with a 7/32 in. wall was then used for the supply connection.

Fluidized bed tests

Instrumentation for the fluidized bed tests was arranged as described in the "Instrumentation" section and as shown in Figures 5 and 6. The first three resistivity readings of a series were taken

1. Of the settled bed
2. At a gas flow rate where the bed resistance was just beginning to increase, and
3. At a flow rate just below the incipient fluidization point.

These three readings could ordinarily be taken with the same instrumentation as for the settled bed readings because there was very little fluctuation in voltage. Resistivity readings were taken just below the incipient fluidization point because the bed was unstable at that point and results were not very repeatable. Values of pressure drop across the bed and flow rate were recorded for the incipient point.

Using the instrumentation of Figure 6, three additional readings were taken at

4. The peak resistivity
5. The minimum fluidized resistivity, and
6. A point beyond the minimum fluidized resistivity.

It was necessary to use the oscilloscope and camera to record the voltages for these three readings because of the fluctuating voltages. The flow rate at which the peak resistivity occurred was determined by using a Brush oscillograph recorder which was connected in place of the oscilloscope. After the incipient fluidization flow rate had been passed, the flow rate was increased in small increments and the voltage drops representing probe voltage and bed current were observed. At some flow rate the probe

voltage was found to be a maximum whereas the bed current was a minimum. This flow rate gave the peak fluidized resistivity. The oscilloscope was then connected in place of the Brush recorder and readings taken. The flow rate which gave the minimum fluidized resistivity was not as readily determined and was arrived at more by experience and intuition. The final reading was taken at the maximum flow rate which could be used without causing excessive elutriation.

Particle size analysis

A particle size analysis was performed on the calcined coke material used in some of the tests. In performing this analysis, an estimate was made of the weight of a sample of each fraction which would contain approximately 500 particles. This amount of material was weighed out on a Cahn Electrobalance and then spread out on a sheet of $8\frac{1}{2}$ x 11 in. graph paper. The paper was sprayed with a clear acrylic coating, using care to keep the spray nozzle at a great enough distance from the paper to prevent the particles from being blown away. The particles were counted using a 20 power Bosch and Lomb zoom microscope. From the data obtained it was possible to calculate the number of particles per gram for each size fraction. Then knowing the number of grams of each size fraction, the total number of particles of each size fraction were calculated.

Angle of repose determination

When granular solids are piled up on a flat surface, the sides of the pile form a definite angle with the horizontal. This angle is known as the angle of repose. The angle of repose of individual size fractions

and of various combinations of size fractions was determined by using the apparatus shown in Figure 16. The apparatus consisted of a Tinker Toy framework which supported a pulley and hoist for raising a brass cylinder having an inside diameter of $1\frac{1}{4}$ in. and a height of 2 in. The brass cylinder was placed on a steel disc having a diameter of 5.02 cm. The cylinder was filled with carbon granules and slowly raised with the crank until it was clear of the pile of granules. The difference in height of the base and apex of the cone was measured using a cathetometer. Knowing the diameter of the base and the height of the cone it was then possible to calculate the tangent of the angle of repose.

Figure 16. Photograph of apparatus used in measuring the angle of repose of some of the fluidized bed materials

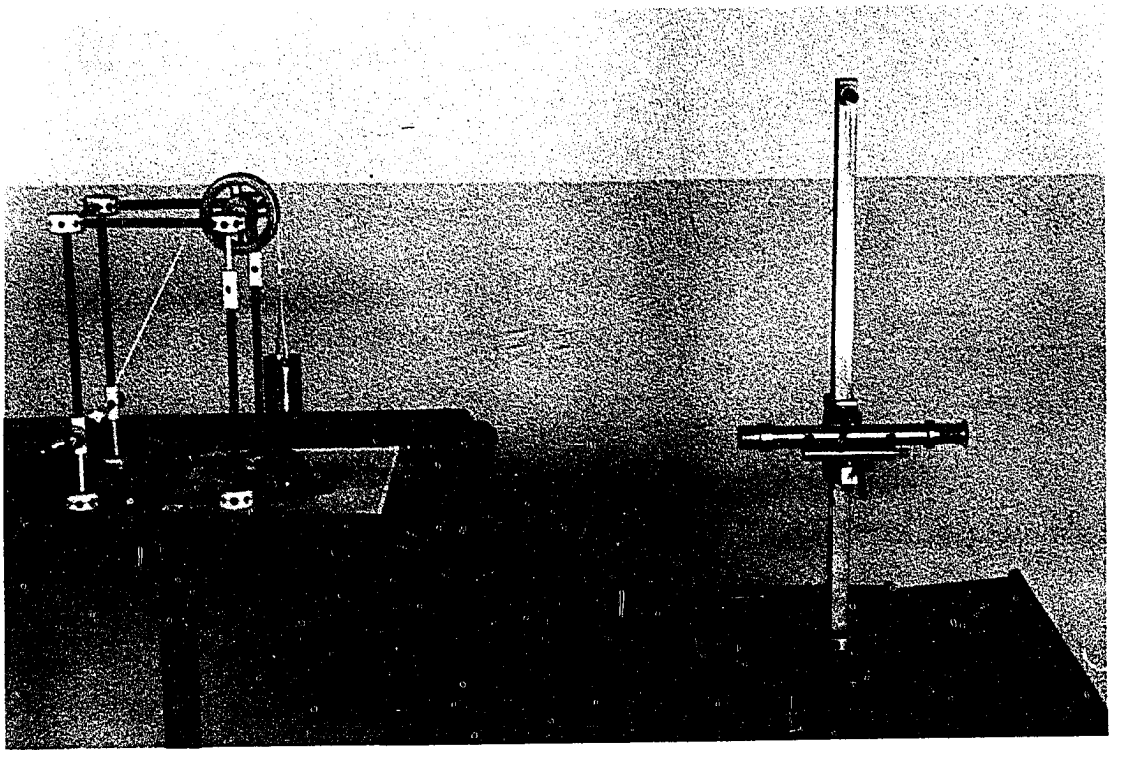

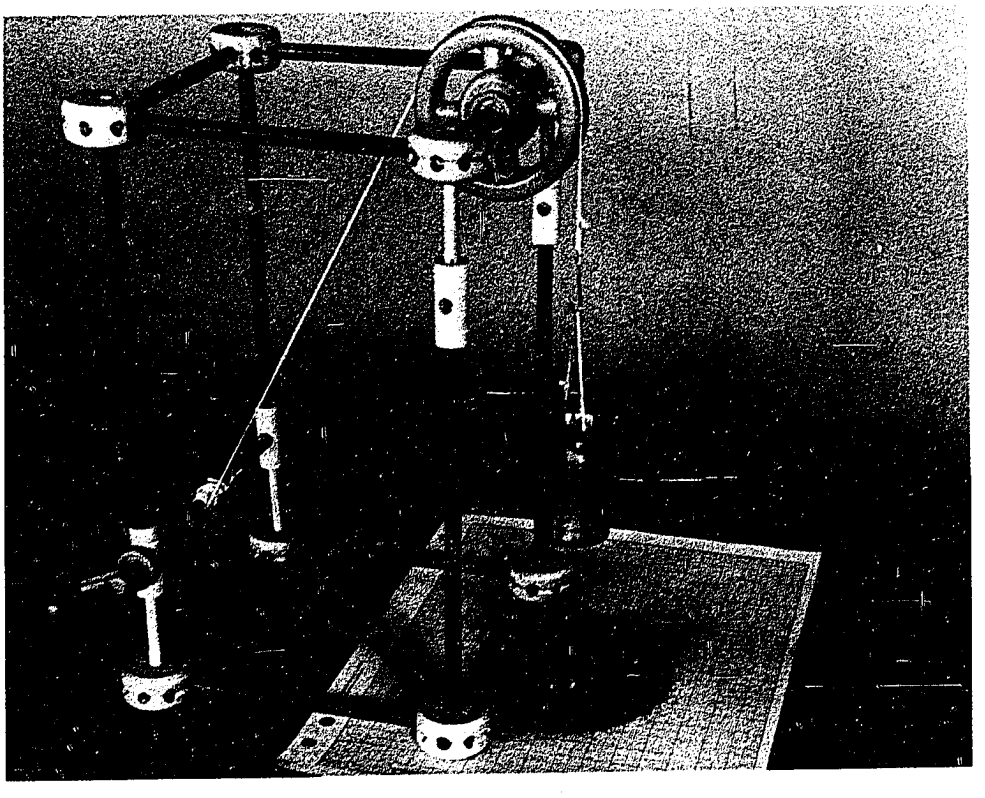

METHOD OF CALCULATION

Gas Velocity

In determining the gas velocity in the fluidized bed, it was necessary to have the average pressure of the gas in the bed $\overline{P}_b$, the temperature of the bed T_b, the rotameter reading Q_{gr}, rotameter pressure P_{gr} and rotameter temperature T_{gr}.

From Schoenborn and Colburn (46) the equation for flow through a rotameter is

$$Q = C\left(\frac{2gv_f(d_f-d_w)}{A_f d_w}\right)^{\frac{1}{2}} A_w \qquad (2)$$

where Q = volume flow rate, cu.ft./min.

C = flow coefficient

g = acceleration of gravity, ft./(sec.)^2

v_f = volume of float, cu.ft.

d_f = density of float, lb./cu.ft.

d_w = density of fluid, lb./cu.ft.

A_f = cross-sectional area of largest part of float, sq.ft.

A_w = cross-sectional area of narrowest part of annulus, sq.ft.

Apply Equation 2 to a rotameter with a particular gas flowing through it at a particular pressure and temperature having a flow rate Q_1, with the float at a certain position. Now apply Equation 2 to the same rotameter with another gas at another pressure and temperature having a flow

rate Q_2 which causes the float to assume the same position as before. The equations can be combined and constant terms canceled to give the following:

$$\frac{Q_2}{Q_1} = \frac{C_2}{C_1} \frac{((d_{f2}-d_{w2})/d_{w2})^{\frac{1}{2}}}{((d_{f1}-d_{w1})/d_{w1})^{\frac{1}{2}}} \tag{3}$$

The subscripts 1 and 2 apply to the two gases respectively. The coefficients C_1 and C_2, can usually be canceled since they are primarily affected by viscosity. The viscosities of the gases will not only be small but also nearly the same value.

Since the density of the float d_f, is so much larger than the density of the gas d_w, no noticeable error is introduced if the (d_f-d_w) terms are cancelled. Equation 3 can then be reduced to

$$\frac{Q_2}{Q_1} = \left(\frac{d_{w1}}{d_{w2}}\right)^{\frac{1}{2}} \tag{4}$$

The scale of the rotameter read in standard cubic feet per minute of air. Considering gases other than air to be measured by the rotameter, Equation 4 can be applied for this situation in the following form:

$$\frac{Q_{cs}}{Q_{gr}} = \left(\frac{d_{gr}}{d_{cs}}\right)^{\frac{1}{2}} \tag{5}$$

where Q_{cs} = corrected scale reading of the rotameter, std.cu.ft./min. of air

Q_{gr} = volume flow rate at rotameter conditions of temperature and pressure, cu.ft./min.

From the continuity equation,

$$M = AVd = Qd \tag{6}$$

where M = mass rate of flow, lb./min.

A = cross-sectional area perpendicular to direction of flow, sq.ft.

V = velocity, ft./min.

d = density, lb./cu.ft.

Q = volume rate of flow, ft./min.

In order to determine the volume flow rate in the fluidized bed, Equation 6 can be written as follows:

$$\frac{Q_{gb}}{Q_{gr}} = \frac{d_{gr}}{d_{gb}} \tag{7}$$

where Q_{gb} = volume flow rate of gas in the fluidized bed at bed conditions of pressure and temperature, cu.ft./min.

The superficial velocity of the gas in the bed, V_b, can be determined from the volume rate of flow, Q_{gb}, and the cross-sectional area, A_b, as follows:

$$V_{gb} = \frac{Q_{gb}}{A_b} \tag{8}$$

Combining Equations 5, 7 and 8 and solving for V_{gb}, the following

result is obtained:

$$V_{gb} = \frac{(d_{cs} d_{gr})^{\frac{1}{2}}}{A_b} \frac{Q_{cs}}{d_{gb}} \tag{9}$$

Combining the equation of state for an ideal gas,

$$P = dR_g T \tag{10}$$

where P = pressure, lb./sq.ft.abs.

d = density, lb./cu.ft.

R_g = gas constant, ft./^{o}R.

T = temperature, ^{o}R.

with Equation 9, gives

$$V_{gb} = \left(\frac{P_{cs} P_{gr}}{R_{cs} T_{cs} R_{gr} T_{gr}} \right)^{\frac{1}{2}} \frac{R_{gb} T_{gb}}{A_b P_{gb}} Q_{cs} \tag{11}$$

Average Particle Size

The particles of any one size fraction were those particles which were retained between two sieves. The size of these particles ranged from the size that would just pass through the mesh opening of the larger sieve above, to the size that was just too large to pass through the mesh opening of the smaller screen upon which the particles were retained. It was assumed that the average particle size of the size fraction was the arithmetic average of the two mesh openings. Table 2 gives the average particle sizes for the screen fractions used.

The average particle size for a mixture of screen fractions was determined by the following expression:

$$D_p = \frac{\sum_i (D_i n_i)}{\sum_i n_i} \tag{12}$$

where D_p = average particle size of mixed fractions, microns

D_i = average size of individual screen fraction, microns

n_i = number of particles in an individual screen fraction

Standard Deviation of Particle Size

The definition for standard deviation can be found in Lindgren and McElrath (47) or any basic statistics text as

$$\sigma_p = \left(\frac{1}{N-1} \left(\sum n_i d_i^2 - \frac{\left(\sum_i n_i D_i\right)^2}{N} \right) \right)^{\frac{1}{2}} \tag{13}$$

where σ_p = standard deviation of particle size, microns

N = total number of particles in mixture

The values of standard deviation determined for the mixtures of size fractions is given in Table 5.

Dimensional Analysis

Preliminary to a statistical analysis of the results of this investigation, a dimensional analysis of the variables which appeared to affect the resistivity of a bed of carbon granules in its fluidized state was

made. The method used was set forth by Murphy (48).

Consider that the resistivity of the fluidized bed is some function of the system parameters as indicated below.

$$\rho_f = f(D_p, V_b, \mu, \rho_s, D_b, H_b, d_p, d_g, \sigma_p) \tag{14}$$

where ρ_f	= resistivity of the fluidized bed, ohm-in.	ML^3/TQ^2
D_p	= average particle diameter, ft.	L
V_b	= superficial gas velocity, ft./sec.	L/T
μ	= viscosity of gas, lb_m./ft.sec.	M/LT
ρ_s	= resistivity of settled bed, ohm-in.	ML^3/TQ^2
D_b	= diameter of bed, ft.	L
H_b	= height of settled bed, ft.	L
d_p	= particle density, lb_m./cu.ft.	M/L^3
d_g	= gas density, lb_m./ft.	M/L^3
σ_p	= standard deviation of particle size, ft.	L

According to the Buckingham Pi Theorem, the number of pi terms will be equal to ten (variables) minus four (basic dimensions) or six pi terms. Equation 1 can be written in the form

$$\rho_f = C\ (D_p^j)\ (V_{gb}^k)\ (\mu^m)\ (\rho_s^n)\ (D_b^p)\ (H_b^g)\ (d_p^r)\ (d_g^s)\ (\sigma_p^t) \tag{15}$$

where C is a coefficient not necessarily a constant. The dimensional equation corresponding to Equation 15 is

$$ML^3T^{-1}Q^{-2} = L^j(LT^{-1})^k(ML^{-1}T^{-1})^m(ML^3T^{-1}Q^{-2})^nL^pL^q(ML^{-3})^r(ML^{-3})^sL^t \tag{16}$$

The four component auxiliary equations are

$$M: \quad 1 = m + n + r + s \tag{17}$$

$$L: \quad 3 = j + k - m + 3n + p + q - 3r - 3s + t \tag{18}$$

$$T: \quad -1 = -k - m - n \tag{19}$$

$$Q: \quad -2 = -2n \tag{20}$$

Since there are nine unknowns and four equations, four of the unknowns may be expressed in terms of the remaining five unknowns

$$j = k - p - q - t \tag{21}$$

$$m = -k \tag{22}$$

$$n = 1 \tag{23}$$

$$r = k - s \tag{24}$$

Substituting these values into Equation (15), there results

$$\frac{\rho_f}{\rho_s} = C \left(\frac{d_p V_{gb} D_p}{\mu}\right)^k \left(\frac{D_b}{D_p}\right)^p \left(\frac{H_b}{D_p}\right)^q \left(\frac{d_g}{d_p}\right)^s \left(\frac{\sigma_p}{D_p}\right)^t \tag{25}$$

In order to have more meaningful dimensionless groups, combine pi terms as follows:

$$\left(\frac{d_p V_{gb} D_p}{\mu}\right)^k \left(\frac{d_g}{d_p}\right)^k = \left(\frac{d_g V_{gb} D_p}{\mu}\right)^k \tag{26}$$

and

$$\left(\frac{H_b}{D_p}\right)^q \left(\frac{D_p}{D_b}\right)^q = \left(\frac{H_b}{D_b}\right)^q \tag{27}$$

Equation (25) then becomes

$$\frac{\rho_f}{\rho_s} = C \left(\frac{d_g V_{gb} D_p}{\mu}\right)^k \left(\frac{D_b}{D_p}\right)^p \left(\frac{H_b}{D_b}\right)^q \left(\frac{d_g}{d_p}\right)^s \left(\frac{\sigma_p}{D_p}\right)^t \tag{28}$$

thus giving six pi terms.

Statistical Analysis

An analysis of variance was made of the test data using the Aardvark computer program of the Iowa State University Statistical Laboratory which was run on the Computation Center's IBM System/360 model 50 digital computer.

A stepwise regression analysis of the data was then made on the test data. This was also a program of the Statistical Laboratory which was run on the computer.

A multiple regression analysis was also made of the data since this method allows one to choose the variables to include in the regression. The regression analysis program is a double precision program and gives more precise results than the stepwise regression analysis program. The regression analysis program is a library program of the Computation Center and the analysis was made with the assistance of the Statistical Laboratory.

RESULTS AND DISCUSSION

Effect of Time on the Fluidized Bed

One of the first studies made in this investigation was concerned with the effect of the length of the fluidization period on the fluidized bed properties. Of particular concern were the following:

1. The possible attrition of particles with its accompanying degradation of size.
2. The elutriation rate from the bed.
3. The change in the resistivity of both settled and fluidized beds.

During the course of any one run, the fluidization process was interrupted at various intervals of time to collect data. An electric clock connected in parallel with the compressor motor would run only when the compressor was running. This clock was used to determine the length of the fluidization period.

A series of three runs was made for determining the effects of time. These runs were made in the four inch column with nitrogen using a settled bed height of 4 3/8 in. above the top voltage probe. In Run A-1 petroleum coke was fluidized for a total of 33 hr., in Run B-1 graphite was fluidized for 72 hr., and in Run C-1 calcined coke was fluidized for 304 hr. During the first two runs periodic screen analyses were made of the bed materials in order to see if any attrition of the particles was taking place. During the last two runs the material elutriated from the beds was collected periodically and weighed to determine the elutriation rates.

The resistivity of the settled beds was measured at frequent intervals throughout all three runs and the resistivity of the fluidized beds was checked frequently during the second and third runs. It was not possible to determine the resistivity of the fluidized petroleum coke used in the first run because its value was too great for measurement. The results of these runs are presented and discussed below.

Screen analysis

Table 1 lists the bed composition by weight per cent for the petroleum coke of Run A-1 and the graphite of Run B-1.

Table 1. Effect of fluidization time on particle size

Screen size	Petroleum coke Run A-1		Graphite Run B-1	
	Initial bed composition, per cent by weight	Bed composition at 33 hr., per cent by weight	Initial bed composition, per cent by weight	Bed composition at 72 hr., per cent by weight
-65/+80	13.04	12.00	22.14	19.72
-80/+100	20.08	19.36	21.23	20.46
-100/+115	19.15	18.62	14.35	13.96
-115/+150	14.29	14.76	12.41	11.90
-150/+170	16.86	17.78	11.67	12.60
-170/+200	4.51	5.49	5.99	6.52
-200/+250	10.24	10.36	8.94	10.12
-250/pan	1.83	1.63	3.27	4.72
Total	100.00	100.00	100.00	100.00

The petroleum coke was a harder material than the graphite and considering the limits of accuracy of the screening operation, there was very little,

if any, degradation in size over the 33 hr. period. The graphite did exhibit some degradation although it was not very great. The small amount of degradation was not considered of great enough consequence to affect any of the results of this investigation.

Elutriated material

The amount of elutriated material which was collected in the filter is shown at different intervals throughout the period of fluidization in Figure 17. It is interesting to note that the average size of the elutriated fines was about 5 microns as determined by microscopic examination. This compares to an average particle size (by weight) of 135 microns for the graphite bed. The arithmetic average of the mesh openings of 100 and 115 mesh screens would be 137 microns. The fines were elutriated quite rapidly during the first hours of fluidization. For the calcined coke (Run C-1), the elutriation rate diminished rapidly after 5 hr, whereas the graphite (Run B-1) elutriation rate did not diminish appreciably until about 20 hr. had passed.

It is also interesting to note the abrupt increase in the amount of elutriated material for Run B-1, at 33 hr. when the fluidization rate was increased from three times minimum fluidization velocity to four times minimum fluidization velocity. An examination of the elutriated fines collected in the filter disclosed that the material elutriated after 33 hr. was of a larger size than that which was elutriated previous to the increase in velocity.

Figure 17. Total amount of elutriated material versus fluidization time

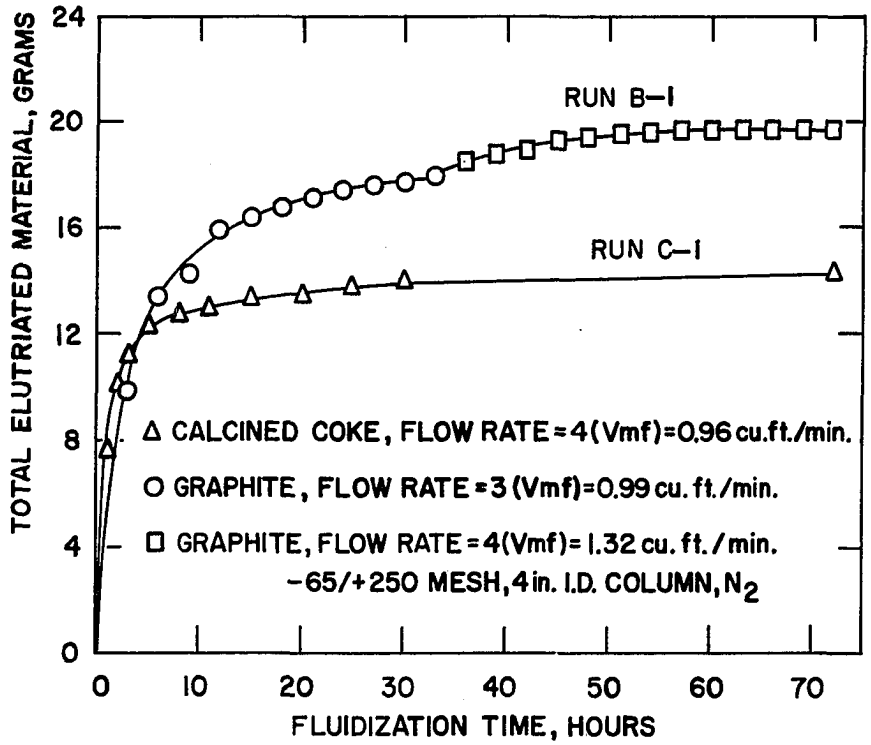
TOTAL ELUTRIATED MATERIAL, GRAMS
24
20
16
12
8
4
0
RUN B–I
RUN C–I
Δ CALCINED COKE, FLOW RATE = 4(Vmf) = 0.96 cu.ft./min.
O GRAPHITE, FLOW RATE = 3 (Vmf) = 0.99 cu. ft./min.
□ GRAPHITE, FLOW RATE = 4(Vmf) = 1.32 cu. ft./min.
-65/+250 MESH, 4 in. I.D. COLUMN, N_2
0
10
20
30
40
50
60
70
FLUIDIZATION TIME, HOURS

Resistivity

Settled bed resistivity The effects of fluidization time are shown in Figure 18 for the settled bed resistivity of calcined coke, petroleum coke and graphite. In Figure 18 (a) is shown the results of fluidizing calcined coke over a period of 304 hr. (Run C-1). The settled bed resistivity increased rapidly at first, but after about 80 hr., the increase was at a nearly constant rate, the rate of increase being approximately 8 per cent in 20 hr. In Figure 18 (b) is shown the results of fluidizing petroleum coke for 33 hr. (Run A-1) and graphite for 72 hr. (Run B-1). These materials did not show as great an increase in settled bed resistivity as did the calcined coke.

Fluidized bed resistivity In Figure 19 is shown the effects of fluidization time on fluidized bed resistivity of both graphite (Run B-1) and calcined coke (Run C-1). The fluidized bed resistivity increased quite rapidly at first and then tended to increase at a decreasing rate. The graphite resistivity had an abruptly increasing rate after about 55 hr. for which there is no logical explanation.

It appears reasonable for both the settled and fluidized bed resistivities to increase more rapidly during the first hours of fluidization since this is the period when the fine particles of the bed are being elutriated. These fine particles would tend to make a greater number of contacts between particles which would result in a greater number of parallel paths between electrodes. From electrical circuit theory it is known that a greater number of equal parallel resistances tend to decrease

Figure 18(a). Settled bed resistivity versus fluidization time for Run C-1 calcined coke

Figure 18(b). Settled bed resistivity versus fluidization time for Run A-1 petroleum coke and Run B-1 graphite

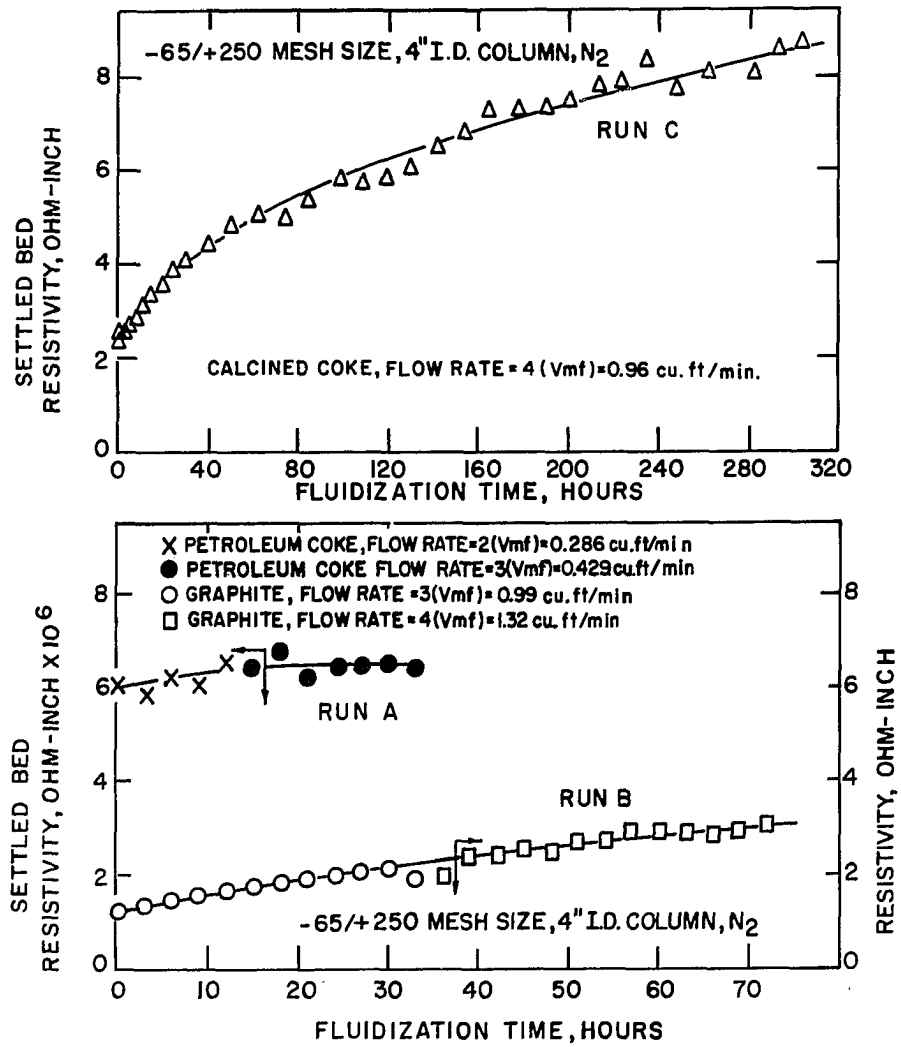
-65/+250 MESH SIZE, 4" I.D. COLUMN, N2
RUN C
CALCINED COKE, FLOW RATE = 4 (Vmf) = 0.96 cu. ft/min.
SETTLED BED RESISTIVITY, OHM-INCH
FLUIDIZATION TIME, HOURS
X PETROLEUM COKE, FLOW RATE = 2(Vmf) = 0.286 cu.ft/min
● PETROLEUM COKE FLOW RATE = 3(Vmf) = 0.429 cu.ft/min
○ GRAPHITE, FLOW RATE = 3(Vmf) = 0.99 cu. ft/min
□ GRAPHITE, FLOW RATE = 4(Vmf) = 1.32 cu. ft/min
RUN A
RUN B
-65/+250 MESH SIZE, 4" I.D. COLUMN, N2
SETTLED BED RESISTIVITY, OHM-INCH X 10^6
RESISTIVITY, OHM-INCH
FLUIDIZATION TIME, HOURS

Figure 19(a). Fluidized bed resistivity versus fluidization time for Run B-1 graphite

Figure 19(b). Fluidized bed resistivity versus fluidization time for Run C-1 calcined coke

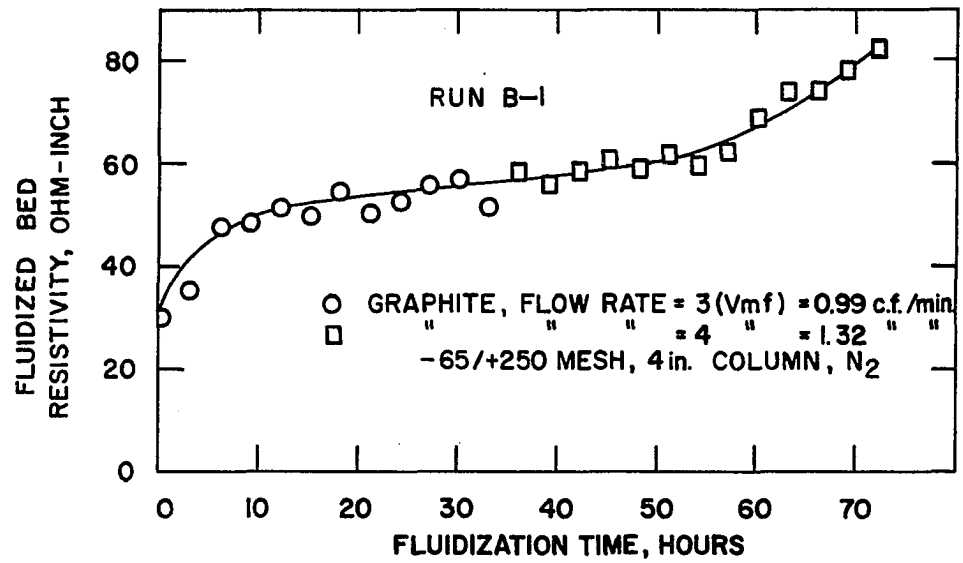
RUN B-I
FLUIDIZED BED RESISTIVITY, OHM-INCH
80
60
40
20
0
0
10
20
30
40
50
60
70
FLUIDIZATION TIME, HOURS
GRAPHITE, FLOW RATE = 3(Vmf) = 0.99 c.f./min.
" " " = 4 " = 1.32 " "
-65/+250 MESH, 4 in. COLUMN, N2

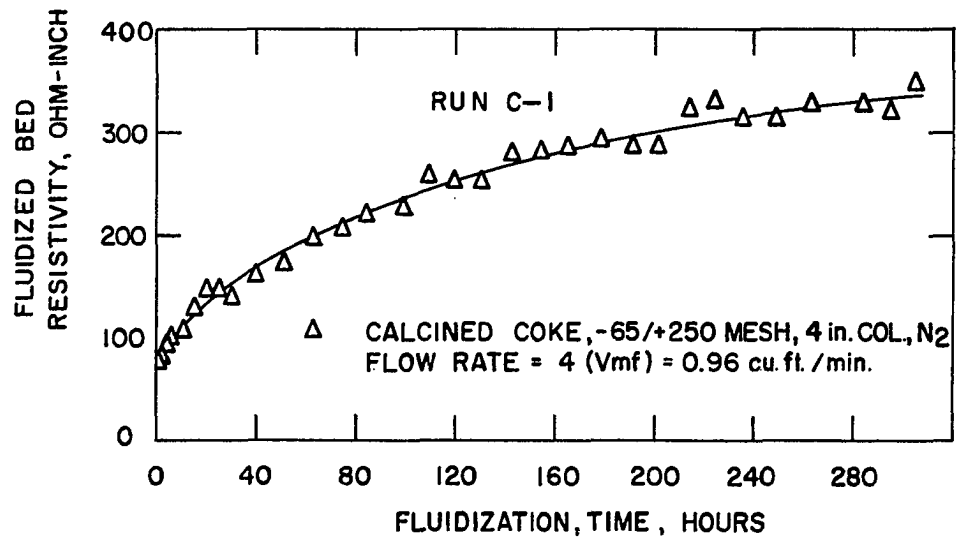
RUN C-I
FLUIDIZED BED RESISTIVITY, OHM-INCH
400
300
200
100
0
0
40
80
120
160
200
240
280
FLUIDIZATION, TIME, HOURS
CALCINED COKE, -65/+250 MESH, 4 in. COL., N2
FLOW RATE = 4 (Vmf) = 0.96 cu. ft./min.

the overall resistance. Therefore, as the number of parallel paths is decreased by the elutriation of fines, it would be expected that the resistance would increase. A microscopic examination of the bed materials before being fluidized showed numerous fines clinging to the larger particles. In later microscopic examinations, the fines were gone and there was a trend toward the removal of sharp corners and projections presumably by attrition. The removal of both the fines and the angular features would reduce the number of contacts between particles, thereby increasing the resistivity.

Since the rate of increase of resistivity for calcined coke was fairly constant after approximately 80 hr., it was decided to prefluidize for about 80 hr. (89 hr. to be exact) the calcined coke material used in subsequent studies of resistivity (Runs D and E).

The elutriated fines from the calcined coke which had been fluidized for 304 hr. (Run C-1) were collected and mixed back in with the bed material and resistivity data taken to determine if the resistivity of the bed would decrease and if so, how close it would come to the initial resistivity of the material. The results were so scattered that no conclusion could be drawn. One problem encountered was the difficulty of handling the elutriated fines. In the first place, there was a relatively small amount of material (16.5 grams) and, in the second place, the material tended to cling to the sides of the container in which it was collected and to the container used to mix the fines with the bed material. The fines tended to elutriate quite rapidly and much of the added

fines had been elutriated before the data were entirely collected.

After fluidizing the calcined coke material (Run C-1) for 304 hr., it was noticed that a carbon coating had been left on the wall of the column where the bed material had rubbed against the wall. In order to determine if this coating might affect the resistivity measurements, the bed material was emptied out and a resistance measurement made between the two current electrodes of the four inch column. The resistance turned out to be 1.1×10^6 ohms for the $7\frac{1}{2}$ in. distance between the current electrodes or 1.47×10^5 ohms per in. This compares with a resistance of 41.6 ohms for the settled bed between the potential probes which were $1\frac{1}{2}$ in. apart. Therefore, the conductivity of the wall was not considered to be great enough to affect the resistivity measurements. The carbon coating was removed by washing the column wall with benzene.

Effect of Flow Rate on Fluidized Bed Characteristics

Two runs were made to determine the effects of gas flow rate on the fluidization characteristics and resistivity of some of the materials which had been fluidized for prolonged periods during the previously described runs. Thus Run B-2 was made with the graphite remaining in the bed after Run B-1, and Run C-2 was made with the calcined coke remaining after Run C-1. Fines which had been elutriated during the preceding runs were not remixed with the bed materials before making the new runs. Runs B-2 and C-2 were made with the four inch column using nitrogen and a settled bed height of 4 3/8 in. above the top potential probe. For each

run the gas flow rate was increased in a step-wise manner until a velocity several times the incipient fluidization velocity was attained. Then the flow rate was reduced in a step-wise manner. For each step the velocity was held constant long enough for the bed to approach a steady-state condition and then the pressure drop across the bed, the bed height, and the resistivity of the bed were measured. The results are discussed below.

Per cent bed expansion

The per cent bed expansion as a function of the volumetric flow rate is shown in Figure 20 (a) for graphite (Run B-2). The procedure of fluidizing the bed to about four times the minimum (incipient) fluidization velocity and then shutting off the compressor and allowing the bed to settle was used to obtain the point of zero per cent expansion. As the flow rate was gradually increased to the incipient fluidization point (0.29 cu.ft./min.) as indicated on Figure 20 (b), the bed expanded quite rapidly with increasing flow rate until the flow reached 0.45 cu.ft./min. Between these two points the bed was essentially in the emulsion phase. As the flow rate approached 0.45 cu.ft./min., small bubbles formed within the bed. With further flow rate increase, the bubbles became larger and any further bed expansion was probably due to the formation of large bubbles. As the flow rate was slowly decreased, a "hysteretic" effect was noted. This was most likely caused by a wedging action between particles brought about by the slow decrease of flow rate.

Pressure drop across the bed

The pressure drop across the bed is shown for both graphite (Run B-2)

Figure 20(a). Per cent bed expansion versus volume flow rate for Run B-2 graphite

Figure 20(b). Pressure drop across the bed versus volume flow rate for Run B-2 graphite

Figure 20(c). Resistivity versus volume flow rate for Run B-2 graphite

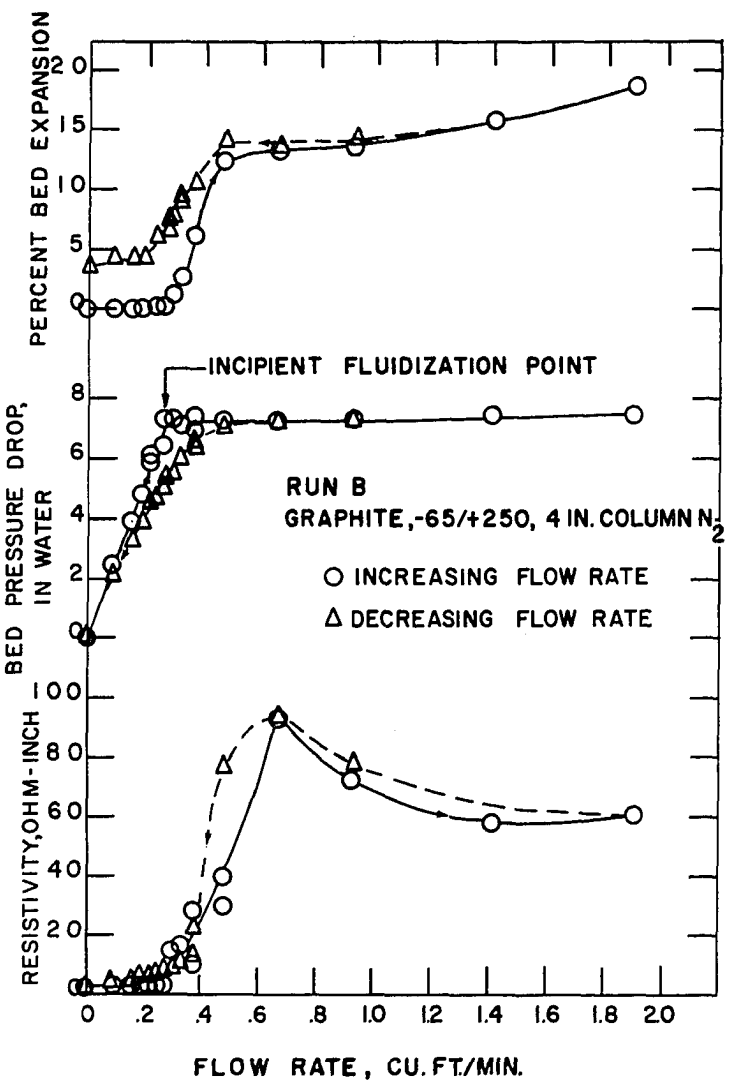
PERCENT BED EXPANSION
BED PRESSURE DROP, IN WATER
RESISTIVITY, OHM-INCH
INCIPIENT FLUIDIZATION POINT
RUN B
GRAPHITE, -65/+250, 4 IN. COLUMN N_2
O INCREASING FLOW RATE
Δ DECREASING FLOW RATE
FLOW RATE, CU. FT./MIN.

and calcined coke (Run C-2) in Figures 20 (b) and 21 (a), respectively. As flow was increased, the pressure drop across the graphite bed (Figure 20 (b)) increased linearly to the point of incipient fluidization, however, the calcined coke of Figure 21 (a) did not exactly display this same linear relationship. In both cases, the pressure drop did not increase appreciably after the incipient fluidization point. As the flow rate was gradually decreased the pressure drop did not have a definite discontinuity at the incipient point. Instead the pressure drop decreased rather gradually as the flow rate was reduced in the vicinity of the incipient point.

Resistivity

The general trend of the resistivity as flow rate increased was to increase rapidly between the incipient fluidization point and a point of peak resistivity which was reached at a velocity of approximately 2.3 times the minimum fluidization velocity for both the graphite (Run B-2) of Figure 20 (c) and the calcined coke (Run C-2) of Figure 21 (b). It was noted that the peak resistivity is more pronounced with the calcined coke than with the graphite. This tendency was found to be the case throughout this investigation. After passing through a peak, the resistivity reached a minimum point (hereafter referred to as the minimum fluidized resistivity) after which the resistivity began a gradual increase. When the flow rate was decreased, resistivity values were nearly the same as values for increasing flow rate.

Figure 21(a). Pressure drop across the bed versus volume flow rate for Run C-2 calcined coke

Figure 21(b). Resistivity versus volume flow rate for Run C-2 calcined coke

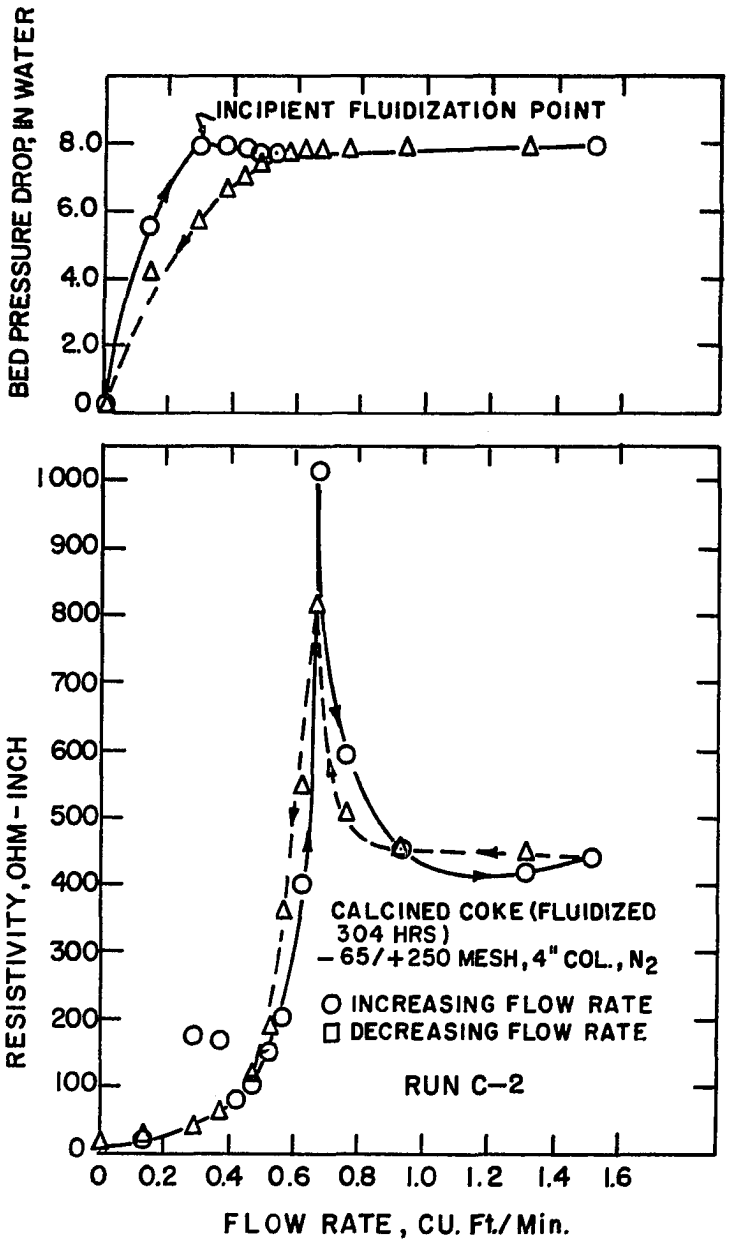
BED PRESSURE DROP, IN WATER
INCIPIENT FLUIDIZATION POINT
8.0
6.0
4.0
2.0
0
RESISTIVITY, OHM - INCH
1000
900
800
700
600
500
400
300
200
100
0
CALCINED COKE (FLUIDIZED 304 HRS)
-65/+250 MESH, 4" COL., N_2
O INCREASING FLOW RATE
□ DECREASING FLOW RATE
RUN C-2
0 0.2 0.4 0.6 0.8 1.0 1.2 1.4 1.6
FLOW RATE, CU. Ft./Min.

Individual Size Fractions

A quantity of calcined coke was ground in a burr mill and screened. The particles which did not pass through a 65 mesh screen and the fines which did pass through a 250 mesh screen were discarded. The material which was retained was placed in the four inch column and fluidized with nitrogen for a total of 89 hr. The material was then screened again and separated into the individual size fractions shown in Table 2. Some degradation of the material apparently took place since a small amount of solids in the -250 to +400 mesh range was recovered and separated.

Table 2. Particle size analysis of calcined coke used in Run D

Pretreatment: Crushed, screened, fluidized for an 89 hr. period, screened

Screen size Tyler mesh	Average particle size, microns	Total number of particles	Tangent of angle	Weight grams
-65/+80	193.5	2.008×10^8	0.7224	1395.641
-80/+100	163.0	3.308 "	0.7310	1496.876
-100/+115	137.0	4.627 "	0.7323	1257.634
-115/+150	115.0	6.739 "	0.7516	1063.727
-150/+170	96.5	11.820 "	0.7722	1125.668
-170/+200	81.0	14.131 "	0.8498	807.513
-200/+250	68.5	24.862 "	0.8937	828.724
-250/+270	58.0	10.323 "	0.9694	224.415
-270/+325	48.5	15.379 "	1.0106	218.143
-325/+400	40.5	3.873 "	1.0789	33.675

The average particle size of each fraction was estimated to be equal to the arithmetic average of the two screen openings which bounded the

fraction. A sample of each fraction was weighed and the number of particles in the sample counted by the method previously described in the section on "EQUIPMENT AND PROCEDURE" under "Particle size analysis." The angle of repose of each fraction was also determined. The results of the angle of repose determination are shown in the semi-log plot of Figure 22. Note the discontinuity in the single size fraction curve at about 150 mesh size. As screen size decreased from 80 mesh to 150 mesh, the angle of repose was nearly constant. Between 150 and 400 mesh the angle of repose increased. One possible explanation for this discontinuity is that the particle sizes became small enough so that the van der Waals (attractive molecular) forces affected the angle of repose. For a free flowing powder, where the force of attraction between particles is negligible compared to the forces of gravity and friction acting on a particle which is sliding down the surface of a pile, it has been shown that the coefficient of friction is equal to the tangent of the angle of repose. For uniformly sized particles the coefficient of friction should be independent of particle size.

All of the size fractions down to +250 mesh were individually fluidized in the two inch column with nitrogen using a settled bed height of 4 3/8 in. above the top potential probe. For each material the settled bed resistivity and fluidized bed resistivity at a series of increasing flow rates were determined. These measurements constituted Run D. In Figure 23 typical resistivity curves are shown for the largest, intermediate and smallest size fractions. These curves have the same characteristic as seen previously, namely, a rapid increase to a peak and then

Figure 22. Angle of repose versus average particle size for Runs D and E calcined coke

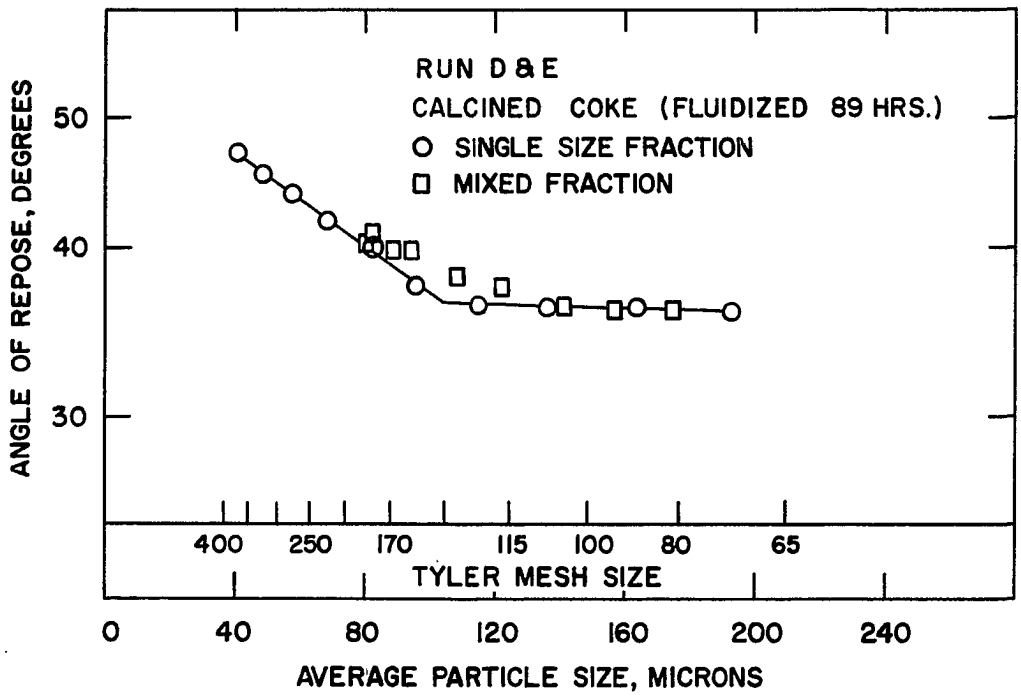
RUN D & E
CALCINED COKE (FLUIDIZED 89 HRS.)
O SINGLE SIZE FRACTION
□ MIXED FRACTION
ANGLE OF REPOSE, DEGREES
50
40
30
400
250
170
115
100
80
65
TYLER MESH SIZE
0
40
80
120
160
200
240
AVERAGE PARTICLE SIZE, MICRONS

Figure 23. Typical resistivity versus volume flow rate curves for Run D calcined coke individual size fractions

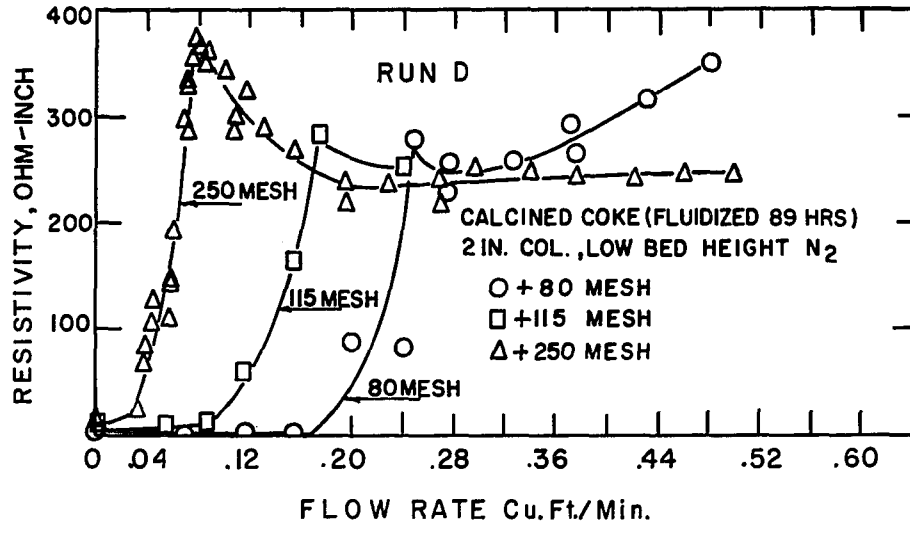
RESISTIVITY, OHM-INCH
400
300
200
100
0
.04
.12
.20
.28
.36
.44
.52
.60
FLOW RATE Cu.Ft./Min.
RUN D
250 MESH
115 MESH
80 MESH
CALCINED COKE (FLUIDIZED 89 HRS)
2 IN. COL., LOW BED HEIGHT N_2
O + 80 MESH
□ + 115 MESH
Δ + 250 MESH

a more gradual decrease to a minimum. The interesting feature of Figure 23 is the tendency for the resistivity curve to shift to the left as the particle size becomes smaller. This is explained by the fact that smaller particles fluidize at a lower velocity than larger particles.

Graphite

Some graphite was crushed and screened and then fluidized for several hours to remove the very fine particles. The material remaining in the fluidization column was separated into two size fractions by screening. Resistivity measurements were made on each individual fraction with the two inch column using nitrogen and a settled bed depth of 4 3/8 in. above the top potential probe. After these measurements were made, the two size fractions of graphite were combined and placed in the four inch column and the resistivity of the mixture was determined using nitrogen and a settled bed depth of 4 3/8 in. above the top potential probe. For each case the resistivity was determined at progressively larger flow rates. These measurements were designated as Run F and the results are summarized in Table 3 and Figure 24.

The settled bed resistivity of the graphite was about 2.5 ohm-in. compared to about 5 ohm-in. for calcined coke. In comparing the peak resistivities of both materials from Figures 23 and 24, the peak resistivity of the graphite was about 100 ohm-in. whereas the peak resistivity of the individual calcined coke fractions was about 300 ohm-in.

Figure 24. Resistivity versus velocity for Run F graphite

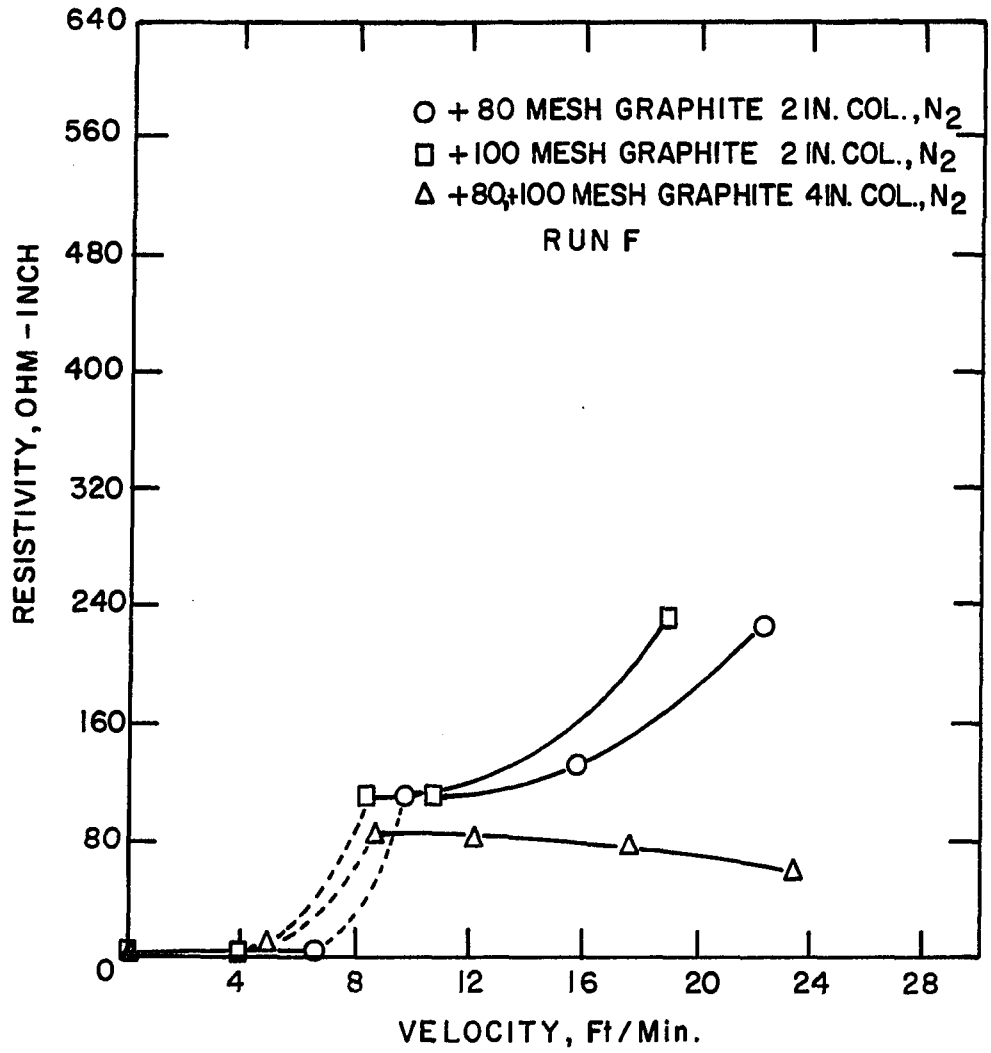
640
560
480
400
320
240
160
80
0
4
8
12
16
20
24
28
RESISTIVITY, OHM - INCH
VELOCITY, Ft/Min.
O + 80 MESH GRAPHITE 2 IN. COL., N2
□ +100 MESH GRAPHITE 2 IN. COL., N2
Δ +80,+100 MESH GRAPHITE 4 IN. COL., N2
RUN F

Table 3. Tabulated results for graphite, Run F

Pretreatment: Crushed, screened, fluidized to remove fines, screened

Screen size Tyler mesh	Gas	Col. dia., in.	Bed height	Bed temp., $^{o}F.$	Average bed press., lb./sq.-in.abs.	Gas velocity, ft./min.	Resistivity, ohm-in.
-65/+80	N_2	2	Lo	78	14.32	0.00	2.63
					14.32	0.00	2.68
					14.32	0.00	2.63
					14.32	0.00	2.81
					18.05	6.64	4.11
					18.08	9.73	109.80
					18.16	15.79	132.51
					18.21	22.32	228.83
-80/+100	N_2	2	Lo	82	14.32	0.00	2.96
					14.32	0.00	2.88
					14.32	0.00	3.04
					17.10	3.95	3.30
					17.95	8.44	108.35
					18.00	10.80	111.62
					18.06	18.96	233.33
-65/+100	N_2	4	Lo	80	14.20	0.00	2.09
					14.20	0.00	2.14
					14.20	0.00	2.16
					17.54	4.10	2.33
					18.44	5.07	6.78
					18.54	8.74	85.06
					18.60	12.24	80.96
					18.61	17.65	76.60
					18.63	23.47	59.44

The shapes of the curves of Figures 23 and 24 are a little different from each other. The most noticeable difference is that the calcined coke curves increase to a peak, decrease somewhat and then increase. There is no peak on the graphite curves. In both figures, the curves for the smaller fractions are shifted to the left of the curves for the larger

fractions. This is due to the fact that the smaller size fractions of a given material fluidize at a lower velocity than the larger size fractions. A pecular characteristic of the curves was noticed in Figure 24. After reaching the point of discontinuity, the resistivity of the individual size fractions begins to increase again, whereas the resistivity of the combined fractions gradually decreases. The explanation for this is that the two inch column has a tendency for the gas bubbles to coalesce and form large bubbles. At high gas flow rates these bubbles would even fill the entire diameter of the column and produce a condition known as "slugging" which occurs when the column contains alternating "slugs" of gas and solids. These large bubbles and slugs of gas would increase the resistivity of the bed by breaking the conducting chains of particles. The four inch column produced much smoother fluidization and did not exhibit the large bubbles and slugging of the two inch column.

Designed Parameter Study

Purpose

The purpose of the designed parameter study was twofold. The first purpose was to determine which parameters affected the electrical resistivity of fluidized beds. The second purpose was to generate an equation representing the response surface of resistivity to the important parameters. By using a statistical design the maximum amount of meaningful data could be obtained from a minimum number of observations.

Description of experimental design

The experimental design was a split-split plot design using nine levels of material (M_b) and two levels each of column diameter (D_b), gas (G) and bed height (H_b). The complete design is shown by Table 4.

The bed materials used were the individual size fractions of calcined coke which had been used in Run D plus an additional quantity of -250/+270, -270/+325 and -325/+400 mesh material which was present after the calcined coke had received its initial 89 hr. fluidization treatment. These size fractions were combined one at a time starting with the largest sizes first. The combining of fractions gave nine bed materials having different average particle sizes. There was more material than could be conveniently mixed with a V-blender so the size fractions were mixed in a large sealed container by simultaneously rolling it and turning it end over end. Table 5 gives the properties of each of the nine mixtures. Each material was subjected to a series of eight runs before another size fraction was mixed with it. Thus a series of eight runs performed on each of nine materials give a total of seventy two runs which were designated as Run E. Runs were made in the sequence listed in Table 4 starting with one and going through seventy two.

The column diameters were two inch and four inch inside diameters. The gases were helium and nitrogen. The bed heights were designated "Hi" and "Lo" where "Hi" refers to a settled bed having a height 18 3/4 in. above the uppermost potential probe and "Lo" refers to a settled bed having a height of 4 3/8 in. above the uppermost potential probe.

Table 4. Experimental design, Run E

			Run number M_b								
D_b	G	H_b	-65/ +100	-65/ +115	-65/ +150	-65/ +170	-65/ +200	-65/ +250	-65/ +270	-65/ +325	-65/ +400
2	He	Hi	6	13	24	25	37	45	56	63	72
2	He	Lo	7	14	23	28	38	46	55	64	71
2	N_2	Hi	5	16	21	26	40	47	53	61	69
2	N_2	Lo	8	15	22	27	39	48	54	62	70
4	He	Hi	1	11	18	30	36	44	49	57	65
4	He	Lo	2	12	19	29	35	43	50	58	66
4	N_2	Hi	4	9	17	31	33	41	51	60	68
4	N_2	Lo	3	10	20	32	34	42	52	59	67

Table 5. Particle size analysis of combined fractions of calcined coke used in Run E.

Screen size Tyler mesh	Average particle size, microns	Total number of particles	Tangent of angle of repose	Weight, grams	Standard deviation of particle size, microns
-65/+100	177.7	5.316×10^8	0.7224	2892.517	15.03
-65/+115	165.4	9.943 "	0.7277	4150.151	15.92
-65/+150	155.1	16.682 "	0.7350	5213.878	24.00
-65/+170	144.7	28.502 "	0.7622	6339.546	28.34
-65/+200	137.5	42.633 "	0.7715	7147.059	30.19
-65/+250	130.3	67.495 "	0.8339	7975.783	30.77
-65/+270	128.3	77.818 "	0.8310	8200.198	31.01
-65/+325	126.3	93.197 "	0.8645	8418.341	32.12
-65/+400	125.9	97.070 "	0.8525	8452.016	32.60

Experimental procedure

The first series of eight runs were made with the -65/+100 mesh mixture. Once the material was mixed, the size of column was chosen by a flip of a coin. The gas and then the bed height were chosen in the same manner. For the second run the remaining bed height was usually used. In the third run, the same column diameter was used but with a different gas and the bed height was chosen by the flip of a coin. The fourth run was the remaining one for that column diameter. The fifth run had to go to the other column diameter and the gas and bed height were chosen by a flip of a coin. The parameters of the remaining sixth through eighth runs were chosen in a manner similar to that described for the second through fourth. Although this was not a completely random choosing of parameters, it did give some randomization while reducing the time consuming work of changing column sizes and conserving on the consumption of the relatively

expensive helium.

Data was recorded for the following items:

1. Run number
2. Size fractions of bed material
3. Column size
4. Gas
5. Bed height
6. Barometric pressure
7. Operating temperature
8. Pressure drop across the bed
9. Rotameter pressure
10. Rotameter reading
11. Voltage drop across the probes
12. Current flowing through the bed
13. Pressure within the column above the fluidized bed
14. Bed pressure drop at the point of incipient fluidization
15. Rotameter reading at the point of incipient fluidization.

All runs were made at room temperature.

Results

After data had been collected, values were calculated for the superficial gas velocities within the column and the electrical resistivities of the bed.

Values of resistivity as a function of gas velocity were plotted

for each of the 72 runs. Typical plots are shown in Figures 25 and 26. Figure 25 is for Runs E-1 through E-8 which were for the -65/+100 mesh mixture. Figure 26 is for Runs E-49 through E-56 which were for a mixture of -65/+270 mesh fractions. Both of these figures demonstrate the same characteristics as was seen previously in Figures 21 (b) and 22, namely the rapid increase to a peak and then a decrease to a minimum. However, it is interesting to note that the curves for the same column diameter are grouped together. In both figures, the curves for the two inch diameter column are grouped above the curves for the four inch diameter column. This seems to indicate that column diameter has a pronounced effect on resistivity of a fluidized bed. Also of note is the tendency of the mixture having smaller screen fractions (Figure 26) to fluidize at a lower velocity and to have more pronounced peaks than the mixture not containing the smaller size fractions (Figure 25).

Since the flow rate at which the minimum fluidized resistivity occurred was not readily predictable, some readings taken for the minimum resistivity were not at that intended point. In these cases it was necessary to estimate the velocity and resistivity from the graph showing resistivity as a function of gas velocity.

Complete tabulated results for all 72 runs are given in Table 17 in the Appendix.

Analysis of variance

In order to determine the significance of the parameters of the experimental design upon settled bed resistivity, peak fluidized

Figure 25. Typical plot of resistivity versus velocity, Run E(1-8)

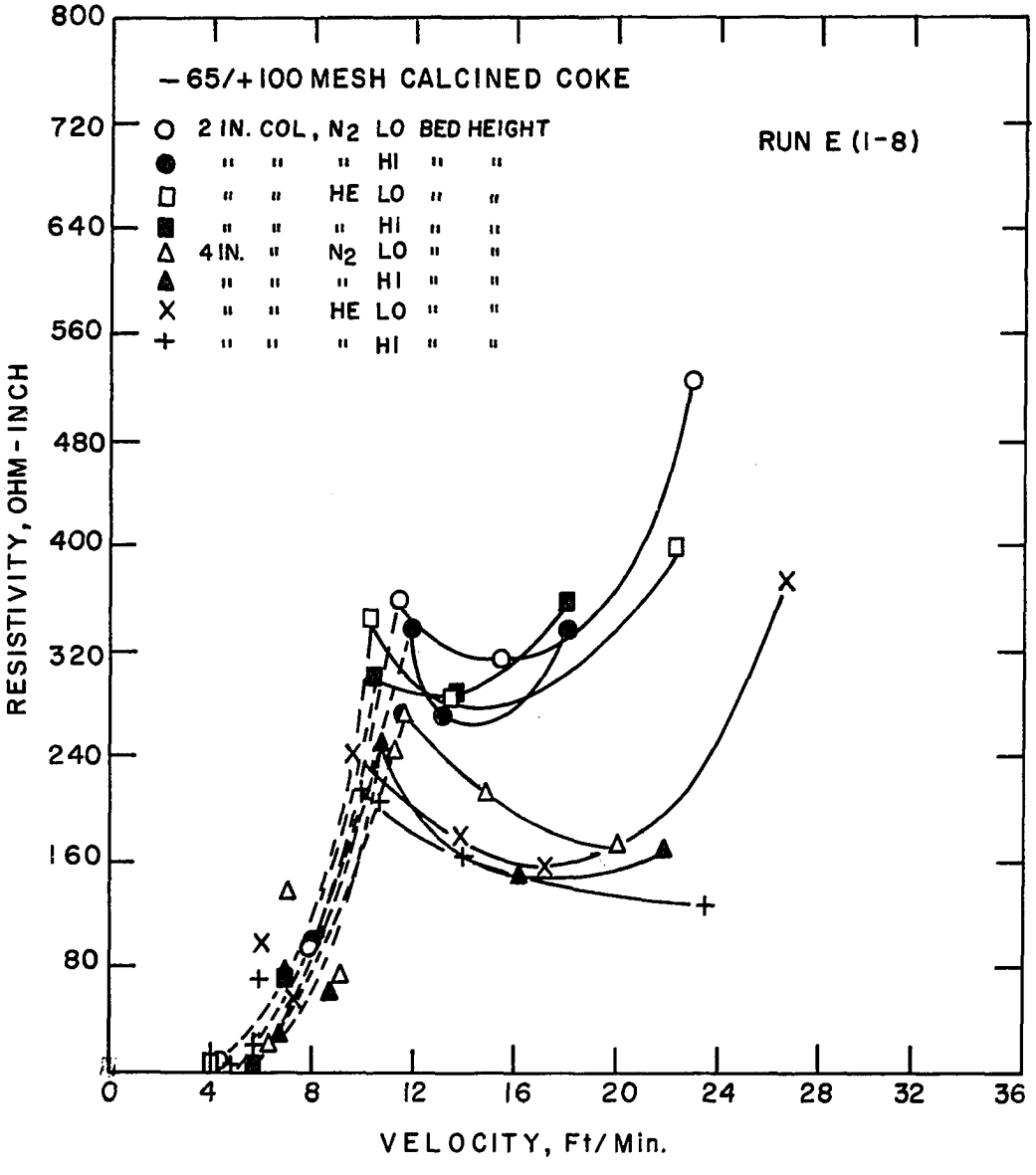
800
720
640
560
480
400
320
240
160
80
0
4
8
12
16
20
24
28
32
36
RESISTIVITY, OHM-INCH
VELOCITY, Ft/Min.
−65/+100 MESH CALCINED COKE
RUN E (1-8)
2 IN. COL, N2 LO BED HEIGHT
" " " HI " "
" " HE LO " "
" " " HI " "
4 IN. " N2 LO " "
" " " HI " "
" " HE LO " "
" " " HI " "

Figure 26. Typical plot of resistivity versus velocity, Run E(49-56)

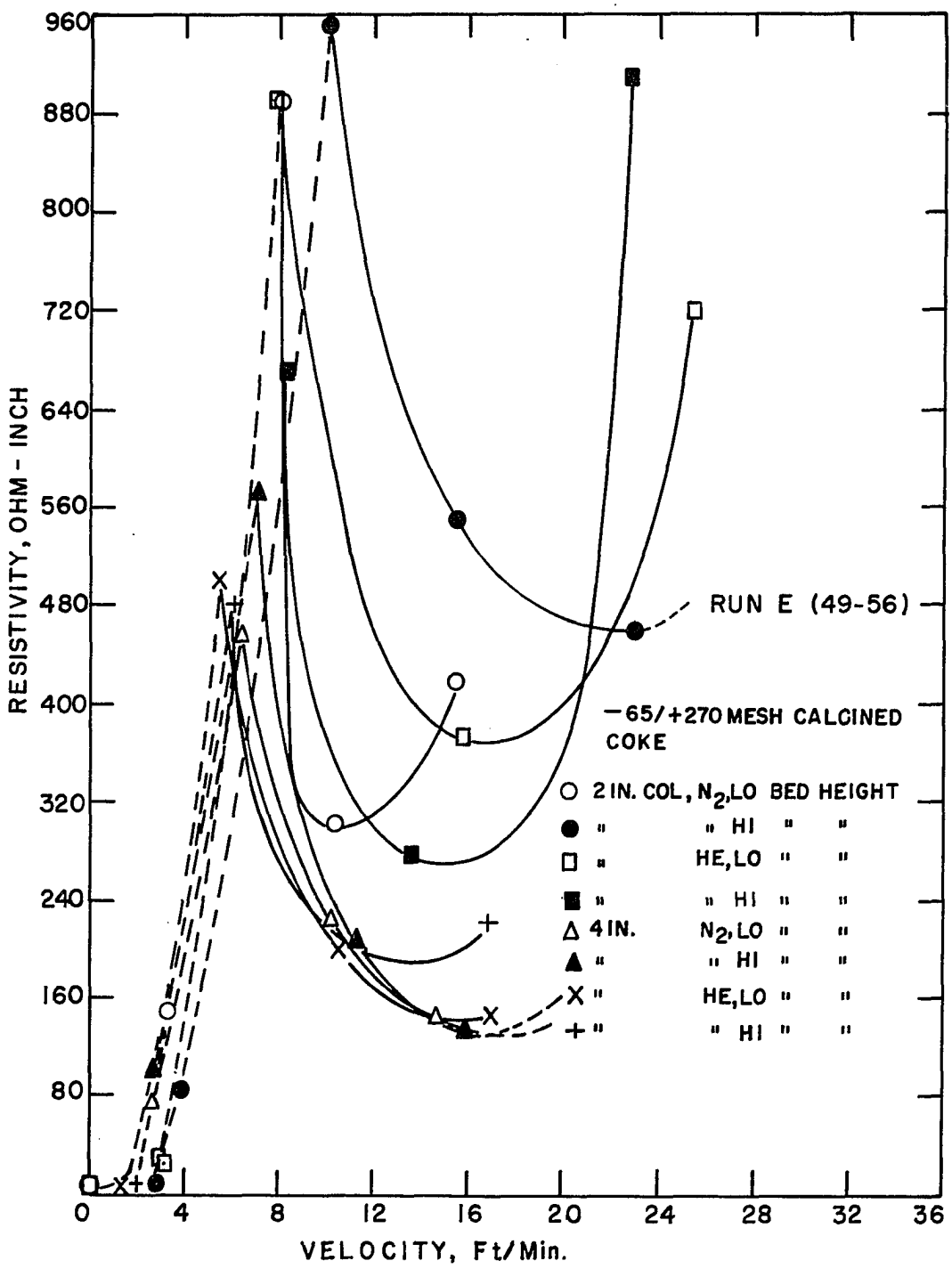
RESISTIVITY, OHM - INCH
960
880
800
720
640
560
480
400
320
240
160
80
0
4
8
12
16
20
24
28
32
36
VELOCITY, Ft/Min.
RUN E (49-56)
-65/+270 MESH CALCINED COKE
2 IN. COL, N2, LO BED HEIGHT
" " HI " "
" HE, LO " "
" " HI " "
4 IN. N2, LO " "
" " HI " "
" HE, LO " "
" " HI " "

resistivity, minimum fluidized resistivity, tne velocity at the peak fluidized resistivity and the velocity at the minimum fluidized resistivity, an analysis of variance of the data was made. All calculations were performed by digital computer using the "Aardvark" computer program.

To test the hypothesis that the parameters have an effect on the settled bed resistivity, for example, a certain significance level was decided upon and the experimental F value was compared with the value found in published F tables. If the calculated F value exceeded the tabulated F value, the hypothesis was accepted, if not, the hypothesis was rejected. Similar F tests were repeated for each parameter and each interaction term.

Settled bed resistivity The results of the analysis of variance for settled bed resistivity are given in Table 6.

Table 6. Analysis of variance (settled bed resistivity)

Source of variation	Degrees of freedom	Sum of squares	Mean square	F value
Material	8	17.381	2.173	92.08
Gas	1	0.027	0.027	1.17
Height	1	33.621	33.621	1424.87
Diameter (of bed)	1	99.991	99.991	4237.62
M x G	8	0.449	0.056	2.38
M x H	8	0.549	0.067	2.91
M x D	8	8.482	1.060	44.93
G x H	1	0.003	0.003	0.15
G x D	1	0.075	0.075	3.17
H x D	1	0.265	0.265	11.21
M x G x H	8	0.527	0.066	2.79
M x G x D	8	0.201	0.025	1.07
M x H x D	8	0.576	0.072	3.05
G x H x D	1	0.003	0.003	0.13
Error	8	0.189	0.024	--

The values of F from the tables are

$$F_{.025(1,8)} = 7.57$$

$$F_{.025(8,8)} = 4.43$$

Therefore, the hypothesis was accepted that material, height, diameter and the two way interactions of material and diameter and height and diameter had an effect on the settled bed resistivity at the 2.5 per cent level of significance. All other parameters and interactions were insignificant.

Peak fluidized resistivity The results of the analysis of variance for peak fluidized resistivity are given in Table 7.

Table 7. Analysis of variance (peak fluidized resistivity)

Source of variation	Degrees of freedom	Sum of squares	Mean square	F value
Material	8	1,324,696	165,587	11.07
Gas	1	113,740	113,740	7.61
Height	1	16,350	16,350	1.09
Diameter (of bed)	1	693,329	693,329	46.37
M x G	8	54,033	6,754	0.45
M x H	8	117,443	14,680	0.98
M x D	8	229,276	28,659	1.92
G x H	1	2,005	2,005	0.13
G x D	1	26,041	26,041	1.74
H x D	1	1,593	1,593	0.11
M x G x H	8	80,419	10,052	0.67
M x G x D	8	49,601	6,200	0.41
M x H x D	8	22,137	2,767	0.19
G x H x D	1	15,782	15,782	1.06
Error	8	119,626	14,953	--

The same tabular F values apply to Table 7 as applied to Table 6. Therefore, the hypothesis was accepted that material, gas and bed diameter had an effect on the peak fluidized resistivity at the 2.5 per cent level of significance. All other parameters and all interactions were insignificant.

Minimum fluidized resistivity The results of the analysis of variance for minimum fluidized resistivity are given in Table 8.

Table 8. Analysis of variance (minimum fluidized resistivity)

Source of variation	Degrees of freedom	Sum of squares	Mean square	F value
Material	8	34,840	4,355.1	2.43
Gas	1	289	289.2	0.16
Height	1	1,389	1,389.8	0.78
Diameter (of bed)	1	671,860	671,860.8	375.58
M x G	8	20,040	2,505.0	1.40
M x H	8	9,911	1,238.9	0.69
M x D	8	13,428	1,678.6	0.94
G x H	1	1,465	1,465.3	0.82
G x D	1	22,456	22,456.7	12.55
H x D	1	2,452	2,452.7	1.37
M x G x H	8	7,979	997.4	0.56
M x G x D	8	27,284	3,410.6	1.91
M x H x D	8	2,862	357.8	0.20
G x H x D	1	1,695	1,695.5	0.95
Error	8	14,310	1,788.9	--

Using the same tabular F values as for Table 5, the hypothesis was accepted that diameter and the two way interaction of gas and diameter had an effect on the minimum fluidized resistivity at the 2.5 per cent level of significance. All other parameters and two and three way

interactions were insignificant.

Velocity at the peak fluidized resistivity The results of the analysis of variance for velocity at the peak fluidized resistivity is given in Table 9.

Table 9. Analysis of variance (velocity at peak fluidized resistivity)

Source of variation	Degrees of freedom	Sum of squares	Mean square	F value
Material	8	193.042	24.130	212.68
Gas	1	27.938	27.938	246.24
Height	1	1.950	1.950	17.19
Diameter (of bed)	1	17.552	17.553	154.71
M x G	8	16.697	2.087	18.40
M x H	8	1.500	0.188	1.65
M x D	8	2.929	0.366	3.23
G x H	1	0.062	0.062	0.54
G x D	1	0.025	0.025	0.22
H x D	1	0.900	0.900	7.93
M x G x H	8	1.874	0.234	2.07
M x G x D	8	1.763	0.220	1.94
M x H x D	8	1.024	0.128	1.13
G x H x D	1	0.009	0.009	0.08
Error	8	0.908	0.113	--

Using the same tabular F values as for Table 6, the hypothesis was accepted that material, gas, bed height, bed diameter and the two way interactions of material and gas and height and diameter had an effect on the velocity at the peak fluidized resistivity at the 2.5 per cent level of significance. All other parameters and interactions were insignificant.

Velocity at the minimum fluidized resistivity The results of the analysis of variance for velocity at the minimum fluidized resistivity is given in Table 10.

Table 10. Analysis of variance (velocity at minimum fluidized resistivity)

Source of variation	Degrees of freedom	Sum of squares	Mean square	F value
Material	8	189.366	23.671	8.38
Gas	1	163.624	163.624	57.92
Height	1	0.029	0.029	0.01
Diameter (of bed)	1	468.281	468.281	165.75
M x G	8	96.300	12.037	4.26
M x H	8	2.531	0.316	0.11
M x D	8	69.886	8.736	3.09
M x H	1	2.777	2.777	0.98
G x D	1	5.917	5.917	2.09
H x D	1	1.350	1.350	0.48
M x G x H	8	41.097	5.137	1.82
M x G x D	8	60.000	7.500	2.65
M x H x D	8	35.786	4.473	1.58
G x H x D	1	-1.312	1.312	0.46
Error	8	22.602	2.825	--

Using the same tabular F values as for Table 6, the hypothesis was accepted that material, gas and bed diameter had an effect on the velocity at the minimum fluidized resistivity at the 2.5 per cent level of significance. All other parameters and all interactions were insignificant.

Summary of analysis of variance The results of the analysis of variance performed on the parameters of the experimental design are summarized in Table 11.

Table 11. Summary of analysis of variance

Dependent variable	Significant parameters
ρ_s	Material, height, diameter, M x D_b
ρ_p	Material, gas, diameter
ρ_m	Diameter, G x D_b
V_p	Material, gas, height, diameter, M x G, H_b x D_b
V_m	Material, gas, diameter

Stepwise regression analysis

It was now known from the analysis of variance just which parameters were the most significant. The next step was to develop a mathematical model which would correlate the five dependent variables listed in Table 11 with the independent variables. To do this, it was necessary that all parameters be represented by some measurable quantity. The bed material could be represented by

1. Particle size
2. Tangent of the angle of repose, and/or
3. Standard deviation of the particle size.

The gas could be represented by

1. Density, and/or
2. Viscosity.

The bed height and bed diameter were directly measurable.

The form of the mathematical model was chosen as

$$\log Y_1 = b_o + b_1 \log X_1 + b_2 \log X_2 \text{ ----- } + b_n \log X_n \qquad (29)$$

where Y = a dependent variable

X = an independent variable

b = a regression coefficient

log = a logarithm to the base 10

A stepwise regression analysis was performed with the aid of a computer program. This was carried out in the following manner:

1. The significance of each independent variable was determined by computing the F level.
2. The most significant variable was chosen and the regression coefficient b_o and the regression coefficient for the most significant variable were computed. The standard error of coefficients and standard error of the estimate were also computed.
3. The second most significant variable was then chosen and the regression coefficients and standard errors were computed for the previous variables as well as the new variable.
4. An F level of 2.00 was arbitrarily chosen as the limit of significance. When no more variables had an F level greater than 2.00, the computation was stopped and a multiple correlation coefficient was calculated.

This type of regression analysis has the advantage over multiple regression analysis of saving computer time that would ordinarily be spent in looking for these significant variables by trial and error methods. In multiple regression analysis it is necessary to select numerous

combinations of variables with the hope of eventually finding those that correlate most highly. By using stepwise regression analysis, the most significant variables are determined immediately. After obtaining the results of the stepwise regression analysis a multiple regression analysis can be performed on any combination of the significant variables plus any other variables of which it may appear advantageous to include.

Results A summary of the results of the stepwise regression analysis are shown in Table 12.

Discussion of results In comparing the results of the analysis of variance with the stepwise regression, the form of the mathematical model was such that no two factor interaction or product terms could be produced by the regression analysis. Therefore, the regression equation produced no interaction terms. A comparison shows the following:

1. For settled bed resistivity, the stepwise regression gave particle size D_p, representing the material term of the analysis of variance, and both gave bed height and bed diameter as significant factors.
2. The results for peak fluidized resistivity and velocity at the peak resistivity agreed exactly if interaction terms for the velocity are not considered.
3. For minimum fluidized resistivity, the stepwise regression gave the tangent of the angle of repose, tan Θ, and particle size, D_p, as significant factors which the analysis of variance did not.
4. Considerable disagreement was seen for the velocity at the

Table 12. Summary of stepwise regression analysis

Dependent variable	Independent variables	F level	Regression coefficient	Multiple correlation coefficient, R (R^2)
ρ_s	Constant	--	1.9225	
	D_b	114.81	-0.6765	
	H_b	106.19	-0.3003	
	D_p	71.75	-0.3068	0.95979 (0.92120)
ρ_p	Constant	--	5.1801	
	D_p	71.18	-1.0471	
	D_b	75.85	-0.5884	
	d_g	9.83	0.0702	0.88197 (0.77787)
ρ_m	Constant	--	3.9840	
	D_b	401.37	-1.1423	
	Tan θ	3.82	-3.3546	
	D_p	5.74	-0.7175	0.92772 (0.86066)
V_p	Constant	--	-0.1431	
	D_p	58.75	0.5831	
	d_g	16.46	0.0769	
	D_b	18.21	-0.2061	
	H_b	5.58	0.0804	0.80742 (0.65193)
V_m	Constant	--	0.3795	
	D_b	46.81	0.4028	
	Tan θ	16.37	-2.1639	
	σ_p	7.89	0.3047	0.73204 (0.53588)

minimum fluidized resistivity. The gas and bed diameter of the analysis of variance were replaced by the tangent of the angle of repose, tan θ, and the standard deviation, σ_p, of the stepwise regression.

The multiple correlation coefficient is a measure of the goodness of fit of the regression equation to the data. A coefficient of 1.00 would be a perfect fit. It could be considered in engineering that a coefficient of 0.90 would be a good fit whereas a coefficient of 0.80 would be a fair fit. However, these values are entirely arbitrary. The square of the multiple correlation coefficient, R^2, is of importance in that it gives the per cent of variation of the dependent variable that is accounted for by the model. As an example, ρ_s in Table 12 has an R^2 of 0.9212. This means that 92.12 per cent of the variation of ρ_s was accounted for by the model as measured by the sum of squares. The other 7.88 per cent was attributed to lack of fit, unconsidered variables and experimental error.

Multiple regression analysis

From the results of the stepwise regression analysis, it was known which independent variables were the most significant with respect to

1. The settled bed resistivity
2. The peak fluidized bed resistivity
3. The minimum fluidized bed resistivity
4. The gas velocity at the peak fluidized bed resistivity, and
5. The gas velocity at the minimum fluidized bed resistivity.

However, a multiple regression analysis was made to further verify the

results of the stepwise regression analysis and also to study the effect of adding some variables or substituting certain variables for those found to be significant by stepwise regression analysis. As an example of the latter, it was felt that the angle of repose might have an effect on the settled bed resistivity. The multiple regression analysis gave a t value which indicated that the angle of repose had no significant effect when added to the other parameters.

Results As a result of the multiple regression analysis, two correlations are presented for the peak fluidized resistivity. One is essentially the same as obtained by stepwise regression and the other has a term for bed height added. Two correlations are presented for minimum fluidized resistivity. One includes the tangent of the angle of repose similar to the stepwise regression results. The other replaces the tangent by the standard deviation of particle size. The results of the multiple regression analysis are shown in Table 13.

Discussion of results In comparing the coefficients of Tables 12 and 13, a slight difference will be noticed between any two equivalent coefficients. The reason for this is the multiple regression program is written for double precision whereas the stepwise regression program is not. Therefore, the coefficients of Table 13 are the more accurate. The "regression equation number" listed in the table identifies the tabulated results with a particular set of computer calculations that determined the results and is used here to put a "tag" on each dependent variable.

Table 13. Summary of multiple regression analysis

Dependent variable	Independent variables	Regression coefficient	t value	Multiple correlation coefficient, R (R^2)
Regression equation 210				
ρ_s	Constant	1.9276	--	
	D_b	-0.6769	24.07	
	H_b	-0.3007	14.70	
	D_p	-0.3090	8.57	0.9630 (0.9274)
Regression equation 201				
ρ_p	Constant	5.1845	--	
	D_p	-1.0489	12.79	
	D_b	-0.5892	9.21	
	d_g	0.07036	3.13	0.8895 (0.7912)
Regression equation 205				
ρ_p	Constant	5.2456	--	
	D_p	-1.0489	12.86	
	D_b	-0.5892	9.27	
	d_g	0.07044	3.15	
	H_b	-0.06243	1.35	0.8926 (0.7967)
Regression equation 217				
ρ_m	Constant	3.9964	--	
	D_b	-1.1429	20.98	
	Tan θ	-3.3800	2.78	
	D_p	-0.7247	2.39	0.9320 (0.8687)

Table 13. (continued)

Dependent variable	Independent variables	Regression coefficient	t value	Multiple correlation coefficient, R (R^2)
Regression equation 219				
ρ_m	Constant	1.3655	--	
	D_b	-1.1429	20.63	
	D_p	0.4669	2.65	
	σ_p	0.3827	2.29	0.9296 (0.8642)
Regression equation 216				
V_p	Constant	0.71986	--	
	D_p	0.5828	9.64	
	d_g	0.0769	4.64	
	D_b	-0.2061	4.37	
	H_b	0.0805	2.35	0.8219 (0.6756)
Regression equation 214				
V_m	Constant	0.3809	--	
	D_b	0.4028	7.85	
	Tan Θ	-2.1611	4.68	
	σ_p	0.3040	2.78	0.7493 (0.5615)

The significance of each variable was determined by the "t test" in which the t value determined from the regression is compared with a value from the t tables. In order to select a t value from the tables it is necessary to know the residual degrees of freedom and also to choose

the significance level. In all cases there were either three or four independent variables which resulted in either 68 or 67 residual degrees of freedom respectively. The significance level chosen was the five per cent level. From the t tables, at the five per cent level

$$t = 2.000 \text{ for } 60 \text{ degrees of freedom}$$

$$t = 1.994 \text{ for } 70 \text{ degrees of freedom}$$

Therefore, any variable having a t value less than 2.00 was considered insignificant. An exception to this is the second of the two correlations for peak fluidized resistivity (regression equation 205) where the bed height was included even though it had a t value of 1.35 which was close. (Bed height would have been significant at the 10 per cent level). Adding the bed height to the three independent variables of equation 201 only increases the multiple correlation coefficient from 0.8895 to 0.8926, an insignificant increase. Therefore, it can be concluded that although intuitively the bed height may have been considered significant, the analysis of the data indicates that it is not.

Actual and predicted values are given in Tables 14, 15 and 16 for settled bed resistivity, peak fluidized resistivity and minimum fluidized resistivity. Table 14 gives values for settled bed resistivity as determined by regression equation 210. Table 15 gives values for peak fluidized resistivity as determined by regression equation 201. Table 16 gives values for minimum fluidized resistivity as determined by regression equation 217. An examination of the actual and predicted values in the tables reveals that the actual and predicted values of Tables 14 and 16

Table 14. Actual and predicted values for settled bed resistivity (regression equation 210) calcined coke, Run E.

Run number	Actual value	Predicted value	Run number	Actual value	Predicted value
1	309.80	296.13	37	592.90	548.45
2	427.00	394.41	38	695.50	730.49
3	427.00	394.41	39	711.00	730.49
4	288.80	296.13	40	591.10	548.45
5	441.60	473.42	41	339.10	358.86
6	452.10	473.42	42	495.60	477.97
7	512.80	630.55	43	518.20	477.97
8	558.80	630.55	44	336.60	358.86
9	319.00	305.89	45	607.20	573.71
10	438.00	407.42	46	717.70	764.14
11	310.60	305.89	47	641.70	573.71
12	431.20	407.42	48	751.80	764.14
13	483.70	489.03	49	348.40	364.62
14	580.60	651.35	50	481.40	486.75
15	618.90	651.35	51	321.60	364.62
16	532.50	489.03	52	472.50	485.63
17	314.00	316.92	53	626.60	582.91
18	331.50	316.92	54	770.40	776.38
19	478.00	422.10	55	784.90	776.38
20	458.80	422.10	56	649.00	582.91
21	533.50	506.65	57	331.50	373.54
22	662.60	674.82	58	538.30	497.52
23	668.70	674.82	59	510.70	497.52
24	532.20	506.65	60	334.00	373.54
25	482.40	528.78	61	669.30	597.18
26	504.60	528.78	62	797.60	795.39
27	603.80	704.29	63	689.90	597.18
28	670.60	704.29	64	792.80	795.39
29	480.60	440.54	65	368.40	375.96
30	319.80	330.75	66	456.30	500.74
31	342.40	330.75	67	469.70	500.74
32	476.40	440.54	68	287.20	375.96
33	333.20	343.06	69	614.90	601.04
34	469.70	456.93	70	826.10	800.54
35	500.50	456.93	71	830.30	800.54
36	316.50	343.06	72	667.90	601.04

Table 15. Actual and predicted values for peak fluidized bed resistivity (regression equation 201) calcined coke, Run E.

Run number	Actual value	Predicted value	Run number	Actual value	Predicted value
1	214.16	217.79	37	701.16	540.13
2	241.45	217.67	38	513.79	539.98
3	273.60	249.87	39	932.89	620.02
4	249.15	249.88	40	510.48	620.32
5	336.76	375.89	41	393.57	480.08
6	299.09	327.52	42	459.54	479.79
7	342.00	328.02	43	425.47	417.80
8	358.10	376.40	44	504.58	418.03
9	248.15	279.46	45	676.63	628.82
10	250.41	279.32	46	697.66	628.42
11	217.50	243.31	47	978.54	722.33
12	231.65	243.24	48	874.29	721.99
13	425.78	366.19	49	480.39	441.40
14	489.43	366.04	50	501.06	441.16
15	396.77	420.50	51	570.73	506.87
16	378.87	420.64	52	454.52	506.60
17	241.87	315.16	53	854.93	762.50
18	256.02	274.33	54	889.53	762.03
19	262.96	274.08	55	893.02	663.51
20	320.15	314.75	56	669.76	663.92
21	450.79	473.93	57	464.48	479.13
22	566.34	473.67	58	562.85	479.10
23	418.60	412.51	59	427.78	550.07
24	457.40	412.68	60	621.54	550.44
25	433.36	477.05	61	727.57	827.93
26	646.93	547.93	62	769.32	826.85
27	484.70	547.67	63	676.04	720.17
28	463.91	477.12	64	390.80	719.56
29	303.09	316.88	65	455.86	489.47
30	283.81	317.01	66	623.13	488.88
31	351.54	364.63	67	785.21	560.13
32	340.57	364.30	68	627.48	562.13
33	428.65	412.54	69	503.87	845.71
34	434.59	414.08	70	934.25	845.07
35	392.65	358.85	71	577.70	735.75
36	309.85	359.10	72	453.28	735.80

Table 16. Actual and predicted values for minimum fluidized bed resistivity (regression equation 217) calcined coke, Run E.

Run number	Actual value	Predicted value	Run number	Actual value	Predicted value
1	127.84	144.89	37	286.00	361.73
2	155.72	144.89	38	316.00	361.73
3	171.96	144.89	39	456.00	361.73
4	148.00	144.89	40	363.00	361.73
5	263.00	319.94	41	103.00	139.97
6	285.00	319.94	42	940.00	139.97
7	279.00	319.94	43	146.00	139.97
8	314.62	319.94	44	142.99	139.97
9	160.00	152.53	45	364.00	309.09
10	168.00	152.53	46	314.00	309.09
11	160.00	152.53	47	284.00	309.09
12	150.00	152.53	48	292.00	309.09
13	268.00	336.82	49	190.00	147.01
14	320.00	336.82	50	142.99	147.01
15	395.00	336.82	51	130.00	147.01
16	368.00	336.82	52	136.00	147.01
17	144.00	160.23	53	460.00	324.63
18	169.00	160.23	54	302.00	324.63
19	174.00	160.23	55	368.00	324.63
20	166.00	160.23	56	270.00	324.63
21	392.00	353.83	57	151.00	136.13
22	416.00	353.83	58	139.00	136.13
23	392.00	353.83	59	129.00	136.13
24	319.00	353.83	60	146.00	136.13
25	279.00	345.93	61	308.00	300.61
26	376.00	345.93	62	305.00	300.61
27	398.00	345.93	63	344.00	300.61
28	375.00	345.93	64	376.00	300.61
29	220.00	156.66	65	190.00	144.90
30	182.00	156.66	66	184.00	144.90
31	155.00	156.66	67	118.00	144.90
32	144.00	156.66	68	123.00	144.90
33	135.00	163.82	69	353.00	319.96
34	128.00	163.82	70	317.00	319.96
35	186.00	163.82	71	263.39	319.96
36	146.00	163.82	72	245.00	319.96

for ρ_s and ρ_m respectively, are in good agreement for all but a few cases. The values in Table 15 for ρ_p have a greater number that have large differences. This is as would be expected from observing the multiple correlation coefficients since the coefficients for ρ_s and ρ_m are 0.9630 and 0.9320 respectively while the coefficient for ρ_p is lower at 0.8895.

Application of correlation to individual size fractions

In Figure 27 is plotted the logarithm of the fluidized resistivity against the logarithm of particle size for the single size fractions of calcined coke which had been fluidized for 89 hr. These values for the seven size fractions were obtained with the two inch diameter bed and with nitrogen as the fluidizing gas during Run D. Shown in comparison with the single size fraction values is a curve representing the second of the two correlation equations for peak fluidized resistivity. Although the results are not too unfavorable, it was expected that the single size fraction would compare more closely with the correlation equation. No explanation can be offered for the discrepancy.

Figure 27. Comparison of regression equation 201 for peak fluidized resistivity with the peak fluidized resistivity values of the single size fractions of Run D calcined coke

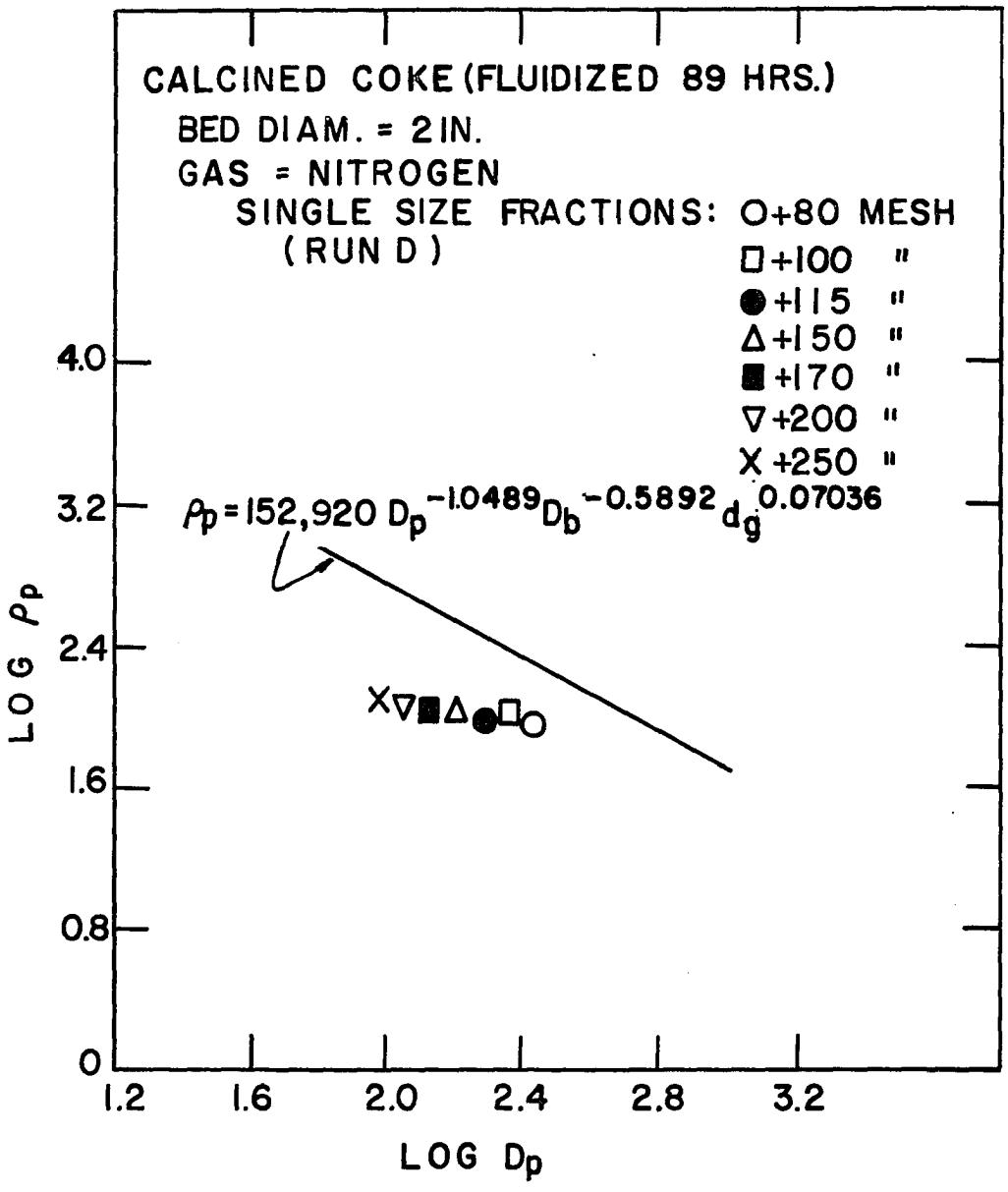
CALCINED COKE (FLUIDIZED 89 HRS.)
BED DIAM. = 2 IN.
GAS = NITROGEN
SINGLE SIZE FRACTIONS: O +80 MESH
(RUN D)
□ +100 "
● +115 "
Δ +150 "
■ +170 "
▽ +200 "
X +250 "
$\rho_p = 152{,}920\, D_p^{-1.0489} D_b^{-0.5892} d_g^{0.07036}$
LOG ρ_p
4.0
3.2
2.4
1.6
0.8
0
1.2
1.6
2.0
2.4
2.8
3.2
LOG D_p

SIGNIFICANT FINDINGS AND RECOMMENDATIONS

1. As the gas flow rate through a fluidized bed of conducting particles is increased, the electrical resistivity increases rapidly at the minimum (incipient) fluidization velocity and then passes through a peak. Then the resistivity usually decreases to a minimum and begins increasing again. The height and steepness of the peak depend on the particle size and nature of the bed material. The calcined coke materials tend to produce resistivity versus gas velocity curves with greater peaks. The resistivity curves for graphite curves show little if any tendency to peak.

2. When a given bed material is divided into its individual size fractions, the smaller fractions fluidize at lower velocities than the larger fractions. The curves of resistivity versus flow rate have more pronounced peaks for the smaller size fractions. However, the individual size fractions do not exhibit as large peaks as beds of mixed sizes.

3. There is a definite increase in resistivity with time as a bed of material is fluidized. The rate of increase is rapid at first but then decreases.

4. Due to the manner in which the electrical resistivity of a fluidized bed of conducting particles changes with gas flow rate, it does not appear feasible to correlate the resistivity over an entire range of flow rates. Therefore, it seems best to correlate the resistivities

at certain prominent points separately. The settled bed resistivity of calcined coke correlates well with bed diameter, bed height and particle size as follows:

$$\rho_s = 84.65\ D_b^{-0.6769}\ H_b^{-0.3007}\ D_p^{-0.3090}$$

The peak fluidized resistivity of calcined coke correlates well with particle size, bed diameter and gas density as follows:

$$\rho_p = 152{,}920\ D_p^{-1.0489}\ D_b^{-0.5892}\ d_g^{0.07036}$$

The minimum fluidized bed resistivity of calcined coke correlates well with bed diameter, particle size and a characteristic of the bed material which may be either standard deviation of the particle size or tangent of the angle of repose. However, the best fit is obtained with the tangent of the angle of repose as follows:

$$\rho_m = 9{,}918\ D_b^{-1.1429}\ (\tan\theta)^{-3.3800}\ D_p^{-0.7247}$$

5. The diameter of the fluidized bed column has a marked effect on the resistivity of a bed. Further investigation should be made to determine to what extent column diameter affects the resistivity in sizes larger than 2 and 4 in. inside diameters.

6. The correlation equations resulting from this investigation are valid only for the calcined coke used. Data should be collected for other carbon materials and the resistivities correlated so as to include

the basic resistivity of the material as a parameter.

7. Since the resistivity of carbon changes considerably as the temperature is increased and since the electrothermal fluidized bed would be used at high temperatures, further investigation should be made at elevated temperatures for the purpose of developing correlations including temperature as a parameter.

NOMENCLATURE

A	cross-sectional area, sq.in. or sq.ft.
A_b	cross-sectional area of the fluidized bed, sq.ft.
A_f	cross-sectional area of largest part of rotameter float, sq.ft.
A_w	cross-sectional area of narrowest part of rotameter annulus, sq.ft.
b	a regression coefficient
C	rotameter flow coefficient or a coefficient
D_b	diameter of bed, ft.
D_i	average particle size of the individual screen fraction, microns
D_p	average particle size of the bed material, microns
d	density, lb./cu.ft.
d_{cs}	density of air at 14.7 lb./sq.in.abs. and $70^{\circ}F$.
d_f	density of rotameter float, lb./cu.ft.
d_g	gas density, lb./cu.ft.
d_{gb}	density of the gas in the fluidized bed at bed conditions
d_{gr}	density of the gas at rotameter conditions of temperature and pressure, lb./cu.ft.
d_m	density of gas at wet test meter conditions of temperature and pressure, lb./cu.ft.
d_p	particle density, lb./cu.ft.
d_w	density of fluid flowing in rotameter, lb./cu.ft.
E	potential difference, millivolts
G	gas used in fluidizing the bed

g	acceleration of gravity, ft./(sec.)^2
H_b	height of settled bed, ft.
I	electric current flowing through the bed, milliamps
L	length of current path, cm.
M	mass rate of flow, lb./min.
M_b	material used in the fluidized bed
N	total number of particles in a mixture
n_i	number of particles in an individual screen fraction
P	pressure, lb./sq.ft.abs.
$\overline{P}_b$	average pressure of the gas in the fluidized bed, lb./sq.in.abs.
P_{gr}	pressure at the entrance to the rotameter, lb./sq.in.abs.
Q	volume flow rate, cu.ft./min.; in dimensional analysis, charge
Q_{cs}	corrected scale reading of the rotameter, std.cu.ft./min. of air
Q_{gb}	volume flow rate of gas in the fluidized bed at bed conditions of pressure and temperature, cu.ft./min.
Q_{gr}	volume flow rate at rotameter conditions of temperature and pressure, cu.ft./min.
Q_m	volume flow rate measured by wet test meter, cu.ft./min.
R	resistance, ohms
R_g	gas constant, ft./^oR.
R_{gb}	gas constant of gas in the fluidized bed, ft./^oR.
R_{gr}	gas constant of gas in rotameter, ft./^oR.
R_m	gas constant of the measured gas, ft./^oR.
T	temperature, ^oR.
T_b	temperature of the bed, ^oR.

T_{gr} temperature of the gas entering the rotameter, ^{o}R.

V velocity, ft./min.

V_b superficial or apparent velocity of the gas in the fluidized bed, ft./min.

V_m superficial velocity of the gas in the fluidized bed at the point of minimum resistivity, ft./min.

V_{mf} minimum fluidization or incipient fluidization velocity, ft./min.

V_p superficial velocity of the gas in the fluidized bed at the point of peak resistivity, ft./min.

v_f volume of rotameter float, cu.ft.

Y a dependent variable

X an independent variable

Greek letters

θ angle of repose of the bed material

μ viscosity of gas, lb./ft.sec.

ρ resistivity, ohm-cm.

ρ_f resistivity of the fluidized bed, ohm-in.

ρ_m minimum resistivity of the fluidized bed after passing the peak resistivity, ohm-in.

ρ_p peak resistivity of the fluidized bed, ohm-in.

ρ_s resistivity of settled bed, ohm-in.

σ_p standard deviation of particle size, microns

LITERATURE CITED

1. Leva, M. Fluidization. New York, N.Y., McGraw-Hill Book Co., Inc. 1959.

2. Zenz, F. A. and Othmer, D. F. Fluidization and fluid-particle systems. New York, N.Y., Reinhold Publishing Corp. 1960.

3. Goldberger, W. M. and Nack, H. Novel uses of fluidized beds in chemical processing. Battelle Technical Review 13, No. 11: 3-9. 1964.

4. Johnson, H. S. and Andersen, A. H. Process for the preparation of carbon monoxide: assigned to Shawinigan Chemicals Limited, Montreal, Canada. U.S. Patent 2,921,840. 19 January 1960.

5. Johnson, H. S. and Andersen, A. H. Process for the preparation of titanium tetrachloride: assigned to Shawinigan Chemicals Limited, Montreal, Canada. U.S. Patent 2,948,587. 9 August 1960.

6. Schenck, H. and Wenzel, W. Electrical heating process and apparatus. U.S. Patent 2,978,315. 4 April 1961.

7. Johnson, H. S. Electrothermic fluidized bed apparatus: assigned to Shawinigan Chemicals Limited, Montreal, Canada. U.S. Patent 3,006,838. 31 October 1961.

8. Othmer, D. F., editor. Fluidization. New York, N.Y., Reinhold Publishing Corp. 1956.

9. Davidson, J. F. and Harrison, D. Fluidized particles. Cambridge, Mass., University Press. 1963.

10. Romero, J. B. and Smith, H. W. Flash X-ray analysis of fluidized beds. American Institute of Chemical Engineers Journal 11: 595-600. 1965

11. Wace, P. F. and Burnett, S. J. Flow patterns in gas-fluidised beds. Institution of Chemical Engineers Transactions 39: 168-174. 1961.

12. Johnson, H. S. and Andersen, A. H. Process for the preparation of carbon disulphide and for the desulphurization of coke: assigned to Shawinigan Chemicals Limited, Montreal, Canada. U.S. Patent 3,009,781. 21 November 1961.

13. Johnson, H. S. and Reid, J. Process for preparation of carbon disulphide: assigned to Shawinigan Chemicals Limited, Montreal, Canada. U.S. Patent 3,034,863. 15 May 1962.

14. Kennedy, D. J. Preparation of hydrocyanic acid: assigned to Shawinigan Chemical Limited, Montreal, Canada. U.S. Patent 3,032,396. 1 May 1962.

15. Johnson, H. S. and Andersen, A. H. Process for preparation of hydrocyanic acid: assigned to Shawinigan Chemicals Limited, Quebec, Canada. U.S. Patent 2,958,584. 1 November 1960.

16. Kennedy, D. J. and Shine, N. R. Production of hydrogen cyanide: assigned to Shawinigan Chemicals Limited, Quebec, Canada. U.S. Patent 3,097,921. 16 July 1963.

17. Waterhouse, D. Possible fluidized bed applications in steel foundries. Journal of steel castings research No. 32: 1-3. January 1964.

18. Johnson, H. S. Electrothermic fluidized bed apparatus: assigned to Shawinigan Chemical Limited, Montreal, Canada. U.S. Patent 3,006,838. 31 October 1961.

19. Johnson, H. S. Reactions in a fluidized coke bed with self-resistive heating. Canadian Journal of Chemical Engineering 39: 145-147. 1961.

20. Winkler, F. Water gas: assigned to I. G. Farbenindustrie. U.S. Patent 1,857,799. 10 May 1932.

21. Garbo, P. W. Fluidization in zinc production: assigned to American Metal Co., Ltd. U.S. Patent 2,475,607. 12 July 1949.

22. Pevere, E. F., Beacon, H. V., Hess, G. and Arnold, G. B. Spark discharge activated chemical reactions: assigned to the Texas Co., New York, N.Y. U.S. Patent 2,799,640. 16 July 1957.

23. Shawinigan unwraps electrofluid reactor. Chemical and Engineering News 38, No. 47: 55-56. 21 November 1960.

24. Goldberger, W. M., Hanway, J. E., Jr. and Langston, B. G. The electrothermal fluidized bed. Chemical Engineering Progress 61, No. 2: 63-67. 1965.

25. Pinnick, H. T. Electronic properties of carbons and graphites. Conferences on Carbon Proceedings 1-2: 3-11. 1956.

26. Mrozowski, S. Semiconductivity and diamagnetism of polycrystalline graphite and condensed ring systems. Physical Review 85: 609-620. 1952.

27. Walker, P. J., Jr. and Rusinko, F., Jr. Determination of the electrical resistivity of particulate carbons. Fuel 36: 43-50. 1957.

28. Takahashi, H. Electrical resistance of carbon powders. II. Electrical resistance of freely heaped carbon powders (translated title). Chemical Society of Japan Journal Pure Chemistry Section 71: 105-108. 1950.

29. Takahashi, H. Electrical resistance of carbon powders. III. Considerations by models on the electrical resistances of freely heaped carbon powders and a report on some related experiments (translated title). Chemical Society of Japan Journal Pure Chemistry Section 71: 108-111. 1950.

30. Goucher, F. S. The carbon microphone: an account of some researches bearing on its action. Franklin Institute Journal 17: 407-442. 1934.

31. Grisdale, R. O. The properties of carbon contacts. Journal of Applied Physics 24: 1288-1296. 1953.

32. Primak, W. and Fuchs, L. The electrical conductivities of natural graphite crystals. Physical Review 86: 651. 1952.

33. White, F. S. Some factors affecting the anisotopy of extruded carbon. Conference on Carbon Proceedings 4: 675-681. 1960.

34. Gopalaswamy, T. R., Subramanian, N. R. and Joglekar, G. D. Measurement of the electrical resistance of sized powders at different bulk densities. Part II. Graphite powders. Journal of Scientific and Industrial Research 18A: 60-65. 1959.

35. Benson, G., Gluck, J., and Kaufmann, C. Electric-conductivity measurements of carbon blacks. Electrochemical Society Transactions 90: 441-447. 1946.

36. Joglekar, G. D., Sen, D. and Gopalaswamy, T. R. Measurement of electrical resistance of sized powders at different bulk densities. Part I. Petroleum coke and retort carbon powders. Journal of Scientific and Industrical Research 18A: 21-24. 1959.

37. Goldschmidt, D. and Le Goff, P. Resistance electrique des lits fluidises. I. Resistances moyennes de grains conducteurs fluidises par air: resultats preliminaires. Chemical Engineering Science 18: 805-806. 1963.

38. Graham, W. and Harvey, E. A. The electrical resistance of fluidized beds of coke and graphite. Canadian Journal of Chemical Engineering 13: 146-149. 1965.

39. Hayakawa, T., Graham, W. and Osberg, G. L. A resistance probe method for determining local solid particle mixing rates in a batch fluidized bed. Canadian Journal of Chemical engineering 42: 99-103. 1964.

40. Graham, W. and Harvey, E. A. The electrical resistance of fluidized beds of coke and graphite. Canadian Journal of Chemical Engineering 13: 146-149. 1965.

41. Goldschmidt, D. Mèthodes electriques d'etude d'un lit fluidisè de grains conducteurs. Unpublished D.Sc. thesis. Nancy, France, Library, University of Nancy. 1965.

42. Reed, A. K. and Goldberger, W. M. Electrical behavior in fluidized beds of conducting solids. Unpublished multilithed paper (preprint 23 D) presented at Symposium on Fundamental and Applied Fluidization, Part II, American Institute of Chemical Engineers, Dallas, Texas, February 6-9, 1966. New York, N.Y., American Institute of Chemical Engineers. ca. 1966.

43. Graham, W. and Harvey, E. A. The electrical conductivity of fluidized beds of coke and graphite up to 1200°C. Canadian Journal of Chemical Engineering 14: 17-19. 1966.

44. Silsbee, F. B. A study of the inductance of four-terminal resistance standards. U.S. Bureau of Standards Bulletin 13: 375-422. 1916-17.

45. Silsbee, F. B. Notes on the design of 4-terminal resistance standards for alternating currents. U.S. Bureau of Standards Journal of Research 4: 73-107. 1930.

46. Schoenborn, E. M., Jr. and Colburn, A. P. The flow mechanism and performance of the rotameter. American Institute of Chemical Engineers Transactions 35: 359-389. 1939.

47. Lindgren, B. W. and McElrath, G. W. Introduction to probability and statistics. New York, N.Y., The Macmillan Company. 1963.

48. Murphy, G. Similitude in engineering. New York, N.Y., Ronald Press. 1950.

ACKNOWLEDGEMENTS

The author wishes to express his appreciation to the following persons and organizations:

Dr. Thomas D. Wheelock for suggesting the problem, for the many hours spent in discussing the problem, for his assistance in obtaining equipment and materials, and for his advice and counsel.

Prof. Henry M. Black for his assistance in expediting equipment purchases during the early phases of the investigation.

Prof. Edward J. Carney and the Statistical Laboratory for assistance in performing the analysis of variance and the multiple regression analysis of the data through the use of computer programs.

Dr. David V. Huntsberger for suggesting the experimental design used in this investigation and for advice regarding the statistical analysis.

Mrs. Gretchen Snowden and the Statistical Laboratory for assistance in performing the stepwise regression analysis through the use of a computer program.

The President's Permanent Objectives Committee of the Alumni Achievement Fund and the Engineering Research Institute for providing funds for the purchase and fabrication of equipment, materials and supplies.

The Iowa State University Computation Center for providing computer time for performing statistical analysis of data.

Numerous colleagues and staff members of the Mechanical Engineering Department who have given suggestions and assistance throughout this investigation.

The Humble Oil and Refining Company, Billings, Montana, for providing petroleum coke without charge.

A special note of appreciation and gratitude goes to the author's wife for her encouragement and untiring support throughout the entire project and for her typing of the manuscript.

APPENDIX

Rotameter Calibration Calculations

By the Continuity Equation, Equation 6, the mass rate of flow is equal to the product of the volume rate of flow and the density and for a given mass rate of flow,

$$\frac{Q_m}{Q_{gr}} = \frac{d_{gr}}{d_m} \tag{30}$$

where Q_m = volume flow rate measured by wet test meter, cu.ft./min.

d_m = density of gas measured at wet test meter conditions of temperature and pressure, lb./cu.ft.

Q_{gr} = volume flow rate of measured gas at rotameter conditions of temperature and pressure, cu.ft./min.

d_{gr} = density of gas at rotameter conditions of temperature and pressure, lb./cu.ft.

Equation 5 relates the flow rates of gases at different densities as measures by a rotameter as follows:

$$\frac{Q_{cs}}{Q_{gr}} = \left(\frac{d_{gr}}{d_{cs}}\right)^{\frac{1}{2}} \tag{5}$$

where Q_{cs} = the corrected scale reading of the rotameter, std.cu.ft./min. of air.

d_{cs} = density of air at standard conditions of 14.7 lb./sq.in.abs. and 70^{o}F.

Combining Equations 5 and 30 results in

$$Q_{cs} = \left(\frac{d_{gr}}{d_{cs}}\right)^{\frac{1}{2}} \frac{d_m}{d_{gr}} Q_m \tag{31}$$

From the equation of state of an ideal gas,

$$P = dR_g T \tag{10}$$

and substituting for density in terms of pressure and temperature, Equation 31 becomes

$$Q_{cs} = \left(\frac{R_{cs} T_{cs}}{P_{cs} P_{gr} R_m T_m}\right)^{\frac{1}{2}} P_m Q_m \tag{32}$$

or

$$Q_{cs} = \left(\frac{53.3 \times 530}{14.7 \times R_m P_{gr} T_m}\right)^{\frac{1}{2}} P_m Q_m \tag{33}$$

$$Q_{cs} = 43.8 \left(\frac{1}{R_m P_{gr} T_m}\right)^{\frac{1}{2}} P_m Q_m \tag{34}$$

Low range rotameter

In calibrating the low range rotameter, the procedure was to measure the flow rate using a wet test meter, and then by knowing the temperatures and pressures of the gas at the wet tesc meter and at the entrance to the rotameter, to calculate the correct scale reading in standard cubic feet per minute of air. As an example, using a spherical model float with nitrogen as the gas flowing the following data were obtained:

$$P_{gr} = 14.28 \text{ lb./sq.in.abs.}$$
$$T_m = 542^{\circ}\text{R.}$$
$$P_m = 14.09 \text{ lb./sq.in.abs.}$$
$$Q_m = 0.1392 \text{ cu.ft./min.}$$
$$R_m = 55.16 \text{ ft./}^{\circ}\text{F.}$$

Substituting into Equation 34,

$$Q_{cs} = 43.8 \left(\frac{1}{55.16 \times 14.28 \times 542} \right)^{\frac{1}{2}} 14.09(0.1392)$$
$$= 0.132 \text{ std.cu.ft./min. of air.}$$

In comparison, the scale reading was 0.137 std.cu.ft./min. of air which gives a difference of 3.8 per cent.

High range rotameter

In calibrating the high range rotameter, the procedure was to measure the flow rate using the displacement of the gas storage tank for a given length of time, and then by knowing the temperatures and pressures of the gas in the storage tank and at the entrance to the rotameter, to calculate the correct scale reading in standard cubic feet per minute of air. As an example, with helium as the gas flowing the following data were obtained:

Tank displaced 1.734 cu. ft. in 1.205 min.

therefore
$$Q_m = \frac{1.734}{1.205} = 1.44 \text{ cu.ft./min.}$$
$$R_m = 386.3 \text{ ft./}^{\circ}\text{R.}$$
$$P_m = 14.29 \text{ lb./sq.in.abs.}$$
$$T_m = 537^{\circ}\text{R.}$$

$$P_{gr} = 14.34 \text{ lb./sq.in.abs.}$$

Substituting the above values in Equation 34

$$Q_{cs} = \left(\frac{1}{386.3 \times 14.34 \times 537}\right)^{\frac{1}{2}} 14.29(1.44)$$

$$= 0.523 \text{ std.cu.ft./min. of air.}$$

In comparison, the scale reading was 0.60 std.cu.ft./min. of air which gives a difference of 14.7 per cent.

Both the high range and low range rotameters were calibrated using nitrogen and helium. Calibration curves were drawn up and were used in determining the corrected scale reading.

Sample Calculations

Gas velocity

The superficial or apparent velocity of the gas in the fluidized bed column based on the cross-sectional area of the column was calculated from Equation 11

$$V_{gb} = \left(\frac{P_{cs}P_{gr}}{R_{cs}T_{cs}R_{gr}T_{gr}}\right)^{\frac{1}{2}} \frac{R_{gb}T_{gb}Q_{cs}}{A_b P_{gb}} \qquad (11)$$

Helium, four inch column Using data from Run E-1, Table 1, in which helium was the fluidizing gas in the four inch inside diameter column and noting that $R_{gr} = R_{gb}$ which is the gas constant for helium and also that $T_{gr} = T_{gb}$ at all times, it follows from Equation 11 that

$$V_{gb} = \left(\frac{14.7 \times 144 \times 16.35 \times 144}{53.3 \times 530 \times 386.3 \times 535}\right)^{\frac{1}{2}} \frac{386.3 \times 535 \times 0.71}{\frac{\pi(2)^2}{144} \times 14.55 \times 144}$$

$$= 23.44 \text{ ft./min.}$$

Nitrogen, two inch column Using data from Run E-1, Table 1, in which nitrogen was the fluidizing gas in the two inch inside diameter column, it follows from Equation 11 that

$$V_{gb} = \left(\frac{14.7 \times 144 \times 15.49 \times 144}{53.3 \times 530 \times 55.16 \times 538}\right)^{\frac{1}{2}} \frac{55.16 \times 538 \times 0.375}{\frac{\pi(1)^2}{144} \times 14.72 \times 144}$$

$$= 18.02 \text{ ft./min.}$$

Electrical resistivity

The expression relating electrical resistance and resistivity is given by Equation 1 as

$$R = \frac{\rho L}{A} \tag{1}$$

or expressing resistivity in terms of resistance.

$$\rho = \frac{RA}{L} \tag{35}$$

By Ohm's Law

$$R = \frac{E}{I} \tag{36}$$

where E = potential difference, millivolts

I = current flowing through the bed, milliamps

Combining Equations 35 and 36 results in

$$\rho = \frac{EA}{IL} \tag{37}$$

From data of Run E-1, Table 1,

$$\rho = \frac{40.0\pi(2)^2}{2.62 \times 1.5}$$

$$= 127.84 \text{ ohms}$$

Average particle size

The average particle size was calculated from Equation 12

$$D_p = \frac{\sum_i (n_i D_i)}{\sum_i n_i} \tag{12}$$

For a mixture of -65/+80, -80/+100 and -100/+115 mesh

$$D_p = \frac{(2.008 \times 10^8)(193.5) + (3.308 \times 10^8)(163) + (4.627 \times 10^8)(137)}{(2.008 \times 10^8) + (3.308 \times 10^8) + (4.627 \times 10^8)}$$

$$= 157.1 \text{ microns.}$$

Standard deviation of particle size

The equation for determining standard deviation of particle size was given as Equation 13

$$\sigma_p = \left(\frac{1}{N-1} \left(\Sigma n_i d_i^2 - \frac{(\Sigma n_i D_i)^2}{N} \right) \right)^{\frac{1}{2}} \tag{13}$$

For large N, Equation 13 reduces to

$$\sigma_p = \left(\frac{1}{N} \Sigma n_i D_i^2 - D_p^2 \right)^{\frac{1}{2}} \tag{38}$$

For -65/+80, -80/+100 and -100/+115 mesh

$$\sigma_p = \left(\frac{(75.2 \times 10^{11}) + (87.9 \times 10^{11}) + (84.8 \times 10^{11})}{9.943 \times 10^{8}} - (157.1)^2 \right)^{\frac{1}{2}}$$

$$= 15.92 \text{ microns.}$$

Table 17. Tabulated results of Run E

Calcined coke

Pretreatment: Crushed, screened, fluidized continuously for 89 hr., screened

Run No.	Average particle diameter, microns	Gas	Col. dia., in.	Bed height	Tangent angle of repose	Particle size standard deviation	Bed temp. $^{o}F.$	Average bed pressure, lb./sq.in.-abs.	Gas velocity, ft./min.	Resistivity, ohm-in.
1	174.5	He	4	Hi[a]	0.7224	15.03	75	14.30	0.00	3.10[b]
								14.48	4.89	3.51
								14.54	5.73	18.47
								14.55	6.05	70.74
								14.54	9.95	214.16[c]
								14.54	10.61	204.61
								14.54	13.87	163.76
								14.54	17.11	139.56
								14.55	23.44	127.84[d]
2	174.5	He	4	Lo	0.7224	15.03	75	14.31	0.00	4.27[b]
								14.40	4.91	6.27
								14.44	6.05	98.45
								14.43	7.34	54.00

[a]Hi and Lo bed height refers to the height of the settled bed as being 13 3/4 and 4 3/8 in. respectively above the uppermost potential probe.

[b]Settled resistivity.

[c]Peak resistivity and velocity values.

[d]Minimum fluidized resistivity and velocity values. Parentheses indicate values were obtained by estimation from a plot of resistivity against velocity.

Table 17. (continued)

Run No.	Average particle diameter, microns	Gas	Col. dia., in.	Bed height	Tangent angle of repose	Particle size standard deviation	Bed temp. °F.	Average bed pressure, lb./sq.in.-abs.	Gas velocity, ft./min.	Resis-tivity, ohm-in.
								14.43	9.62	241.45[c]
								14.44	13.85	175.81
								14.43	17.12	155.72[d]
								14.44	26.61	372.55
3	174.5	N_2	4	Lo	0.7224	15.03	74	14.50	0.00	4.27[b]
								14.61	6.34	21.35
								14.62	7.07	135.38
								14.62	9.14	72.67
								14.62	11.24	242.79
								14.62	11.61	273.60[c]
								14.62	14.86	211.06
								14.62	20.99	171.96[d]
4	174.5	N_2	4	Hi	0.7224	15.03	78	14.50	0.00	2.89[b]
								14.67	4.96	3.37
								14.73	6.61	27.21
								14.74	6.96	77.19
								14.73	8.80	61.12
								14.73	10.70	249.15[c]
								14.74	16.23	150.70
									(18.00)	(148.00)[d]
								14.74	21.88	168.28
5	174.5	N_2	2	Hi	0.7224	15.03	78	14.48	0.00	4.42[b]
								14.65	6.02	4.56
								14.71	8.05	97.43
								14.71	11.52	274.60
								14.71	11.91	336.76[c]

Table 17. (continued)

Run No.	Average particle diameter, microns	Gas	Col. dia., in.	Bed height	Tangent angle of repose	Particle size standard deviation	Bed temp. $^{o}F.$	Average bed pressure, lb./sq.in.-abs.	Gas velocity, ft./min.	Resistivity, ohm-in.
								14.71	13.16	271.88
									(14.50)	(263.00)[d]
								14.72	18.02	334.88
6	174.5	He	2	Hi	0.7224	15.03	75	14.24	0.00	4.52[b]
								14.42	5.56	4.71
								14.47	7.09	28.86
								14.46	10.41	299.09[c]
									(12.60)	(285.00)[d]
								14.47	13.63	286.95
								14.48	18.04	356.23
7	174.5	He	2	Lo	0.7224	15.03	72	14.59	0.00	5.13[b]
								14.65	4.11	5.46
								14.69	6.99	74.09
								14.69	10.26	342.00[c]
								14.69	13.43	282.30
									(14.60)	(279.00)[d]
								14.69	22.28	396.62
8	174.5	N_2	2	Lo	0.7224	15.03	71	14.70	0.00	5.59[b]
								14.75	4.31	5.80
								14.80	7.85	96.28
								14.80	11.37	358.10[c]
								14.80	15.38	313.90[d]
								14.81	22.85	523.25
9	157.1	N_2	4	Hi	0.7277	15.92	76	14.44	0.00	3.19[b]
								14.94	3.48	3.38

Table 17. (continued)

Run No.	Average particle diameter, microns	Gas	Col. dia., in.	Bed height	Tangent angle of repose	Particle size standard deviation	Bed temp. $^{o}F.$	Average bed pressure, lb./sq.in.-abs.	Gas velocity, ft./min.	Resistivity, ohm-in.
								15.03	5.68	44.83
								15.04	10.58	248.15[c]
								15.05	16.99	173.89
								15.07	22.66	159.49
									(25.00)	(160.00)[d]
								15.04	13.47	182.93
10	157.1	N_2	4	Lo	0.7277	15.92	74	14.40	0.00	4.39[b]
								14.82	3.53	5.41
								14.87	5.80	52.93
								14.87	10.18	250.41[c]
								14.87	11.68	200.93
									(17.00)	(168.00)[d]
								14.89	19.54	172.46
								14.90	23.29	577.00
11	157.1	He	4	Hi	0.7277	15.92	76	14.40	0.00	3.11[b]
								14.67	4.27	4.14
								14.70	4.91	6.68
								14.69	9.11	217.50[c]
								14.71	17.07	161.16
									(17.10)	(160.00)[d]
								14.72	23.33	480.13
								14.70	13.73	170.62
12	157.1	He	4	Lo	0.7277	15.92	75	14.43	0.00	4.31[b]
								14.55	3.25	5.02
								14.61	5.23	61.94
								14.61	9.75	231.65[c]

Table 17. (continued)

Run No.	Average particle diameter, microns	Gas	Col. dia., in.	Bed height	Tangent angle of repose	Particle size standard deviation	Bed temp. $^{o}F.$	Average bed pressure, lb./sq.in.-abs.	Gas velocity, ft./min.	Resistivity, ohm-in.
								14.62	16.88	160.07
									(23.00)	(150.00)[d]
								14.62	26.43	149.61
								14.63	36.33	176.23
13	157.1	He	2	Hi	0.7277	15.92	74	14.47	0.00	4.84[b]
								14.64	3.64	4.84
								14.73	5.77	32.19
								14.73	10.05	425.78[c]
								14.73	13.47	299.01
									(15.60)	(268.00)[d]
								14.74	20.04	363.18
								14.75	25.14	394.84
14	157.1	He	2	Lo	0.7277	15.92	73	14.47	0.00	5.81[b]
								14.57	3.47	6.19
								14.61	5.77	140.73
								14.61	9.63	489.43[c]
									(15.60)	(320.00)[d]
								14.61	15.64	381.16
								14.62	25.17	644.64
15	157.1	N_2	2	Lo	0.7277	15.92	70	14.46	0.00	6.19[b]
								14.85	3.32	6.55
								14.90	7.04	146.51
								14.90	6.09	42.86
								14.90	11.35	396.77[c]
									(12.50)	(395.00)[d]
								14.91	17.72	457.68

Table 17. (continued)

Run No.	Average particle diameter, microns	Gas	Col. dia., in.	Bed height	Tangent angle of repose	Particle size standard deviation	Bed temp. $^{o}F.$	Average bed pressure, lb./sq.in.-abs.	Gas velocity, ft./min.	Resistivity, ohm-in.
16	157.1	N_2	2	Hi	0.7277	15.92	71	14.44	0.00	5.33[b]
								14.97	5.45	5.97
								15.00	6.67	39.64
								15.00	11.38	378.87[c]
									(14.20)	(368.00)[d]
								15.01	17.75	382.73
								15.02	27.52	852.42
17	140.1	N_2	4	Hi	0.7350	24.00	75	14.44	0.00	3.14[b]
								15.06	3.55	3.78
								15.00	4.40	4.88
								15.03	9.75	241.87[c]
								15.03	13.42	175.81
								15.05	17.99	171.63
									(26.20)	(144.00)[d]
								15.07	27.02	144.84
18	140.1	He	4	Hi	0.7350	24.00	76	14.39	0.00	3.32[b]
								14.65	4.22	3.70
								14.65	4.13	4.23
								14.67	4.56	81.61
								14.68	8.64	256.02[c]
								14.69	15.41	184.50
								14.70	23.27	169.37
									(24.00)	(169.00)[d]
								14.71	29.54	171.80
19	140.1	He	4	Lo	0.7350	24.00	78	14.37	0.00	4.78[b]
								14.48	2.61	5.35

Table 17. (continued)

Run No.	Average particle diameter, microns	Gas	Col. dia., in.	Bed height	Tangent angle of repose	Particle size standard deviation	Bed temp. $^{o}F.$	Average bed pressure, lb./sq.in.-abs.	Gas velocity, ft./min.	Resistivity, ohm-in.
								14.53	4.47	10.08
								14.54	8.98	262.96
								14.55	16.98	180.33
									(21.60)	(174.00)[d]
								14.56	23.33	176.06
								14.57	36.26	207.88
20	140.1	N_2	4	Lo	0.7350	24.00	78	14.37	0.00	4.59[b]
								14.78	2.59	5.33
								14.83	4.45	17.23
								14.84	9.18	320.15[c]
								14.85	15.94	169.53
									(18.20)	(166.00)[d]
								14.87	20.89	218.84
								14.87	25.95	180.58
21	140.1	N_2	2	Hi	0.7350	24.00	76	14.41	0.00	5.34[b]
								14.93	4.73	5.70
								14.96	5.66	69.07
								14.96	10.79	375.71
								14.96	10.80	450.79[c]
								14.97	13.05	398.67
									(14.50)	(392.00)[d]
								14.98	20.28	545.56
22	140.1	N_2	2	Lo	0.7350	24.00	76	14.40	0.00	6.63[b]
								14.77	1.59	6.29
								14.83	4.72	23.04
								14.85	10.21	566.34[c]

Table 17. (continued)

Run No.	Average particle diameter, microns	Gas	Col. dia., in.	Bed height	Tangent angle of repose	Particle size standard deviation	Bed temp. $^{o}F.$	Average bed pressure, lb./sq.in.-abs.	Gas velocity, ft./min.	Resistivity, ohm-in.
								14.85	13.06	420.65
									(14.40)	(416.00)[d]
								14.85	20.29	613.94
23	140.1	He	2	Lo	0.7350	24.00	76	14.43	0.00	6.69[b]
								14.51	3.27	6.37
								14.57	4.78	17.14
								14.57	8.84	418.60[c]
								14.56	13.69	392.73
									(14.20)	(392.00)[d]
								14.58	22.61	654.06
24	140.1	He	2	Hi	0.7350	24.00	77	14.43	0.00	5.32[b]
								14.65	4.06	5.76
								14.69	4.79	11.04
								14.69	9.14	457.40[c]
									(14.60)	(319.00)[d]
								14.70	14.62	318.93
								14.71	22.62	577.00
25	122.0	He	2	Hi	0.7622	28.34	78	14.42	0.00	4.82
								14.67	4.06	5.48
								14.68	4.54	7.81
								14.68	9.25	433.36[c]
								14.69	13.55	279.06
									(14.40)	(279.00)[d]
								14.70	22.67	443.80
26	122.0	N_2	2	Hi	0.7622	28.34	77	14.43	0.00	5.05[b]

Table 17. (continued)

Run No.	Average particle diameter, microns	Gas	Col. dia., in.	Bed height	Tangent angle of repose	Particle size standard deviation	Bed temp. $^{o}F.$	Average bed pressure, lb./sq.in.-abs.	Gas velocity, ft./min.	Resistivity, ohm-in.
								14.94	4.01	5.48
								14.98	4.72	5.51
								14.99	10.55	646.93[c]
								14.99	15.45	376.74
									(15.50)	(376.00)[d]
								15.00	20.29	638.91
27	122.0	N_2	2	Lo	0.7622	28.34	76	14.42	0.00	6.04[b]
								14.82	3.02	7.47
								14.86	4.72	115.97
								14.86	10.68	484.70[c]
								14.87	15.46	397.67
									(15.50)	(398.00)[d]
								14.87	20.28	523.25
28	122.0	He	2	Lo	0.7622	28.34	73	14.43	0.00	6.71[b]
								14.52	2.42	7.10
								14.56	4.77	14.70
								14.57	8.25	463.91[c]
									(15.40)	(375.00)[d]
								14.57	15.63	377.43
								14.58	28.19	714.09
29	122.0	He	4	Lo	0.7622	28.34	76	14.31	0.00	4.81[b]
								14.42	2.12	5.43
								14.47	3.61	14.17
								14.48	8.00	303.49[c]
									(15.40)	(220.00)[d]
								14.49	17.02	220.10

Table 17. (continued)

Run No.	Average particle diameter, microns	Gas	Col. dia., in.	Bed height	Tangent angle of repose	Particle size standard deviation	Bed temp. $^{o}F.$	Average bed pressure, lb./sq.in.-abs.	Gas velosity, ft./min.	Resistivity, ohm-in.
								14.49	26.71	265.89
								14.51	36.23	307.00
30	122.0	He	4	Hi	0.7622	28.34	77	14.31	0.00	3.20[b]
								14.57	3.14	4.25
								14.59	3.61	9.55
								14.59	8.01	283.81[c]
								14.61	17.01	188.37
									(21.60)	(182.00)[d]
								14.62	26.71	193.19
								14.64	36.46	321.48
31	122.0	N_2	4	Hi	0.7622	28.34	70	14.44	0.00	3.42[b]
								15.02	3.45	4.69
								15.03	3.80	5.11
								15.04	7.92	351.54[c]
								15.05	13.40	220.10
								15.06	20.61	162.33
									(25.80)	(155.00)[d]
								15.08	28.62	157.56
32	122.0	N_2	4	Lo	0.7622	28.34	72	14.44	0.00	4.76[b]
								14.85	2.35	5.38
								14.89	3.97	79.53
								14.90	8.55	340.57[c]
								14.91	14.62	209.89
								14.92	20.71	171.37
								14.94	28.27	145.09
									(31.00)	(144.00)[d]

Table 17. (continued)

Run No.	Average particle diameter, microns	Gas	Col. dia., in.	Bed height	Tangent angle of repose	Particle size standard deviation	Bed temp. $^{o}F.$	Average bed pressure, lb./sq.in.-abs.	Gas velocity, ft./min.	Resistivity, ohm-in.
33	108.4	N_2	4	Hi	0.7715	30.19	75	14.46	0.00	3.33[b]
								15.02	2.58	3.94
								15.06	3.24	15.36
								15.07	7.64	428.65[c]
								15.08	13.45	200.93
								15.08	18.30	148.44
									(22.00)	(135.00)[d]
								15.08	23.29	135.29
34	108.4	N_2	4	Lo	0.7715	30.19	76	14.46	0.00	4.70[b]
								14.86	2.03	5.40
								14.91	3.24	91.59
								14.92	7.47	434.59[c]
								14.93	13.48	194.48
								14.94	18.35	137.38
								14.95	23.34	138.05
									(27.00)	(128.00)[d]
35	108.4	He	4	Lo	0.7715	30.19	77	14.44	0.00	5.01[b]
								14.54	1.63	5.53
								14.60	3.13	26.25
								14.60	6.11	392.65[c]
								14.61	16.96	186.03
									(19.00)	(186.00)[d]
								14.62	26.58	194.73
								14.63	35.97	188.12
36	108.4	He	4	Hi	0.7715	30.19	76	14.44	0.00	3.17[b]
								14.70	2.81	4.06

Table 17. (continued)

Run No.	Average particle diameter, microns	Gas	Col. dia., in.	Bed height	Tangent angle of repose	Particle size standard deviation	Bed temp. $^{o}F.$	Average bed pressure, lb./sq.in.-abs.	Gas velocity, ft./min.	Resistivity, ohm-in.
								14.73	3.16	21.88
								14.72	6.69	309.85[c]
								14.74	16.92	162.00
									(22.80)	(146.00)[d]
								14.75	26.49	150.28
								14.76	35.83	195.99
37	108.4	He	2	Hi	0.7715	30.19	77	14.44	0.00	5.93[b]
								14.68	3.27	6.23
								14.70	3.80	46.34
								14.70	8.66	701.16[c]
								14.71	13.52	286.82
									(14.00)	(286.00)[d]
								14.71	20.13	538.49
38	108.4	He	2	Lo	0.7715	30.19	75	14.45	0.00	6.96[b]
								14.57	2.85	8.79
								14.59	3.69	33.55
								14.59	8.64	513.79[c]
								14.60	13.49	316.08
									(14.50)	(316.00)[d]
								14.60	20.08	377.77
39	108.4	N_2	2	Lo	0.7715	30.19	76	14.43	0.00	7.11[b]
								14.82	1.69	7.43
								14.88	3.74	29.51
								14.89	9.32	932.87[c]
								14.89	15.41	461.05
									(17.00)	(456.00)[d]

Table 17. (continued)

Run No.	Average particle diameter, microns	Gas	Col. dia., in.	Bed height	Tangent angle of repose	Particle size standard deviation	Bed temp. $^{o}F.$	Average bed pressure, lb./sq.in.-abs.	Gas velocity, ft./min.	Resistivity, ohm-in.
								14.89	26.40	702.16
40	108.4	N_2	2	Hi	0.7715	30.19	76	14.41	0.00	5.91[b]
								14.92	2.71	6.16
								14.98	3.99	34.22
								14.99	9.34	510.48[c]
								15.00	13.31	389.40
									(14.60)	(363.00)[d]
								15.00	22.73	837.20
41	93.7	N_2	4	Hi	0.8339	30.77	78	14.29	0.00	3.39[b]
								14.84	2.12	4.23
								14.88	2.60	10.05
								14.89	6.89	393.57[c]
								14.89	10.23	207.21
								14.90	13.58	129.43
									(17.40)	(103.00)[d]
42	93.7	N_2	4	Lo	0.8339	30.77	78	14.29	0.00	4.96[b]
								14.70	1.69	5.48
								14.76	2.61	40.31
								14.76	7.37	459.54[c]
								14.76	10.24	274.77
								14.77	13.59	145.00
									(18.40)	(94.00)[d]
43	93.7	He	4	Lo	0.8339	30.77	78	14.30	0.00	5.18[b]
								14.41	1.68	5.90
								14.46	2.73	38.78

Table 17. (continued)

Run No.	Average particle diameter, microns	Gas	Col. dia., in.	Bed height	Tangent angle of repose	Particle size standard deviation	Bed temp. $^{o}F.$	Average bed pressure, lb./sq.in.-abs.	Gas velocity, ft./min.	Resistivity, ohm-in.
								14.46	6.05	425.47[c]
								14.46	9.02	225.54
									(16.20)	(146.00)[d]
								14.47	16.35	147.77
44	93.7	He	4	Hi	0.8339	30.77	78	14.29	0.00	3.37[b]
								14.45	1.20	4.55
								14.58	2.77	50.96
								14.58	6.87	504.58[c]
								14.59	12.14	196.24
								14.60	17.00	141.65
									(17.20)	(142.00)[d]
45	93.7	He	2	Hi	0.8339	30.77	78	14.29	0.00	6.07[b]
								14.54	2.88	7.27
								14.55	3.16	46.34
								14.55	8.33	676.63[c]
								14.56	13.61	390.14
									(15.00)	(364.00)[d]
								14.56	20.26	427.33
46	93.7	He	2	Lo	0.8339	30.77	78	14.29	0.00	7.18[b]
								14.38	1.73	7.55
								14.42	2.74	13.56
								14.42	5.66	697.66[c]
								14.43	13.62	315.37
									(14.10)	(314.00)[d]
								14.43	20.27	475.86

Table 17. (continued)

Run No.	Average particle diameter, microns	Gas	Col. dia., in.	Bed height	Tangent angle of repose	Particle size standard deviation	Bed temp. $^{o}F.$	Average bed pressure, lb./sq.in.-abs.	Gas velocity, ft./min.	Resistivity, ohm-in.
47	93.7	N_2	2	Hi	0.8339	30.77	77	14.31	0.00	6.42[b]
								14.84	2.55	6.45
								14.88	4.01	140.63[c]
								14.88	9.80	978.54
								14.89	11.42	265.12
									(12.00)	(284.00)[d]
								14.89	15.52	449.66
48	93.7	N_2	2	Lo	0.8339	30.77	76	14.31	0.00	7.52[b]
								14.70	1.53	7.90
								14.76	3.23	7.39[c]
								14.76	8.80	874.29
								14.76	11.48	296.52
									(12.20)	(292.00)[d]
								14.76	15.51	439.53
49	89.0	He	4	Hi	0.8310	31.01	77	14.35	0.00	3.48[b]
								14.58	2.01	4.03
								14.63	2.68	81.77[c]
								14.64	6.23	480.39
								14.65	10.63	209.30
									(13.50)	(190.00)[d]
								14.66	16.86	223.28
50	89.0	He	4	Lo	0.8310	31.01	77	14.35	0.00	4.81[b]
								14.45	1.28	5.35
								14.51	2.69	77.16[c]
								14.52	5.48	501.06
								14.53	10.63	200.93

Table 17. (continued)

Run No.	Average particle diameter, microns	Gas	Col. dia., in.	Bed height	Tangent angle of repose	Particle size standard deviation	Bed temp. $^{o}F.$	Average bed pressure, lb./sq.in.-abs.	Gas velocity, ft./min.	Resistivity, ohm-in.
									(16.00)	(142.00)[d]
								14.53	17.00	145.09
51	89.0	N_2	4	Hi	0.8310	31.01	78	14.35	0.00	3.22[b]
								14.90	2.60	3.67
								14.94	2.60	99.38
								14.94	7.11	570.72[c]
								14.95	11.18	206.12
								14.96	15.92	133.28
									(17.30)	(130.00)[d]
52	89.0	N_2	4	Lo	0.8310	31.01	77	14.35	0.00	4.73[b]
								14.76	1.84	5.50
								14.82	2.60	73.54
								14.82	6.44	454.52[c]
								14.83	10.20	222.36
								14.83	14.74	145.09
									(16.80)	(136.00)[d]
53	89.0	N_2	2	Hi	0.8310	31.01	78	14.38	0.00	6.27[b]
								14.91	2.72	8.44
								14.92	3.76	84.66
								14.94	10.00	954.93[c]
								14.96	15.48	550.17
									(22.40)	(460.00)[d]
								14.96	23.01	460.46
54	89.0	N_2	2	Lo	0.8310	31.01	78	14.38	0.00	7.70[b]
								14.75	1.54	8.25

Table 17. (continued)

Run No.	Average particle diameter, microns	Gas	Col. dia., in.	Bed height	Tangent angle of repose	Particle size standard deviation	Bed temp. $^{o}F.$	Average bed pressure, lb./sq.in.-abs.	Gas velocity, ft./min.	Resistivity, ohm-in.
								14.81	3.35	148.83
								14.81	8.01	889.53[c]
									(10.40)	(302.00)[d]
								14.81	10.44	302.06
								14.82	15.51	418.80
55	89.0	He	2	Lo	0.8310	31.01	79	14.38	0.00	7.85[b]
								14.49	1.89	8.51
								14.52	2.87	26.58
								14.52	7.92	893.02[c]
								14.53	15.78	372.09
									(16.80)	(368.00)[d]
								14.53	25.41	719.47
56	89.0	He	2	Hi	0.8310	31.01	79	14.38	0.00	6.49[b]
								14.64	2.87	7.27
								14.62	2.59	6.75
								14.65	3.16	25.05
								14.65	8.31	669.76[c]
								14.66	13.57	278.12
									(17.10)	(270.00)[d]
								14.66	22.69	908.97
57	82.3	He	4	Hi	0.8645	32.12	79	14.40	0.00	3.32[b]
								14.65	2.12	3.95
								14.69	2.48	12.26
								14.69	6.50	464.48[c]
								14.69	8.99	235.34
									(15.00)	(151.00)[d]

Table 17. (continued)

Run No.	Average particle diameter, microns	Gas	Col. dia., in.	Bed height	Tangent angle of repose	Particle size standard deviation	Bed temp. $^{o}F.$	Average bed pressure, lb./sq.in.-abs.	Gas velocity, ft./min.	Resistivity, ohm-in.
								14.70	16.14	153.63
								14.70	12.13	167.44
58	82.3	He	4	Lo	0.8645	32.12	77	14.43	0.00	5.38[b]
								14.56	1.57	6.49
								14.70	2.45	21.90
								14.61	5.78	562.85[c]
								14.61	10.59	216.08
								14.62	15.41	142.66
									(16.80)	(139.00)[d]
59	82.3	N_2	4	Lo	0.8645	32.12	78	14.43	0.00	5.11[b]
								14.83	1.37	6.06
								14.89	2.35	79.83
								14.89	5.94	427.73[c]
								14.90	9.65	248.06
								14.91	13.53	148.35
									(16.20)	(129.00)[d]
60	82.3	N_2	4	Hi	0.8645	32.12	77	14.42	0.00	3.34[b]
								14.98	2.28	4.19
								15.01	2.30	86.15
								15.01	7.33	620.11[c]
								15.01	11.17	185.77
								15.02	14.68	146.01
									(14.70)	(146.00)[d]
61	82.3	N_2	2	Hi	0.8645	32.12	77	14.41	0.00	6.69[b]
								14.93	2.55	7.57

Table 17. (continued)

Run No.	Average particle diameter, microns	Gas	Col. dia., in.	Bed height	Tangent angle of repose	Particle size standard deviation	Bed temp. $^{o}F.$	Average bed pressure, lb./sq.in.-abs.	Gas velocity, ft./min.	Resistivity, ohm-in.
								14.96	3.35	107.73
								14.96	8.97	727.57[c]
									(13.00)	(308.00)[d]
								14.97	13.04	307.57
								14.98	17.86	586.04
62	82.3	N_2	2	Lo	0.8645	32.12	79	14.30	0.00	7.98[b]
								14.67	1.58	8.50
								14.74	3.03	59.80
								14.74	8.04	769.32[c]
								14.74	9.52	372.09
									(12.10)	(305.00)[d]
								14.75	15.54	401.17
63	82.3	He	2	Hi	0.8645	32.12	80	14.26	0.00	6.90[b]
								14.51	2.54	7.50
								14.52	3.05	25.68
								14.52	7.58	676.04[c]
								14.53	14.76	344.28
									(15.00)	(344.00)[d]
								14.54	21.57	458.24
64	82.3	He	2	Lo	0.8645	32.12	82	14.25	0.00	7.93[b]
								14.35	1.74	8.48
								14.39	2.60	46.90
								14.39	7.41	817.94[c]
								14.39	14.79	378.35
									(15.40)	(376.00)[d]
								14.38	22.92	435.34

Table 17. (continued)

Run No.	Average particle diameter, microns	Gas	Col. dia., in.	Bed height	Tangent angle of repose	Particle size standard deviation	Bed temp. $^{o}F.$	Average bed pressure, lb./sq.in.-abs.	Gas velocity, ft./min.	Resistivity, ohm-in.
65	80.6	He	4	Hi	0.8525	32.60	80	14.29	0.00	3.68[b]
								14.53	1.98	4.24
								14.58	2.40	37.59
								14.58	5.84	455.86[c]
								14.59	10.67	213.40
									(14.10)	(190.00)[d]
								14.60	16.52	206.45
66	80.6	He	4	Lo	0.8525	32.60	81	14.20	0.00	4.56[b]
								14.29	1.15	4.98
								14.36	2.63	75.62
								14.36	6.55	623.13[c]
								14.37	10.78	230.40
								14.37	13.91	188.87
									(15.40)	(184.00)[d]
67	80.6	N_2	4	Lo	0.8525	32.60	81	14.20	0.00	4.70[b]
								14.57	1.19	5.08
								14.65	2.33	72.70
								14.66	6.68	785.21[c]
								14.66	10.31	228.22
								14.66	13.69	142.83
									(17.40)	(118.00)[d]
68	80.6	N_2	4	Hi	0.8525	32.60	75	14.16	0.00	2.87[b]
								14.70	2.04	3.32
								14.75	2.49	46.15
								14.75	7.13	627.48[c]
								14.75	10.25	220.69

Table 17. (continued)

Run No.	Average particle diameter, microns	Gas	Col. dia., in.	Bed height	Tangent angle of repose	Particle size standard deviation	Bed temp. $^{o}F.$	Average bed pressure, lb./sq.in.-abs.	Gas velocity, ft./min.	Resistivity, ohm-in.
								14.76	13.60	144.00
									(16.80)	(123.00)[d]
69	80.6	N_2	2	Hi	0.8525	32.60	72	14.12	0.00	6.15[b]
								14.63	2.29	8.36
								14.66	2.86	24.89
								14.68	9.61	503.87[c]
								14.69	11.93	365.77
									(13.20)	(353.00)[d]
								14.69	17.98	543.49
70	80.6	N_2	2	Lo	0.8525	32.60	73	14.12	0.00	8.26[b]
								14.50	1.54	8.43
								14.55	2.74	51.22
								14.55	7.79	934.25[c]
								14.56	10.50	320.88
									(12.40)	(317.00)[d]
								14.56	18.00	418.60
71	80.6	He	2	Lo	0.8525	32.60	73	14.08	0.00	8.30[b]
								14.18	1.55	9.09
								14.23	2.54	31.75
								14.23	6.55	577.70[c]
									(11.60)	(264.00)[d]
								14.23	11.63	263.93
								14.23	18.08	441.85
72	80.6	He	2	Hi	0.8525	32.60	77	14.07	0.00	6.68[b]
								14.32	2.55	7.37

Table 17. (continued)

Run No.	Average particle diameter, microns	Gas	Col. dia., in.	Bed height	Tangent angle of repose	Particle size standard deviation	Bed temp. $^{o}F.$	Average bed pressure, lb./sq.in.-abs.	Gas velocity, ft./min.	Resistivity, ohm-in.
								14.34	2.76	28.49
								14.34	7.19	453.28[c]
								14.35	12.72	245.97
									(13.40)	(245.00)[d]
								14.35	20.39	386.41